SCATTERING PROCESSES
IN ATOMIC PHYSICS, NUCLEAR PHYSICS, AND COSMOLOGY

By

Gavriil Shchedrin

A DISSERTATION

Submitted to
Michigan State University
in partial fulfillment of the requirements
for the degree of

PHYSICS - DOCTOR OF PHILOSOPHY

2013

ABSTRACT

SCATTERING PROCESSES IN ATOMIC PHYSICS, NUCLEAR PHYSICS, AND COSMOLOGY

By

Gavriil Shchedrin

The universal way to probe a physical system is to scatter a particle or radiation off the system. The results of the scattering are governed by the interaction Hamiltonian of the physical system and scattered probe. An object of the investigation can be a hydrogen atom immersed in a laser field, heavy nucleus exposed to a flux of neutrons, or space-time metric perturbed by the stress-energy tensor of neutrino flux in the early Universe. This universality of scattering process designates the *Scattering Matrix*, defined as the unitary matrix of the overlapping *in* and *out* collision states, as the central tool in theoretical physics.

In this Thesis we present our results in atomic physics, nuclear physics, and cosmology. In these branches of theoretical physics the key element that unifies all of them is the scattering matrix. Additionally, within the scope of Thesis we present underlying ideas responsible for the unification of various physical systems. Within atomic physics problems, namely the axial anomaly contribution to parity nonconservation in atoms, and two-photon resonant transition in a hydrogen atom, it was the scattering matrix which led to the Landau-Yang theorem, playing the central role in these problems. In scattering problems of cosmology and quantum optics we developed and implemented mathematical tools that allowed us to get a new point of view on the subject. Finally, in nuclear physics we were able to take advantage of the target complexity in the process of neutron scattering which led to the formulation of a new resonance width distribution for an open quantum system.

ACKNOWLEDGMENTS

In this section I would like to give a credit to many physicists and mathematicians who shared their knowledge and shaped my understanding of this beautifully designed Physical and Mathematical World whose elegance can be appreciated by mere mortals.

The first in the list is my Thesis advisor, Prof. Vladimir G. Zelevinsky, whose knowledge and real understanding of theoretical physics and in particular nuclear physics is truly remarkable. My advisor expertise in atomic physics, nuclear physics and cosmology made possible the very existence of the present Thesis. Also his teaching talent is of the same caliber as his physics expertise. Here I would like to mention that MSU Physics & Astronomy Outstanding Faculty Teaching Award of 2003, 2004, and in the unprecedented period of 6 consecutive years from 2006 till 2011 was given to my advisor. So I am very much privileged and grateful to my great advisor for his willingness to work with such a troublemaker and crazy guy like me. Most importantly for me, besides physics of course, was his company where we shared a great deal of fun.

I am very thankful to the Condensed Matter group at Michigan State. First of all, I am thankful to great physicist Prof. Mark Dykman for his active position in every respect and his teaching style. The very special thank you goes to Prof. Norman Birge, remarkable physicist and great experimentalist. His way of explaining physics was absolutely new experience for me. It was a refreshing point of view on the subject which gave me a practical understanding. Prof. Thomas Kaplan is the great soul of the condensed matter body at Michigan State. Prof. Chih-Wei Lai and Prof. John McGuire were very kind to share their time and ideas with me.

I am grateful to the High Energy group at Michigan State. I am thankful to Prof. Wayne Repko for an exciting problem in cosmology and for the reference to a jewel in the modern physics literature, a masterpiece by the greatest living physicist Steven Weinberg, named *Cosmology*, published by the Oxford University Press in 2008. If someone wants to appreciate a truth beauty of the Physical World, this book will blow someone's mind as it happened with me while I was writing this Thesis. I would like to thank Prof. Carl Schmidt for his courses on Quantum Field Theory and Mathematical Physics. Also I would like to thank Prof. James Linnemann, Prof. Carl Bromberg and Prof. Kirsten Tollefson, supported by the team of Tibor Nagy, Richard Hallstein and Mark Olson, who guided me thorough my teaching courses at Michigan State. On the top of that, Prof. James Linnemann has always been a great audience to discuss theoretical physics.

The physics division where I finally settled down had become Nuclear Cyclotron facility at Michigan State. Prof. Scott Pratt who is the Graduate Program Director and who was a witness of my ups and downs during my four years long graduate life, has always been a great audience to discuss physics in a "five minutes" format. I would like to thank Prof. Alex Brown and Prof. Remco Zegers for their time and efforts during my nuclear graduate life. I am thankful to Prof. Michael Thoennessen whose invisible help has always been very much appreciated.

Mathematics department at Michigan State has a number of great mathematicians. I am very thankful to great mathematician Prof. Alexander Volberg for his keen interest in physics that resulted in our joint paper. The chapter on quantum optics in this Thesis is based on our work. Also I am indebted to a wonderful mathematician Prof. Michael Shapiro, who shared his time and mathematical insights on the mathematical structures appearing in nuclear physics problems.

From my undergraduate life in St. Petersburg I would like to thank remarkable physicist Prof. Alexander N. Vasil'ev for his rich contribution to my undergraduate physics life which would have been completely empty otherwise. Also I am grateful to my undergraduate advisor, great physicist Prof. Leonti N. Labzowsky, who shared quite a bit of his time and knowledge with me. Most importantly, he shared a very interesting problem on axial anomaly that grew into a single chapter on atomic physics in this Thesis.

The present list would never be a complete one without paying a tribute to a truly remarkable people, Anna G. Reznikova, Sergey G. Maloshevsky, and Inna D. Mints, all wonderful mathematicians, who helped me get started and supported me wholeheartedly during my rough undergraduate years in St. Petersburg.

Finally I would like to thank all of my fellow physics graduate students at Michigan State, and in particular Pawin Ittisamai and Scott Bustabad who shared a great deal of humor during my graduate life. Also I am grateful to my undergraduate students who suffered at my physics classes and from whom I have learned quite a bit.

Thank all of you!

TABLE OF CONTENTS

LIST OF FIGURES

Chapter 1

Introduction

In this Thesis we summarize our results in atomic physics, quantum optics, nuclear physics, and cosmology unified by various aspects of quantum scattering theory.

In *Chapter 2* our object of investigation is the scattering matrix corresponding to the axial anomaly contribution to parity nonconservation in atoms. Here we explain physics of parity nonconservation in complex atoms and discuss the contribution of the axial anomaly to parity nonconservation in atomic cesium. The main result is the prediction of the emission of an electric photon by the magnetic dipole which has not been observed yet. The probability of this process is very small but the non-zero result is important from theoretical point of view.

The main aspect of our calculation is related to the well known theorem of axial anomaly cancellation in the Standard Model. According to the Landau-Yang theorem, it is impossible for the real Z-boson of spin $J = 1$ to decay into two real photons in contrast to the allowed two-photon decay of the spinless π^0-meson. However, if one of the photons that connects the triangular graph of the axial anomaly with the electron atomic transition, e.g., $6s - 7s$ transition in cesium, is virtual, the axial anomaly does not vanish. We have shown that one can see the impact of the axial anomaly in atomic physics through the parity violation in atoms.

Chapter 3 is devoted to the electron scattering process off an arbitrary central potential in the presence of strong laser field. Here we introduce a new method that allows one to obtain an analytical cross section for the laser-assisted electron-ion collision. As an example we perform a calculation for the hydrogen laser-assisted recombination. The standard S-matrix formalism is used for describing the collision process. The S-matrix is constructed from the electron Coulomb-Volkov wave function in the combined Coulomb-laser field and the hydrogen perturbed state. By the aid of the Bessel generating function, the S-matrix is decomposed into an infinite series of the field harmonics. We have introduced a new step that results in an analytical expression for the cross section of the process. The theoretical novelty is in the application of the Plancherel theorem to the Bessel generating function. This allows one to perform summation of the infinite series of Bessel functions and thus obtain a closed analytical expression for the laser-assisted hydrogen photo-recombination process.

In the field of nuclear physics presented in *Chapter 4* we investigate the resonance width distribution for low-energy neutron scattering off heavy nuclei. Our interest was ignited by the recent experiments that claimed significant deviations from the routinely used chi square, or the Porter-Thomas, distribution. The unstable complex nucleus is an open quantum system, where the intrinsic dynamics has to be supplemented by the coupling of chaotic internal states through the continuum. We propose a new width distribution based on random matrix theory for a chaotic quantum system with a single decay channel as well as for an open quantum system with an arbitrary number of open channels. The revealed statistics of the width distribution exhibits distinctive properties that are characteristically different from the regularities shared by closed quantum systems.

In *Chapter 5* our object of investigation is the space-time metric perturbed by the stress-energy tensor of neutrino scattering in the early Universe. In this Chapter we have developed a mathematical machinery that allows one to evaluate gravitational wave damping due to freely streaming neutrinos in the early Universe. The solution is represented by a convergent series of spherical Bessel functions derived with the help of a new compact formula for the convolution of spherical Bessel functions of integer order. These calculations can be compared to the tensor fluctuations of the Cosmic Microwave Background in order to reveal direct evidence of the presence of gravitational waves in the early Universe. The developed technique can be applied for the analysis of the scalar Cosmic Microwave Background fluctuations which provides a direct test of the standard inflationary cosmological model.

Finally, *Chapter 6* summarizes the results of our investigation on scattering processes in atomic physics, quantum optics, nuclear physics, and cosmology. Basic governing principles, such as conservation laws and detailed balance principle, unitarity and gauge invariance of the scattering matrix are given special attention throughout the Thesis.

Chapter 2

Atomic Physics

In this chapter the main interest is parity violation in atomic physics. Parity operation is defined as a coordinate inversion $\vec{r} \to -\vec{r}$, which tests the coordinate symmetry of the physical system, as well as intrinsic symmetries of fundamental physical objects. In quantum electrodynamics (QED) that fully describes electron-photon interaction, parity is conserved due to the invariance of the QED action under the spatial inversion.

However, in the Standard Model that treats electromagnetic and weak forces as a unified electroweak interaction, which led to a prediction and subsequent discovery of the W and Z bosons, parity is violated. The W and Z bosons are the carriers of the so-called weak axial currents which are responsible for the parity violation.

In addition to the high energy experiments, that aim at the verification of the Standard Model on a very high energy scale, one can test its predictions on a low energy scale by running tabletop experiments. In particular, we are interested in parity non-conservation effects in atoms, driven by the effective parity nonconserving interaction of electrons with the nucleus.

This chapter is organized as follows. In the first subsection we briefly review the general scope of the problem. In the section on the *Furry theorem* we provide an important result for the fermion loop diagrams with an odd number of interaction vertices, e.g. one on Fig. 2.1. Next subsection stands for a general physical idea behind axial anomaly calculation in atomic physics. The actual calculation is presented in section *Axial Anomaly S-matrix*. In this

section we explicitly write the S-matrix for the decay of the Z-boson into two photons and apply it to our calculation. We show that due to the transversality conditions and on-shell constraint for real photons and the Z-boson, the axial anomaly diagram identically vanishes, in a full accordance with the Landau-Yang theorem. However, if one of the photons that connects the triangular graph of the axial anomaly with the electron atomic transition, e.g., $6s - 7s$ transition in cesium, is virtual, the axial anomaly does not vanish and contributes to the effect of parity nonconservation.

The results of this chapter are based on our paper,
GS and L. Labzowsky, Phys. Rev. A **80**, 032517 (2009).

2.1 Standard Model in low-energy physics

The problem of testing the Standard Model (SM) in the low-energy physical phenomena is one of the interesting topics in physics actively pursued in the last few decades. The SM in the low energy limit is tested in nuclei, where significant many-body enhancement of the parity nonconservation (PNC) effects was predicted and confirmed. Along with the PNC effects in nuclei, atomic physics experiments offer a high precision for validating the SM predictions. The most accurate of atomic experiments is the one with the neutral cesium atom, first proposed in [1] and performed with the utmost precision in [2].

The basic atomic transition employed in the cesium experiment was the strongly forbidden $6s - 7s$ transition of the valence electron with the absorption of a magnetic dipole photon, $M1$. In the real experiment this very weak transition was opened by the external electric field but it does not matter for our further derivations. The Feynman graphs

illustrating the PNC effect in cesium are given below in Fig. 2.2.

The atomic experiments are indirect and require very accurate calculations of the PNC effects to extract the value of the characteristic parameter of the SM, the Weinberg angle, which can be compared with the corresponding high-energy value. The main difficulty with the PNC calculations in neutral atoms is the necessity to take into account the electron correlations within the complex atom. Therefore the experiments with much simpler systems, such as few-electron highly charged ions (HCI) would be highly desirable. Several proposals on the subject were considered in [3–6]. At the same time relativistic corrections make heavy-Z atoms preferable due the enhancement factor for electronic wave functions.

The radiative corrections to the PNC effect are important in cesium calculations to reach the agreement with the high-energy SM predictions. These radiative corrections include electron self-energy, vertex and vacuum polarization Feynman diagrams. They are even more important in the case of the HCI. The entire set of these corrections for the neutral cesium atom was calculated in [7–10]. The electron self-energy and vertex corrections for HCI were obtained in [11]; the vacuum polarization correction was given in [12].

The full set of radiative corrections including Z-boson loops has not been calculated, neither for a neutral atom nor for the HCI. Therefore the problem still cannot be considered as fully solved.

2.2 Furry theorem

In quantum field theory Feynman diagrams with a high number of vertices are notoriously difficult for calculation. However, in the special case of a fermion loop diagram with an odd number of identical interaction vertices, its contribution, according to the `Furry theorem`,

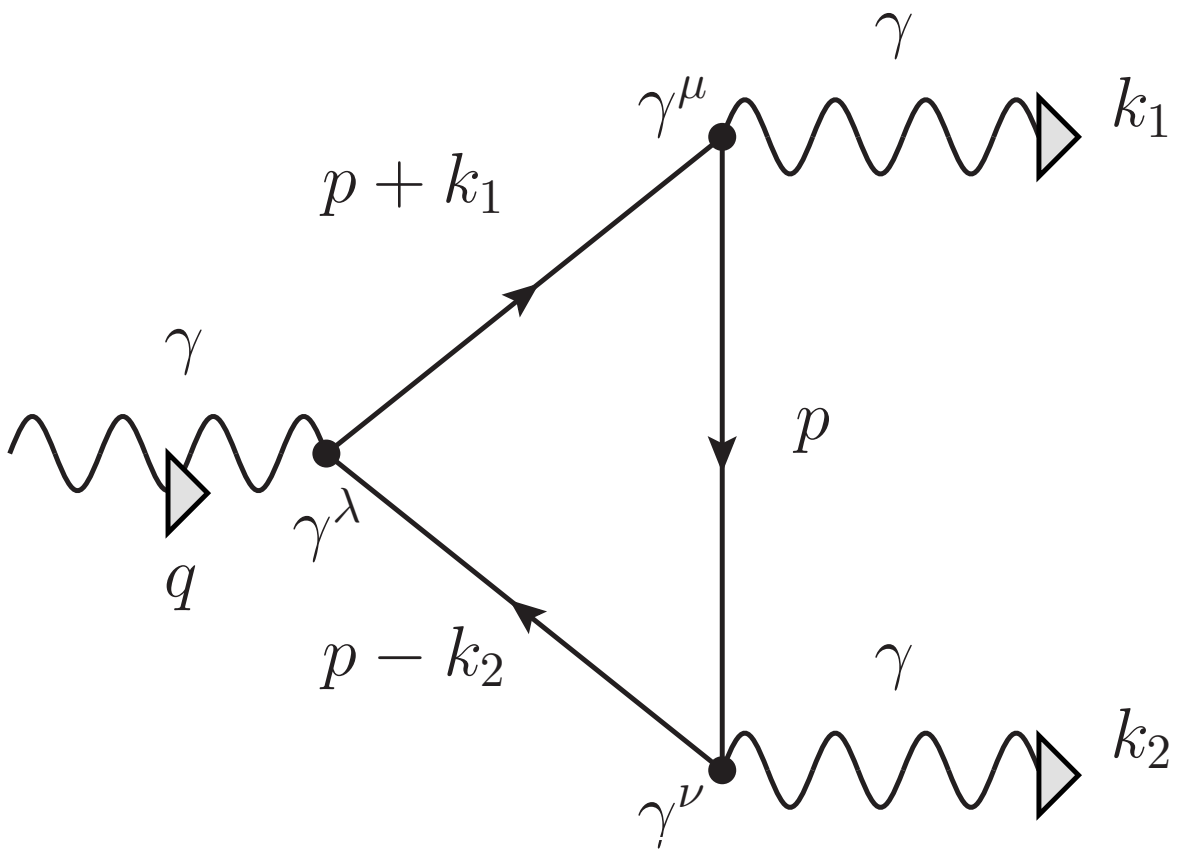

Figure 2.1: Proof of the Furry theorem on the example of a triangle Feynman graph.

is identically zero. To illustrate the proof of the Furry theorem we recognize that the Dirac matrices γ^μ change sign and get transposed, $\widehat{\gamma}^\mu$, under charge conjugation C,

$$C^{-1}\gamma^\mu C = -\widehat{\gamma}^\mu, \tag{2.1}$$

while the charge conjugated fermion propagator modifies according to

$$C^{-1}G(p)C = C^{-1}\left[\frac{p_\nu\gamma^\nu + m_e}{p^2 - m_e^2}\right]C = \left[\frac{-p_\nu\widehat{\gamma}^\nu + m_e}{p^2 - m_e^2}\right] = \widehat{G}(-p). \tag{2.2}$$

Therefore a typical triangle amplitude will change sign under charge conjugation,

$$A^{\mu\nu\lambda}(k_1,k_2) = \tag{2.3}$$
$$\int d^4p \ \mathrm{Tr}\left[\gamma^\mu \frac{\not p + m_e}{p^2-m_e^2}\gamma^\nu \frac{\not p - \not k_2 + m_e}{(p-k_2)^2-m_e^2}\gamma^\lambda \frac{\not p + \not k_1 + m_e}{(p+k_1)^2-m_e^2}\right]$$
$$\longrightarrow (-1)^3 \int d^4p \ \mathrm{Tr}\left[\gamma^\mu \frac{\not p + m_e}{p^2-m_e^2}\gamma^\nu \frac{\not p - \not k_2 + m_e}{(p-k_2)^2-m_e^2}\gamma^\lambda \frac{\not p + \not k_1 + m_e}{(p+k_1)^2-m_e^2}\right] \equiv 0.$$

The same argument holds for a Feynman diagram with an arbitrary number of odd fermion-boson vertices, and we thus prove the Furry theorem.

However, if a Feynman diagram has an odd number of vertices of a *different* kind, for instance, two vector photon vertices, and a single π^0 pseudo-scalar vertex, or a single Z-boson pseudo-vector vertex, the corresponding Feynman diagram has a non-zero value.

2.3 Axial Anomaly

In the present work we consider a very special radiative correction to the PNC effect, presented by a triangular Feynman graph, or axial anomaly (AA). We understand the triangle AA as a fermion loop with at least one weak vertex [13]. Our conclusion will be that in a neutral atom the contribution of the axial anomaly is non-zero albeit relatively small.

The leading contribution of the AA to the atomic PNC effect is depicted in Fig. 2.2 (c). This contribution corresponds to the Adler-Bell-Jackiw anomaly [14]. In this work we will concentrate exclusively on this term.

The final answer, that looks like the emission of the electric photon by the magnetic dipole, can be easily understood before any real calculations are made. Suppose we have the *6s-7s* transition in cesium. The virtual photon in this transition that connects the atomic electron line with the triangular graph of the axial anomaly must be of a magnetic dipole type $M1$. This virtual photon is absorbed by the fermion current in the axial anomaly

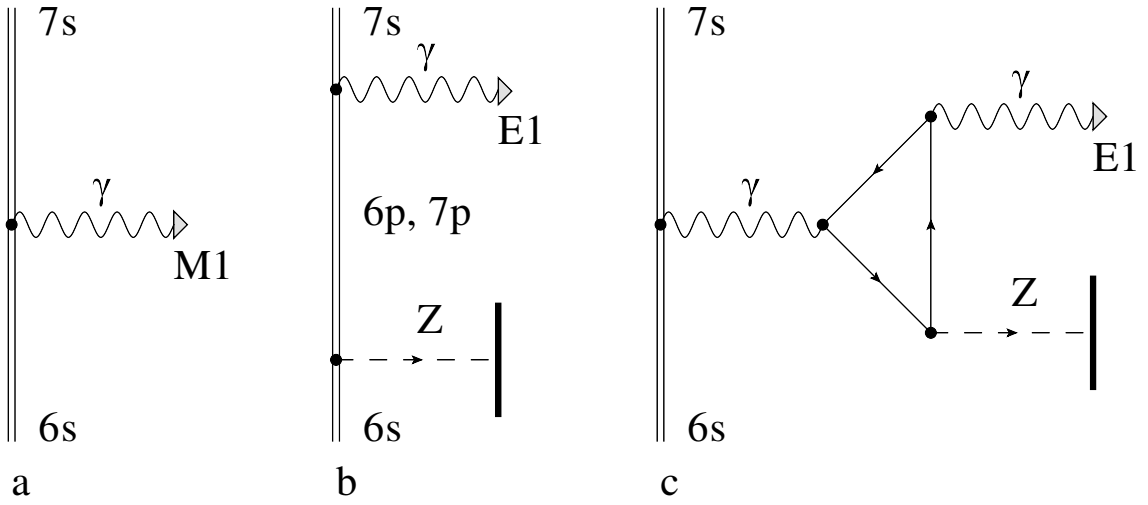

Figure 2.2: The Feynman graphs that describe PNC effect in cesium. The double solid line denotes the electron in the field of the nucleus. The wavy line denotes the photon (real or virtual) and the dashed horizontal line with the short thick solid line at the end denotes the effective weak potential, i.e. the exchange by Z-boson between the atomic electron and the nucleus. Graph (a) corresponds to the basic $M1$ transition amplitude, graph (b) corresponds to the $E1$ transition amplitude, induced by the effective weak potential. The latter violates the spatial parity and allows for the arrival of p-states in the electron propagator in graph (b), of which the contributions of *6p* and *7p* states dominate. The standard PNC effect arises due to the interference between graphs (a) and (b). Graph (c) corresponds to the axial anomaly. The thin solid lines represent virtual electrons and positrons. To graph (c), the Feynman diagram with interchanged external photon and Z-boson lines should be added.

triangle, through a first vertex, and cannot change the parity of the fermion current flowing through this vertex. Now, the second vertex in the axial anomaly triangle that is responsible for exchange of the Z-boson between the fermion line and the cesium nucleus has the Dirac matrix γ^5 that changes the parity of the fermion line. As the result, the third vertex in the axial anomaly triangle that connects two fermion lines with an opposite parity must emit the *electric* photon type $E1$.

2.4 Axial Anomaly S-matrix

We employ the standard expression for the effective parity nonconserving interaction of the atomic electron with the nucleus [15] in the form

$$H_W = A_{\rm PNC}\rho_0(\vec{r})\gamma^5, \tag{2.4}$$

with parity nonconservation vertex $A_{\rm PNC}$,

$$A_{\rm PNC} = -\frac{G_F Q_W}{2\sqrt{2}}, \tag{2.5}$$

Dirac pseudoscalar matrix γ^5,

$$\gamma^5 = i\gamma^0\gamma^1\gamma^2\gamma^3 = -\frac{i}{4!}\varepsilon_{\mu\nu\rho\sigma}\gamma^\mu\gamma^\nu\gamma^\rho\gamma^\sigma = \begin{pmatrix} 0 & \mathbf{1} \\ \mathbf{1} & 0 \end{pmatrix}, \tag{2.6}$$

and contact electron-nucleus interaction $\rho_0(\vec{r})$, where one can neglect the finite size of an atomic nucleus,

$$\rho_0(\vec{r}) = \delta(\vec{r}). \tag{2.7}$$

G_F is the Fermi constant given in terms of the proton mass m_p by

$$G_F = 1.027 \times 10^{-5} \frac{1}{m_p^2} = 1.166 \times 10^{-5} \frac{1}{\mathrm{GeV}^2}. \tag{2.8}$$

Q_W is the weak charge of the nucleus,

$$Q_W = -N + Z(1 - 4\sin^2\theta_w), \tag{2.9}$$

while Z and N are the numbers of protons and neutrons in the nucleus, and θ_w is the Weinberg angle. The currently accepted value for this parameter is

$$\sin^2\theta_w \simeq 0.23. \tag{2.10}$$

The singular δ-function potential acting in the space of Dirac electron wave functions does not vanish only when electron and nucleon coordinates coincide. This approximation is valid if the transferred momentum q is much less than the mass of Z-boson, which is clearly valid for the atomic electron. For the electron in the loop this approximation is valid due to the fact that the momentum transfer to the nucleus, as one can see on Fig. 2.3, is $(q-k)$ where $q^2 \ll m_Z^2$, and as the consequence $(q-k)^2 \ll m_Z^2$. Therefore we can parametrize the coupling of the electron-nucleon interaction by the contact interaction (2.4).

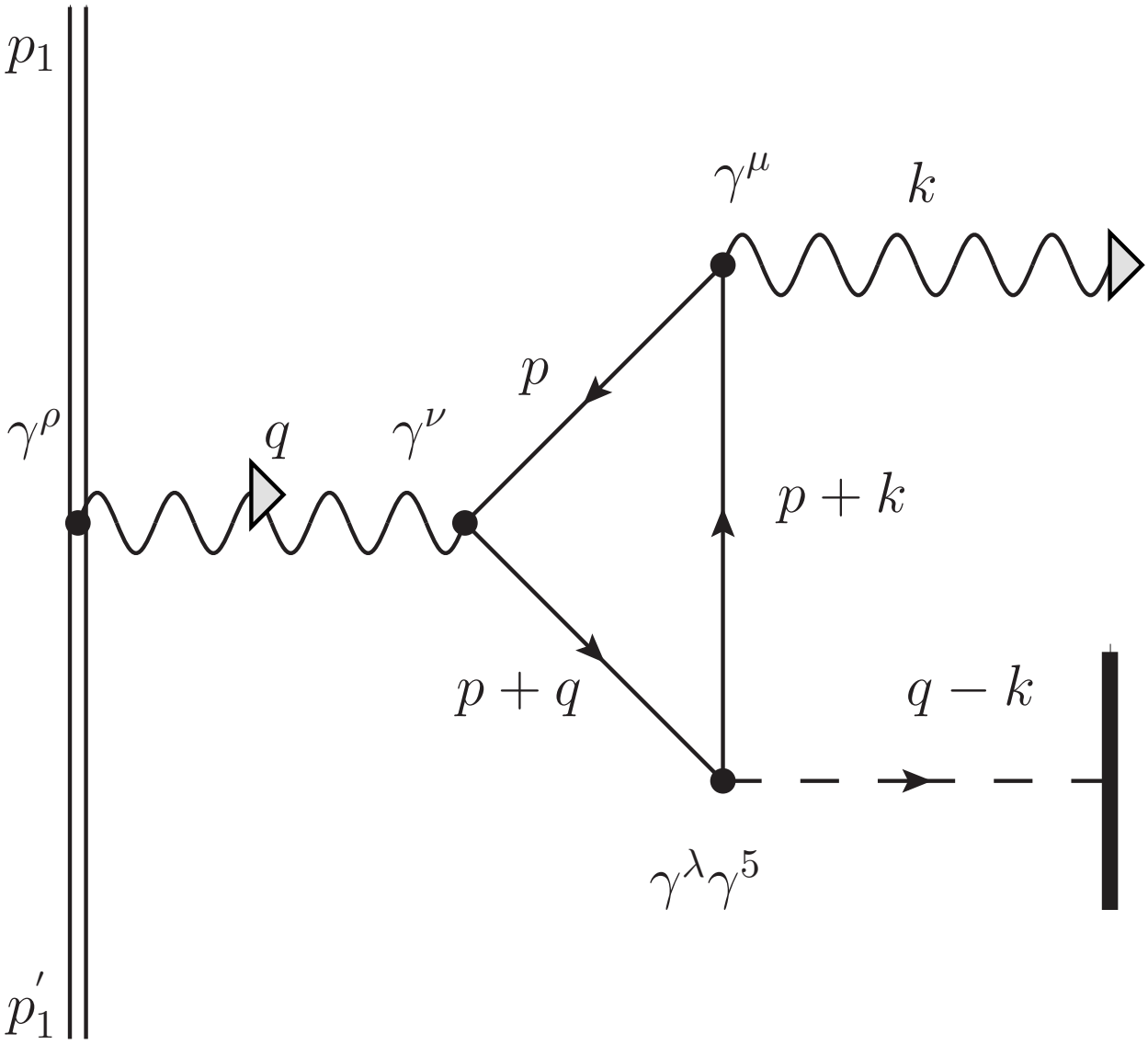

Figure 2.3: Flow of momenta in the axial anomaly.

We write down the S-matrix corresponding to the amplitude Fig. 2.2 (c) in the momentum representation (see Fig. 2.3):

$$S = (ie)^3 \int \frac{d^4p_1'}{(2\pi)^4}\frac{d^4p_1}{(2\pi)^4}\frac{d^4p}{(2\pi)^4}\,\overline{\Psi}_{n's}(p_1)\gamma^\rho\Psi_{ns}(p_1')\frac{g_{\rho\nu}}{q^2+i\epsilon} \tag{2.11}$$
$$\times\mathrm{Tr}\left[\gamma^\mu\frac{\not p+m_e}{p^2-m_e^2}\gamma^\nu\frac{\not p+\not q+m_e}{(p+q)^2-m_e^2}\gamma^\lambda\gamma^5\frac{\not p+\not k+m_e}{(p+k)^2-m_e^2}\right]V_\lambda^{\mathrm{PNC}}(q-k)A_\mu(k).$$

Here e and m_e are the electron charge and mass,

$$\Psi_{ns}(p) = \Psi_{ns}(\vec{p})\delta(p_0 - \varepsilon_{ns}) \tag{2.12}$$

is the wave function of the bound atomic electron in the state $|ns\rangle$ with ε_{ns} being the energy of this state, the transferred momentum q is

$$q = p_1 - p_1', \tag{2.13}$$

$g_{\rho\nu}$ is the pseudo-Euclidean metric tensor,

$$g_{\rho\nu} = \begin{pmatrix} 1 & 0 & 0 & 0 \\ 0 & -1 & 0 & 0 \\ 0 & 0 & -1 & 0 \\ 0 & 0 & 0 & -1 \end{pmatrix}, \tag{2.14}$$

γ^μ are the Dirac matrices,

$$\gamma^\mu = \begin{pmatrix} 0 & \sigma^\mu \\ -\sigma^\mu & 0 \end{pmatrix} \equiv \begin{pmatrix} 0 & \boldsymbol{\sigma} \\ -\boldsymbol{\sigma} & 0 \end{pmatrix}, \tag{2.15}$$

$$\gamma^0 \equiv \beta = \begin{pmatrix} \mathbf{1} & 0 \\ 0 & \mathbf{-1} \end{pmatrix}, \tag{2.16}$$

and $A_\mu(k)$ is the wave function of the emitted photon,

$$A_\mu(x) = \sqrt{\frac{2\pi}{\omega}}\epsilon_\mu e^{-ikx}, \tag{2.17}$$

in the momentum representation. Here ϵ_μ and $k = (\omega, \mathbf{k})$ are the four-vectors of the polarization and the momentum of the emitted photon, correspondingly.

In the momentum representation the potential $V_\lambda^{\rm PNC}$ for the parity-nonconserving interaction of the electron with the nucleus is

$$V_\lambda^{\rm PNC}(q-k) = A_{\rm PNC}\rho_0(q-k)\delta_{\lambda 0}, \tag{2.18}$$

where the nucleon density in the particular case of the point-like nucleus is

$$\rho_0(q-k) = 2\pi\delta(q_0 - k_0). \tag{2.19}$$

In this chapter we use the relativistic units with $\hbar = c = 1$.

2.5 Z-boson decay

The central element in the Feynman diagram of Fig. 2.3, the fermion triangle, involves two photon vertices and a single Z-boson vertex. First we consider the Z-boson (with spin $J(Z) = 1$) decay [16] into two photons, Fig. 2.4. The Landau theorem forbids this decay because a two-photon system cannot exist with angular momentum $J = 1$ [17, 18], in contrast to the allowed decay $\pi^0 \to \gamma\gamma$ since $J(\pi^0) = 0$ [19], see Fig. 2.5. We shall derive this result in the Feynman diagram language for the S-matrix of Fig. 2.4, and see implications for the diagram in Fig. 2.3.

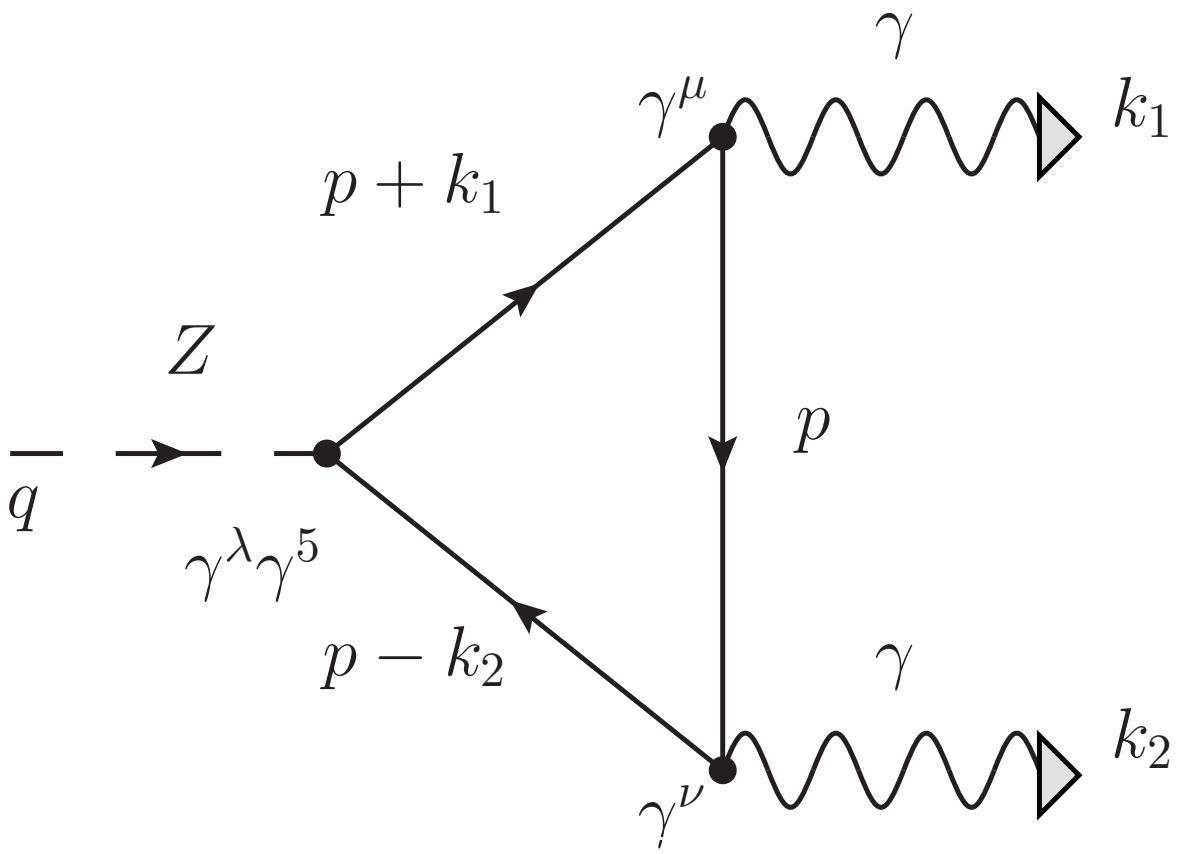

Figure 2.4: Feynman diagram of Z-boson decay into two photons.

The S-matrix of the Z-boson decay into two photons, Fig. 2.4, is proportional to

$$S^{\mu\nu\lambda}(k_1,k_2) = \int d^4p \ \mathrm{Tr}\left[\gamma^\mu \frac{\not{p} + m_e}{p^2 - m_e^2}\gamma^\nu \frac{\not{p} - \not{k}_2 + m_e}{(p-k_2)^2 - m_e^2}\gamma^\lambda\gamma^5 \frac{\not{p} + \not{k}_1 + m_e}{(p+k_1)^2 - m_e^2}\right]. \tag{2.20}$$

A simple change of variables in the Z-boson amplitude (2.20),

$$\begin{aligned} k_1 &\to k, \\ k_2 &\to -q, \end{aligned} \tag{2.21}$$

leads to the loop integral in the original PNC-amplitude, eq. (2.11).

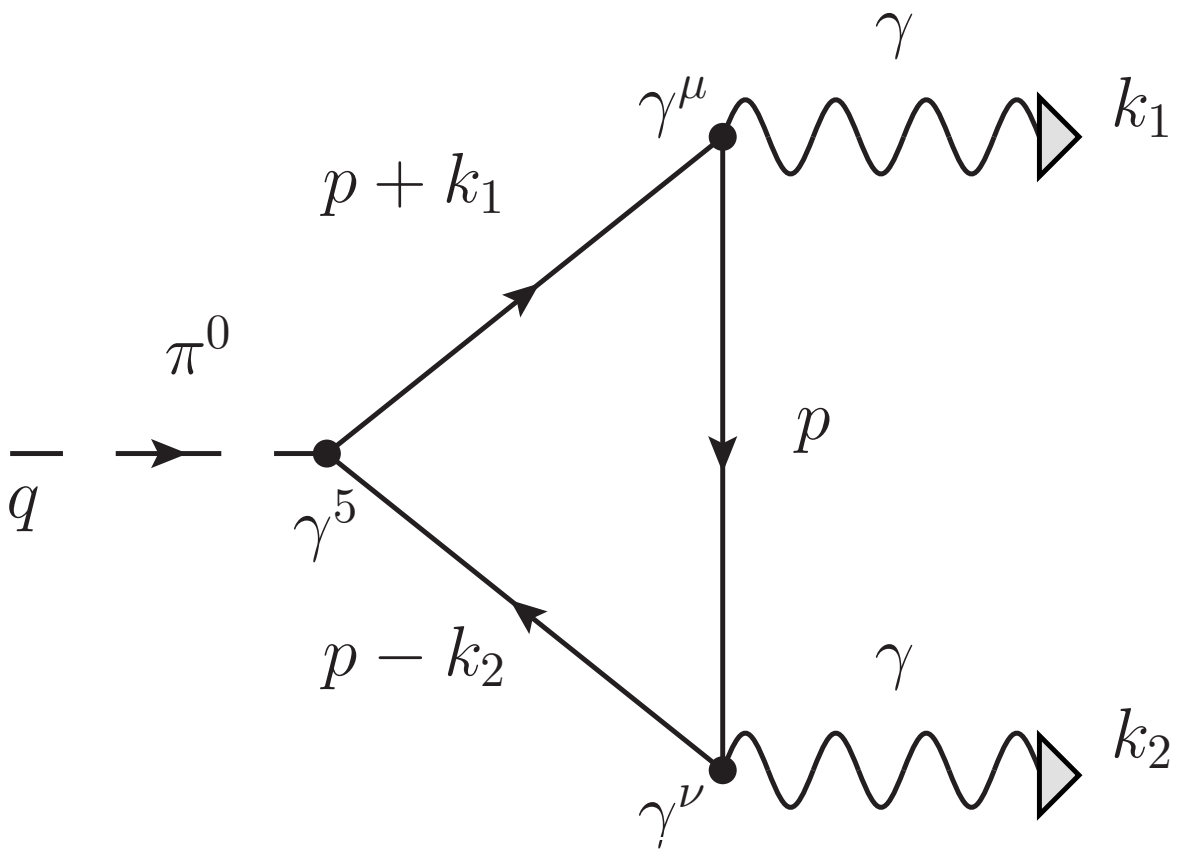

Figure 2.5: Feynman diagram of π^0-meson decay into two photons.

Here we shall note that the trace of a product of the Dirac γ^5 matrix with the four other distinct Dirac matrices leads to a non-vanishing result,

$$\mathrm{Tr}\left[\gamma^5\gamma^\tau\gamma^\mu\gamma^\nu\gamma^\lambda\right] = 4i\varepsilon_{\tau\mu\nu\lambda}, \tag{2.22}$$

where $\varepsilon_{\tau\mu\nu\lambda}$ is the unit antisymmetric fourth rank tensor defined as $\varepsilon_{0123} = -1$. All other combinations return zero result. Therefore the most general expression for the Z-

boson decay amplitude $S_{\lambda\mu\nu}(k_1, k_2)$ is

$$S_{\mu\nu\lambda}(k_1,k_2) = A_1 k_{1\tau}\varepsilon_{\tau\mu\nu\lambda} + A_2 k_{2\tau}\varepsilon_{\tau\mu\nu\lambda} + A_3 k_{1\nu}k_{1\xi}k_{2\tau}\varepsilon_{\xi\tau\mu\lambda} \quad (2.23)$$
$$+A_4 k_{2\nu}k_{1\xi}k_{2\tau}\varepsilon_{\xi\tau\mu\lambda} + A_5 k_{1\mu}k_{1\xi}k_{2\tau}\varepsilon_{\xi\tau\nu\lambda} + A_6 k_{2\mu}k_{1\xi}k_{2\tau}\varepsilon_{\xi\tau\nu\lambda}.$$

The expressions for A_i with $3 \leq i \leq 6$ represent convergent integrals and are evaluated using the standard Feynman technique. The first step is to introduce Feynman variables ξ_i which simplify the loop integral (2.20),

$$\frac{1}{\alpha_1\alpha_2\alpha_3} = 2!\int_0^1 d\xi_1 \int_0^1 d\xi_2 \int_0^1 d\xi_3 \frac{\delta(1-\xi_1-\xi_2-\xi_3)}{(\alpha_1\xi_1+\alpha_2\xi_2+\alpha_3\xi_3)^3} \quad (2.24)$$
$$\equiv 2!\int_0^1 d\xi_1 \int_0^{\xi_1} d\xi_2 \frac{1}{(\alpha_1\xi_2+\alpha_2(\xi_1-\xi_2)+\alpha_3(1-\xi_1))^3}.$$

In our specific case the variables α_i are

$$\alpha_1 = (p+k_1+k_2)^2 - m_e^2, \quad (2.25)$$

$$\alpha_2 = (p+k_2)^2 - m_e^2, \quad (2.26)$$

$$\alpha_3 = p^2 - m_e^2. \quad (2.27)$$

Therefore the loop integral becomes

$$\frac{1}{\alpha_1\alpha_2\alpha_3} \equiv \frac{1}{[(p+k_1+k_2)^2-m_e^2][(p+k_2)^2-m_e^2][p^2-m_e^2]} \\ = 2!\int_0^1 d\xi_1 \int_0^{\xi_1} d\xi_2 \frac{1}{(\alpha_1\xi_2+\alpha_2(\xi_1-\xi_2)+\alpha_3(1-\xi_1))^3}. \tag{2.28}$$

First we shall simplify the denominator in eq. (2.28) as follows:

$$[(p+k_1+k_2)^2-m_e^2]\xi_2 + [(p+k_2)^2-m_e^2](\xi_1-\xi_2) + [p^2-m_e^2](1-\xi_1) \\ = p^2 - 2p(-k_2\xi_1 - k_1\xi_2) + (-m^2 + 2k_2k_1\xi_2 + k_1^2\xi_2 + k_2^2\xi_1). \tag{2.29}$$

Further we notice a common integral

$$\int \frac{d^4p}{(p^2+l-2pk)^3} = \frac{i\pi^2}{2(l-k^2)}, \tag{2.30}$$

and the loop integral becomes

$$\int d^4p \ \frac{1}{[(p+k_1+k_2)^2-m_e^2][(p+k_2)^2-m_e^2][p^2-m_e^2]} \\ = 2!\left(\frac{i\pi^2}{2}\right)\int_0^1 d\xi_1 \int_0^{\xi_1} d\xi_2 \frac{1}{-m^2+2k_2k_1\xi_2+k_1^2\xi_2+k_2^2\xi_1-(k_2\xi_1+k_1\xi_2)^2}. \tag{2.31}$$

Finally the expression of eq. (2.31) can be simplified by the change of variable

$$\xi_1 \longrightarrow 1-\xi_1, \tag{2.32}$$

and the denominator in eq. (2.31) becomes

$$-m^2 + 2k_2k_1\xi_2 + k_1^2\xi_2 + k_2^2(1-\xi_1) - (k_2(1-\xi_1) + k_1\xi_2)^2 \qquad (2.33)$$
$$= -m^2 + k_1^2\xi_2 + k_2^2\xi_1 - (k_2\xi_1 - k_1\xi_2)^2.$$

Finally the expressions for A_i with $3 \leq i \leq 6$ will be expressed in terms of the convergent integrals

$$J_{rst}(k_1,k_2) = \frac{1}{\pi^2}\int_0^1 d\xi_1 \int_0^1 d\xi_2 \int_0^1 d\xi_3 \frac{({\xi_1}^r {\xi_1}^s {\xi_3}^t)\delta(1-\xi_1-\xi_2-\xi_3)}{(\xi_1\xi_2(k_1+k_2)^2 + \xi_1\xi_3k_1^2 + \xi_2\xi_3k_2^2 - m^2)}. \qquad (2.34)$$

In order to obtain a convergent and gauge invariant expression for the amplitude $S_{\mu\nu\lambda}$ we impose the `Ward` identities,

$$k^{1\mu}S_{\mu\nu\lambda} = 0, \qquad (2.35)$$

$$k^{2\nu}S_{\mu\nu\lambda} = 0. \qquad (2.36)$$

In terms of the general expression (2.23), eqs. (2.35) and (2.36) lead to the desirable constraints on the divergent integrals

$$[-A_2 + k_1^2A_5 + (k_1k_2)A_6]k_{1\xi}k_{2\tau}\varepsilon_{\xi\tau\nu\lambda} = 0, \qquad (2.37)$$

$$[-A_1 + k_2^2A_4 + (k_1k_2)A_3]k_{1\xi}k_{2\tau}\varepsilon_{\xi\tau\mu\lambda} = 0. \qquad (2.38)$$

In this way the amplitude $S_{\mu\nu\lambda}$ will be finite and gauge-invariant if we choose $A_2(k_1,k_2)$ and $A_1(k_1,k_2)$ in the form

$$A_2(k_1,k_2) = k_1^2 A_5 + (k_1 k_2) A_6, \tag{2.39}$$

$$A_1(k_1,k_2) = k_2^2 A_4 + (k_1 k_2) A_3. \tag{2.40}$$

Finally we come to the Z-boson amplitude $S_{\mu\nu\lambda}$,

$$\begin{aligned} S_{\mu\nu\lambda}(k_1,k_2) &= J_{110}(k_1,k_2)\varepsilon_{\mu\nu\alpha\beta}k_{1\alpha}k_{2\beta}(k_1+k_2)_\lambda \\ &+J_{101}(k_1,k_2)(\varepsilon_{\lambda\nu\alpha\beta}k_{1\alpha}k_{2\beta}k_{1\mu} + k_1^2\varepsilon_{\lambda\mu\nu\alpha}k_{2\alpha}) \\ &+J_{011}(k_1,k_2)(\varepsilon_{\lambda\mu\alpha\beta}k_{1\alpha}k_{2\beta}k_{2\nu} + k_2^2\varepsilon_{\lambda\mu\nu\alpha}k_{1\alpha}), \end{aligned} \tag{2.41}$$

with the integrals $J_{rst}(k_1,k_2)$ given by eq. (2.34).

Due to the transversality conditions for the Z-boson and *on-shell* photons expressed as

$$\begin{aligned} (k_1+k_2)_\lambda \epsilon_\lambda &= 0, \\ \epsilon_{1\mu}k_{1\mu} &= 0, \\ \epsilon_{2\nu}k_{2\nu} &= 0, \end{aligned} \tag{2.42}$$

and conditions for the real photons,

$$\begin{aligned} k_1^2 &= 0, \\ k_2^2 &= 0, \end{aligned} \tag{2.43}$$

we arrive at the result of the Landau theorem $S_{Z\gamma\gamma} = 0$. But in our case one of the photons (e.g. with index 2) is virtual, as well as the Z-boson. Therefore the initial S-matrix (2.11) returns a nonzero result.

2.6 PNC amplitude

The next step is to contract the Z-boson amplitude $S_{\mu\nu\lambda}$ with the Z-boson δ-potential, photon polarization vector, and photon propagator,

$$S_{\mu\nu\lambda}(k,q)\delta_{\lambda 0}\epsilon_{1\mu}a_{2\nu}, \tag{2.44}$$

where

$$a_{2\nu} = \frac{\gamma^0\gamma^\rho g_{\rho\nu}}{q^2} = \frac{\alpha^\rho g_{\rho\nu}}{q^2} = \frac{\alpha_\nu}{q^2}, \tag{2.45}$$

with Dirac α-matrices

$$\alpha^\mu = \gamma^0\gamma^\mu = \begin{pmatrix} 0 & \boldsymbol{\sigma} \\ \boldsymbol{\sigma} & 0 \end{pmatrix}. \tag{2.46}$$

By noticing

$$\varepsilon_{0\mu\nu\alpha} = -\varepsilon_{\mu\nu\alpha}, \tag{2.47}$$

we finally arrive at the axial anomaly amplitude,

$$S_{\mu\nu\lambda}(k,q)\delta_{\lambda 0}\epsilon_{1\mu}\frac{\alpha_\nu}{q^2} = J_{011}(k,q)[\varepsilon_{\mu\alpha\beta}k_\alpha q_\alpha \epsilon_{1\mu}(\alpha,q) + \varepsilon_{\mu\nu\alpha}\epsilon_{1\mu}k_\alpha\alpha_\nu]$$
$$= J_{011}(k,q)\left\{\frac{(\epsilon,[k\times q])(\alpha,q)}{q^2} + (\epsilon,[\alpha\times k])\right\}, \tag{2.48}$$

and S-matrix for the PNC effect is

$$S = (ie)^3 A_{\rm PNC}\delta(E_f - E_{in} - \omega_0)\sqrt{\frac{4\pi}{2\omega_0}} \tag{2.49}$$
$$\times \int \frac{d^3p_1'}{(2\pi)^3}\frac{d^3p_1}{(2\pi)^3}\,\Psi^+(p_1)J_{011}(k,q)\left[\frac{(\epsilon,[k\times q])(\alpha,q)}{q^2} + (\epsilon,[\alpha\times k])\right]\Psi(p_1').$$

Next we turn our attention to non-relativistic analysis of the S-matrix. The lower component of the Dirac electron wave function χ is expressed in terms of the upper one φ via

$$\chi = \frac{(\sigma p)}{2m}\varphi. \tag{2.50}$$

Dirac α-matrices mix these components,

$$\left(\begin{array}{cc}\varphi_1^* & \chi_1^*\end{array}\right)\left(\begin{array}{cc}0 & \boldsymbol{\sigma}\\ \boldsymbol{\sigma} & 0\end{array}\right)\left(\begin{array}{c}\varphi_1'\\ \chi_1'\end{array}\right), \tag{2.51}$$

which reduces to

$$\varphi_1^*\left[\sigma\frac{(\sigma p_1')}{2m} + \frac{(\sigma p_1)}{2m}\sigma\right]\varphi_1'. \tag{2.52}$$

The first term in square brackets in eq. (2.49) can be simplified to

$$\frac{(q,[\epsilon\times k])(\sigma,q)}{q^2}(\sigma p_1')+(\sigma p_1)\frac{(q,[\epsilon\times k])(\sigma,q)}{q^2}, \tag{2.53}$$

while the second term reduces to

$$(\sigma,[k\times\epsilon])(\sigma p_1')+(\sigma p_1)(\sigma,[k\times\epsilon]). \tag{2.54}$$

Further we employ the well-known identity for the Pauli matrices,

$$(\sigma a)(\sigma b)=(ab)+i(\sigma,[a\times b]), \tag{2.55}$$

and owing to the transferred momentum is $q=p_1-p_1'$, eq. (2.53) becomes

$$\frac{(q,[\epsilon\times k])(\sigma,q)}{q^2}(\sigma p_1')+(\sigma p_1)\frac{(q,[\epsilon\times k])(\sigma,q)}{q^2}=(q,p_1+p_1')\frac{(q,[\epsilon\times k])}{q^2}. \tag{2.56}$$

In order to simplify eq. (2.54) we use the identities

$$(\sigma,[k\times\epsilon])(\sigma p_1')=([k\times\epsilon],p_1')+i(\sigma,[[k\times\epsilon]\times p_1']]), \tag{2.57}$$

$$(\sigma p_1)(\sigma,[k\times\epsilon])=(p_1,[k\times\epsilon])+i(\sigma,[p_1\times[k\times\epsilon]]). \tag{2.58}$$

Therefore the sum of these terms is

$$
\begin{aligned}
&(\sigma,[k\times\epsilon])(\sigma p_1')+(\sigma p_1)(\sigma,[k\times\epsilon]) \\
&=(p_1+p_1',[k\times\epsilon])+i(\sigma,[q\times[k\times\epsilon]]) \\
&=(p_1+p_1',[k\times\epsilon])+i(\sigma k)(q\epsilon)-i(\sigma\epsilon)(qk),
\end{aligned}
\tag{2.59}
$$

which represents the final expression for eq. (2.54). For the sake of convenience we introduce

$$
P=p_1+p_1', \tag{2.60}
$$

and then the square brackets of the S-matrix in eq. (2.49) will be represented as

$$
(q,P)\frac{(q,[\epsilon\times k])}{q^2}+(P,[k\times\epsilon])+i(\sigma k)(q\epsilon)-i(\sigma\epsilon)(qk). \tag{2.61}
$$

Now we have to explore how the obtained expression changes under change of integration variables

$$
\begin{aligned}
p_1 &\longrightarrow -p_1, \\
p_1' &\longrightarrow -p_1'.
\end{aligned}
\tag{2.62}
$$

The expression in eq. (2.59) changes sign and therefore we shall turn our attention to the integral (2.34) which simplifies in the case for a real emitted photon $k_1^2=0$,

$$
I(k,q)=\frac{1}{\pi^2}\int_0^1 d\xi_1\int_0^{1-\xi_1}d\xi_2\frac{\xi_1(\xi_1+\xi_2-1)}{-m^2+2\xi_1\xi_2(kq)+\xi_1(1-\xi_1)q^2}, \tag{2.63}
$$

and in the non-relativistic limit we obtain

$$\frac{1}{m^2 - 2\xi_1\xi_2(kq)} = \frac{1}{m^2}\left[1 + \frac{2\xi_1\xi_2(kq)}{m^2} + O\left(\frac{1}{m^4}\right)\right]. \tag{2.64}$$

Finally, we have the expression which is even under the inversion (2.62),

$$(q,P)\frac{(q,[\epsilon\times k])}{q^2}(qk) + (P,[k\times\epsilon])(qk) + i(\sigma k)(q\epsilon)(qk) - i(\sigma\epsilon)(qk)^2. \tag{2.65}$$

After integration over $\left(p_1, p_1'\right)$ or similarly over (P,q), the first two terms in eq. (2.65) vanish because of the contraction with the external vectors ϵ_μ and k_μ. The third term in eq. (2.65) will disappear in the final expression due to the Wigner-Eckart theorem as we show later.

The only nonvanishing term in eq. (2.65) that contributes to the probability of the PNC effect is

$$-i(\sigma\epsilon)(qk)^2, \tag{2.66}$$

and therefore the S-matrix in the nonrelativistic limit is

$$\begin{aligned} S &= (ie)^3 A_{\rm PNC}\delta(E_f - E_{in} - \omega_0)\sqrt{\frac{4\pi}{2\omega_0}} \\ &\times \int \frac{d^3p_1'}{(2\pi)^3}\frac{d^3p_1}{(2\pi)^3}\frac{I}{m^5}\,\Psi^+(p_1)[-i(\sigma\epsilon)(qk)^2]\Psi(p_1'), \end{aligned} \tag{2.67}$$

where

$$I = -\frac{1}{\pi^2}\int_0^1 d\xi_1 \int_0^{1-\xi_1} d\xi_2(\xi_1^2\xi_2)(\xi_1+\xi_2-1) = \frac{1}{360\pi^2}. \tag{2.68}$$

After performing the Fourier transformation,

$$\int \frac{d^3p_1'}{(2\pi)^3}\frac{d^3p_1}{(2\pi)^3}\,\varphi^*_{6s}(p_1)[(qk)^2]\varphi_{7s}(p_1') \tag{2.69}$$
$$= m^6\varphi^*_{6s}(0)[-(k\nabla)^2]\varphi_{7s}(0) = -m^6\varphi^*_{6s}(0)k^2\,\frac{d^2\varphi_{7s}(r)}{dr^2}\bigg|_{r=0}$$

For brevity we will write

$$\frac{d^2\varphi(r)}{dr^2}\bigg|_{r=0} \equiv \varphi''(0), \tag{2.70}$$

and the S-matrix takes the form

$$S = e^3 m A_{\rm PNC}\delta(E_f - E_{in} - \omega_0)\sqrt{\frac{4\pi}{2\omega_0}}\left(\frac{1}{360\pi^2}\right)\,(\sigma\epsilon)k^2\varphi^*_{6s}(0)\varphi''_{7s}(0) \tag{2.71}$$
$$= -e^3\frac{(G_F m_p^2)Q_W}{2\sqrt{2}}\delta(E_f - E_{in} - \omega_0)\left(\frac{m_e}{m_p}\right)^2\frac{\sqrt{2\pi}}{360\pi^2}\frac{\omega_0^{3/2}}{m_e}(\sigma\epsilon)\varphi^*_{6s}(0)\varphi''_{7s}(0),$$

and, owing to the standard correspondence between the S-matrix and amplitude of the process $\widehat{F}_{\rm PNC}$,

$$S = -2\pi i\widehat{F}_{\rm PNC}\delta(E_{n's} - E_{ns} - \omega_0), \tag{2.72}$$

we obtain for the parity-nonconserving amplitude,

$$\widehat{F}_{\rm PNC} = \frac{e^3}{2\pi i}\frac{(G_F m_p^2)Q_W}{2\sqrt{2}}\left(\frac{m_e}{m_p}\right)^2\frac{\sqrt{2\pi}}{360\pi^2}\frac{\omega_0^{3/2}}{m_e}(\sigma\epsilon)\varphi^*_{6s}(0)\varphi''_{7s}(0). \tag{2.73}$$

For the Feynman diagrams a and c, Fig. 2.2, we have

$$\widehat{F}_{7s\to 6s} = \widehat{F}_{\rm M1} + \widehat{F}_{\rm PNC}, \tag{2.74}$$

and the corresponding expression for the probability of the process, after averaging over the initial electron spin projections and summing over the final spin projections,

$$W_{7s\to 6s} = W_{\rm M1} + \frac{1}{2j_0+1}\sum_{m_0 m_1} 2{\rm Re}\left[F_{\rm M1}F_{\rm PNC}\right] + O\left(F^2_{\rm PNC}\right), \qquad (2.75)$$

where the matrix element for $F_{\rm PNC}$ is

$$F_{\rm PNC} = \frac{e^3}{2\pi i}\frac{(G_F m_p^2)Q_W}{2\sqrt{2}}\left(\frac{m_e}{m_p}\right)^2 \frac{\sqrt{2\pi}}{360\pi^2}\frac{\omega_0^{3/2}}{m_e}\varphi^*_{6s}(0)\varphi''_{7s}(0) \qquad (2.76)$$
$$\times\langle n_1 j_1 l_1 m_1 s_1|(\sigma\epsilon)|n_0 j_0 l_0 m_0 s_0\rangle.$$

In the specific case of the cesium transition we have

$$\langle n_1 j_1 l_1 m_1 s_1| = \langle 6s_{1/2}|, \qquad (2.77)$$
$$|n_0 j_0 l_0 m_0 s_0\rangle = |7s_{1/2}\rangle.$$

Following Landau [20] we estimate the electron wavefunction (in atomic units) in the region $r \sim 1/Z$ (see *Appendix A*) as

$$\varphi(r) \sim Z^{1/2}, \qquad (2.78)$$
$$\varphi''(r) \sim Z^{5/2}.$$

Therefore the expression (2.76) becomes

$$F_{\rm PNC} = \frac{e^3}{2\pi i}\frac{(G_F m_p^2)Q_W}{2\sqrt{2}}\left(\frac{m_e}{m_p}\right)^2 \frac{\sqrt{2\pi}}{360\pi^2}\frac{\omega_0^{3/2}}{m_e} Z^3 \langle n_1 j_1 l_1 m_1 s 1_1|(\sigma\epsilon)|n_0 j_0 l_0 m_0 s_0\rangle. \tag{2.79}$$

The matrix element in eq. (2.79) is evaluated by means of the `Wigner-Eckart` theorem,

$$\langle n' j' l' m'|A_{JLM}|njlm\rangle = (-1)^{j'-m'}\begin{pmatrix} j' & J & j \\ -m' & M & m \end{pmatrix}\langle n' j' l'||A_{JL}||njl\rangle. \tag{2.80}$$

In the following we shall evaluate the product of two matrix elements,

$$\sum_{m_0 m_1}\left(\langle n_1 j_1 l_1 m_1|\sum_q (-1)^q \mu_q [\epsilon\times k]_{-q}|n_0 j_0 l_0 m_0\rangle^* \right. \tag{2.81}$$
$$\left. \times \langle n_1 j_1 l_1 m_1|\sum_{q'}(-1)^{q'}\sigma_{q'}\epsilon_{-q'}|n_0 j_0 l_0 m_0\rangle\right),$$

where $\widehat{\mu} = \mu_0 \widehat{s}$ is the magnetic moment of electron. Owing to the orthogonality relation between $3j$-symbols,

$$(2j+1)\sum_{m_1 m_2}\begin{pmatrix} j_1 & j_2 & j \\ m_1 & m_2 & m \end{pmatrix}\begin{pmatrix} j_1 & j_2 & j' \\ m_1 & m_2 & m' \end{pmatrix} = \delta_{jj'}\delta_{mm'}, \tag{2.82}$$

we can perform the summation over the spin projections and obtain the mixed product

$$i\sum_q (-1)^q \epsilon_q [\epsilon^*\times k]_{-q} = i(\epsilon,[\epsilon^*\times k]) = i(k,[\epsilon\times\epsilon^*]) \equiv (k s_{ph}), \tag{2.83}$$

where we have introduced a photon spin variable in terms of the vector product of the photon

polarization vectors,

$$s_{ph} = i[\epsilon \times \epsilon^*]. \tag{2.84}$$

Now we return to eq. (2.65), where we disregarded the term (σk) which corresponds to

$$\sum_{m_0 m_1} \left(\langle n_1 j_1 l_1 m_1 | \sum_q (-1)^q \mu_q [\epsilon \times k]_{-q} | n_0 j_0 l_0 m_0 \rangle^* \right. \tag{2.85}$$
$$\left. \times \langle n_1 j_1 l_1 m_1 | \sum_{q'} (-1)^{q'} \sigma_{q'} k_{-q'} | n_0 j_0 l_0 m_0 \rangle \right).$$

The orthogonality relation between $3j$-symbols leads to

$$i \sum_q (-1)^q k_q [\epsilon \times k]_{-q} = i(k, [\epsilon \times k]) = 0, \tag{2.86}$$

and therefore this term does not contribute to the probability of the PNC process.

The expression (2.81) simplifies to a product of the reduced matrix elements,

$$(k s_{ph}) \langle n_1 j_1 l_1 || \mu || n_0 j_0 l_0 \rangle \langle n_1 j_1 l_1 || \sigma || n_0 j_0 l_0 \rangle. \tag{2.87}$$

Rewriting in terms of the spin operator $\widehat{s}$,

$$\widehat{\mu} = \mu_0 \widehat{s}, \tag{2.88}$$
$$\widehat{\sigma} = 2\widehat{s},$$

and owing to the reduced matrix elements of the spin operator,

$$\langle s_1||\widehat{s}||s_0\rangle = \delta_{s_0 s_1}\sqrt{s_0(s_0+1)(2s_0+1)}, \tag{2.89}$$

we get the final expression for eq. (2.81) for $s_0 = 1/2$

$$\mu_0(k s_{ph}). \tag{2.90}$$

Introducing the probability of the process on Fig. 2.2 (a),

$$W_{M1} = \frac{4}{3}\omega_0^3\mu_0^2, \tag{2.91}$$

we get the final answer in the form

$$W_{7s\to 6s} = W_{M1}(1 + R(\vec{\nu}\cdot\vec{s}_{ph})), \tag{2.92}$$

where $\nu = \vec{k}/|\vec{k}|$ is the unit vector in the direction of the emitted photon momentum. In our case R is equal to the ratio $F_{\rm PNC}/F_{M1}$, where the amplitudes are expressed via the angular reduced matrix elements.

Using the estimate $\varphi(0)\varphi''(0) \sim \alpha^5 Z^3$ for neutral atoms [20], we get for the anomaly contribution to the PNC-amplitudes on Fig. 2.2 (c)

$$F_{\rm PNC} \sim \frac{1}{360\pi^2}\left(\frac{m_e}{m_p}\right)^2 \alpha^{3/2}(G_F m_p^2) Q_W \alpha^5 Z^3. \tag{2.93}$$

Using a well-known estimate for the PNC-amplitude [15], Fig. 2.2 (b), in neutral atoms

without the contribution from the axial anomaly

$$F^0_{\rm PNC} \sim \left(\frac{m_e}{m_p}\right)^2 \alpha^{3/2} Z^2 (G_F m_p^2) Q_W, \tag{2.94}$$

we get for the relative axial anomaly contribution (2.93) in terms of $F^0_{\rm PNC}$,

$$\frac{F_{\rm PNC}}{F^0_{\rm PNC}} \sim (10)^{-3} \alpha^5 Z. \tag{2.95}$$

We should admit that contribution of the axial anomaly to the PNC effects in neutral atoms is small for an observation in real experiments but the nonzero result is important from the theoretical point of view for understanding the axial anomaly mechanism.

Chapter 3

Quantum Optics

In this chapter we introduce a new method that allows one to obtain in a closed form an analytical cross section for the laser-assisted electron-ion interaction. As an example we perform a calculation for the hydrogen laser-assisted recombination.

The results of this chapter are based on our paper,
GS and A. Volberg, J. Phys. A: Math. Theor. **44**, 245301 (2011).

3.1 Introduction

Electron scattering processes in the presence of a laser field play a significant role in the contemporary atomic physics [21]. A simple but sufficiently accurate theoretical model for laser-assisted atomic scattering would be helpful for many experimental studies. The standard theoretical approach for laser-assisted electron-ion collisions requires the construction of the S-matrix for the corresponding process. The electron wave function in a combined Coulomb-laser field is given by the well known Coulomb–Volkov solution. The dressed state of the atom is described by the time-dependent perturbation series.

In our work we have developed a new method that allows one to derive in a closed form an analytical expression for the cross section of a laser-assisted atomic scattering. The new mathematical step is in using the Bessel generating function as an argument for

the Plancherel theorem. This allows one to perform the summation over the number of field harmonics so that the analytical expression for the cross section of the process can be explicitly written. As an example, we perform a calculation for the laser-assisted hydrogen recombination.

3.2 Laser-assisted hydrogen recombination

The proposed method will be illustrated on a typical example of the laser-assisted hydrogen recombination process,

$$p + e + L\hbar\omega_0 \longrightarrow H + \hbar\omega. \tag{3.1}$$

The additional term $L\hbar\omega_0$, where L is the number of exchanged laser quanta, indicates the presence of a laser field,

$$\vec{\varepsilon} = \vec{\varepsilon}_0 \sin\omega_0 t, \tag{3.2}$$

and points out the conservation of quasienergy. Here $\vec{\varepsilon}_0$ is the amplitude of the field and ω_0 is the field frequency.

The differential cross section of the reaction for the standard field-free hydrogen recombination process is known [20] due to the detailed balance between the differential cross section of photo-recombination, $d\sigma_{fi}/d\Omega_f$, and that of photo-ionization, $d\sigma_{if}/d\Omega_i$,

$$\frac{d\sigma_{fi}}{d\Omega_f} = \frac{k^2}{q^2}\frac{d\sigma_{if}}{d\Omega_i}, \tag{3.3}$$

where k and q are the momenta of the outgoing photon and electron, respectively.

The differential photo-ionization cross section $d\sigma_{if}/d\Omega_i$ is given by [18, 30]

$$\frac{d\sigma_{if}}{d\Omega_i} = 2^7 \frac{\pi e^2}{\hbar c} \left(\frac{\hbar^2}{mZe^2}\right)^2 \left(\frac{W_0}{\hbar\omega}\right)^4 \frac{e^{-4\xi \mathrm{arccot}\xi}}{1-e^{-2\pi\xi}} (1-\cos^2\theta), \tag{3.4}$$

where W_0 is the ionization potential of the hydrogen atom from the continuum threshold to the ground state. Here ω is the frequency of the photon emitted at an angle θ relative to the incoming electron, and m and e are the mass and electric charge of the electron. The dimensionless parameter ξ is defined as

$$\xi = \frac{Z\hbar}{a_0 q} = \frac{\eta}{q}, \tag{3.5}$$

where Z is the nuclear charge ($Z = 1$), a_0 is the Bohr radius, and $\eta = Z\hbar/a_0$.

3.3 S-matrix

The S-matrix describing the photo-recombination process (3.1) in the presence of the laser field (3.2) is given by [18, 28, 29]

$$S = -ie \int dt \langle \Psi_0^H(\vec{r},t) | (\vec{\epsilon}\cdot\nabla) e^{-i(\vec{k}\cdot\vec{r}/\hbar - \omega t)} | \chi^e(\vec{r},t) \rangle, \tag{3.6}$$

where $\chi^e(\vec{r},t)$ is the Coulomb-Volkov wave function of the electron in the field of the proton and external laser field, $\vec{\epsilon}, \vec{k}$ and ω are the polarization vector, momentum and frequency of the emitted photon, respectively, and $\Psi_0^H(\vec{r},t)$ is the electron wave function in the hydrogen atom in $1s$ state in the laser field $\vec{\varepsilon}$, eq. (3.2).

Using the standard technique of transformation to the rotating frame we can obtain the

electron wave function in the total Coulomb-laser field [31]

$$\chi^e(\vec{r},t) = e^{\frac{\pi\xi}{2}}\Gamma(1-i\xi)F(i\xi,1;i(qr-\vec{q}\cdot\vec{r})/\hbar) \tag{3.7}$$
$$\times \exp\left[-\frac{ie}{\hbar mc}\int_0^t \vec{q}\cdot\vec{A}(\tau)d\tau - \frac{ie^2}{2\hbar mc^2}\int_0^t A^2 d\tau + \frac{i\vec{q}\cdot\vec{r}}{\hbar} - \frac{iE_i t}{\hbar}\right],$$

where $\vec{q}$ is the asymptotic value of the incoming electron momentum, $q = |\vec{q}|$, $r = |\vec{r}|$, $F(a,b;x)$ is the confluent hypergeometric function, E_i is the initial kinetic energy of the incoming electron, and c is the speed of light.

In the harmonic laser field (3.2) the vector-potential $\vec{A}$ is defined as

$$\vec{A}(t) = \frac{c\vec{\varepsilon}_0}{\omega_0}\cos\omega_0 t \equiv \vec{A}_0\cos\omega_0 t. \tag{3.8}$$

The quadratic term in the square brackets (3.7), $(ie^2/2\hbar mc^2)\int_0^t A^2 d\tau = O\left(1/c^2\right)$, will be neglected [31]. Evaluation of the remaining integral over τ in (3.7) yields

$$\chi^e(\vec{r},t) = \Gamma(1-i\xi)F(i\xi,1;i(qr-\vec{q}\cdot\vec{r})/\hbar) \tag{3.9}$$
$$\times \exp i\left[\frac{\vec{q}\cdot\vec{r}}{\hbar} + z\sin\omega_0 t - \frac{E_i t}{\hbar} - \frac{i\pi\xi}{2}\right],$$

where the atomic parameter ξ was defined in eq. (3.5), and the field parameter z is given by

$$z = \frac{e}{m\hbar}\frac{(\vec{q}\cdot\vec{\varepsilon}_0)}{\omega_0^2}, \tag{3.10}$$

The exact solution for the electron wave function in the discrete spectrum of a combined Coulomb-laser field is known. However, in our calculation we will assume that laser field introduces only a small perturbation for the ground state of electron in hydrogen. Therefore

we can use first-order perturbation theory for deriving the hydrogen wave function in the presence of the laser field [20, 28, 29],

$$\Psi_n^H(\vec{r},t) = e^{-iW_nt/\hbar} \times \left\{ \psi_n(\vec{r}) - \frac{1}{2}\sum_{m\neq n}\left(\frac{e^{i\omega_0 t/\hbar}}{\omega_{mn}+\omega_0} + \frac{e^{-i\omega_0 t/\hbar}}{\omega_{mn}-\omega_0}\right)\langle m|\frac{e\vec{A}_0\cdot\vec{p}}{\hbar mc\omega_0}|n\rangle\psi_m(\vec{r})\right\}, \tag{3.11}$$

where $\psi_m(\vec{r})$ is the wave function for the atomic electron in the field-free state $|m\rangle$ with energy W_m, and $\omega_{mn} = (W_m - W_n)/\hbar$. The summation in (3.11) is extended over the full set of atomic electron states in the absence of the laser field. In the derivation of (3.11) it was assumed that none of the denominators were close to zero [20].

For the optical frequency of the laser we have $\omega_0 \ll \omega_{n0}$ and therefore we get the following expression for $\Psi_0^H(\vec{r},t)$, which holds true even over a broader frequency range [28],

$$\Psi_0^H(\vec{r},t) = e^{-iW_0t/\hbar}\left(1 + \frac{ie(\vec{\varepsilon}_0\cdot\vec{r})}{\hbar\omega_0}\cos\omega_0 t\right)\psi_0^H(\vec{r}), \tag{3.12}$$

where

$$\psi_0^H(\vec{r}) = \sqrt{\frac{Z^3}{\pi a_0^3}}e^{-\eta r/\hbar} \equiv C_0 e^{-\eta r/\hbar}. \tag{3.13}$$

3.4 The Coulomb-Volkov wave function

In order to perform the time integration in the S-matrix (3.6) we decompose the electron wave function $\chi^e(\vec{r},t)$ given by (3.9) over the Bessel functions $J_L(z)$ of integer order L and argument z given by (3.10). For this purpose we introduce the Bessel generating function

$$\exp\left[iz\sin u\right] = \sum_{L=-\infty}^{L=+\infty} J_L(z)\exp(iLu). \tag{3.14}$$

To simplify the S-matrix (3.6) we use the recurrence relation for the Bessel functions

$$J_{L+1}(z) + J_{L-1}(z) = \frac{2L}{z}J_L(z). \tag{3.15}$$

Performing the time integration in eq. (3.6) and applying the Gauss theorem we obtain the following expression for the S-matrix in the dipole approximation, $(\vec{k}\cdot\vec{r})/\hbar \ll 1$,

$$S = -2\pi i \sum_{L=-\infty}^{L=+\infty} f_L \delta(W_0 + \hbar\omega - E_i + L\hbar\omega_0), \tag{3.16}$$

where

$$f_L = e^{\frac{\pi\xi}{2}}\Gamma(1-i\xi)C_0\left[J_L(z)\omega(L)\left(I_1 + \frac{L}{z}I_2\right)\right]. \tag{3.17}$$

Here we have introduced the following notations:

$$I_1 = \eta\hbar\int d\vec{r}\psi_0^H(\vec{r})\frac{(\vec{\epsilon}\cdot\vec{r})}{r}\chi^e(\vec{r}), \tag{3.18}$$

$$I_2 = \frac{ie}{\omega_0}\int d\vec{r}\psi_0^H(\vec{r})\left(-(\vec{\varepsilon}_0\cdot\vec{\epsilon}) + \frac{\eta}{\hbar}\frac{(\vec{\varepsilon}_0\cdot\vec{r})(\vec{\epsilon}\cdot\vec{r})}{r}\right)\chi^e(\vec{r}), \tag{3.19}$$

and

$$\hbar\omega(L) = E_i - W_0 - L\hbar\omega_0 \equiv E_{i0} - L\hbar\omega_0. \tag{3.20}$$

Exploiting the integral involving the confluent hypergeometric function [18, 32],

$$\int d\vec{r} e^{i(\vec{q}-\vec{p})\cdot\vec{r}/\hbar - \eta r/\hbar} \frac{F(i\xi, 1, i(qr - \vec{q}\cdot\vec{r}))}{r} = 4\pi\hbar^2 \frac{[\vec{p}^2 + (\eta - iq)^2]^{-i\xi}}{[(\vec{q}-\vec{p})^2 + \eta^2]^{1-i\xi}}, \tag{3.21}$$

we obtain the following expression for the integral I_1, eq. (3.18),

$$I_1 = 8\pi i\hbar^4 (\vec{\epsilon}\cdot\vec{e}_q) \frac{\xi(1-i\xi)}{q^2(1+\xi^2)^2} e^{-2\xi \mathrm{arccot}\xi}, \tag{3.22}$$

and the corresponding expression for the integral I_2, eq. (3.19),

$$I_2 = -8\pi i\hbar^4 \frac{\xi e}{\omega_0} \frac{e^{-2(1+\xi)\mathrm{arccot}\xi}}{q^3(1+\xi^2)^2} \left((\vec{\varepsilon}_0\cdot\vec{\epsilon}) - 2(\vec{\epsilon}\cdot\vec{e}_q)(\vec{\varepsilon}_0\cdot\vec{e}_q) \frac{(2-i\xi)}{(1-i\xi)} \right), \tag{3.23}$$

where $\vec{e}_q \equiv \vec{q}/q$ is a unit vector along the electron momentum.

3.5 The partial cross section

The partial cross section of the reaction (3.1) with fixed L is given by

$$d\sigma_L = 2\pi \frac{e^2}{2q\omega(L)} |f_L|^2 \delta(W_0 + \hbar\omega - E_i + L\hbar\omega_0) \frac{d^3k}{(2\pi)^3}. \tag{3.24}$$

The integration over ω yields

$$\frac{d\sigma_L}{d\Omega} = \frac{e^2 C_0^2}{8\pi^2 q(1-e^{-2\pi\xi})} \left(E_i - W_0 - L\hbar\omega_0\right)^3 \times |J_L(z)|^2 \left(|I_1|^2 + \frac{2L}{z}\mathrm{Re}(I_1 I_2) + \frac{L^2}{z^2}|I_2|^2\right). \tag{3.25}$$

The conservation of quasi-energy uniquely specifies the frequency of the emitted photon, eq. (3.20), in terms of the number of exchanged laser quanta L. In order to obtain the total cross section of the reaction (3.1) in the laser field (3.2) we must count all possibilities for the number of exchanged laser quanta. In other words, we have to perform the summation over all possible L,

$$\frac{d\sigma}{d\Omega} = \sum_{L=-\infty}^{L=+\infty} \frac{d\sigma_L}{d\Omega}. \tag{3.26}$$

3.6 The summation procedure and cross section

We introduce a new step that allows one to analytically sum up the infinite series (3.26). The summation over L in (3.26) is performed with the aid of the Plancherel theorem [33],

$$\frac{1}{2\pi}\int_0^{2\pi} |f(x)|^2 dx = \sum_{n=-\infty}^{n=+\infty} |c_n|^2, \tag{3.27}$$

where c_n are the Fourier coefficients of the function $f(x)$,

$$c_n = \frac{1}{2\pi}\int_0^{2\pi} f(x) e^{i\pi n x} dx. \tag{3.28}$$

The application of the Plancherel theorem to the Bessel generating function (3.14) leads to the following equalities [34] :

$$\sum_{L=-\infty}^{L=+\infty} J_L^2(z) = 1, \tag{3.29}$$

$$\sum_{L=-\infty}^{L=+\infty} L^2 J_L^2(z) = \frac{z^2}{2}, \tag{3.30}$$

$$\sum_{L=-\infty}^{L=+\infty} L^{2n-1} J_L^2(z) = 0, n \in Z_+ \tag{3.31}$$

$$\sum_{L=-\infty}^{L=+\infty} L^4 J_L^2(z) = \frac{z^2(4+3z^2)}{8}. \tag{3.32}$$

Performing the summation over the photon polarizations we obtain the closed analytical expression for the cross section of the process (3.1)

$$\begin{aligned} &\frac{d\sigma}{d\Omega} = \frac{e^2 C_0^2 E_{i0}^3}{8\pi^2 q(1-e^{-2\pi\xi})}\left[|I_1|^2 + F\right], \\ &F = \frac{|I_2|^2}{2} + \frac{3\hbar\omega_0 z^2}{2E_{i0}^2}\left(\frac{2E_{i0}}{z}\mathrm{Re}(I_1 I_2) + \hbar\omega_0 |I_1|^2\right) \\ &+\frac{\hbar^2\omega_0^2 z^2(4+3z^2)}{8E_{i0}^3}\left(\frac{3E_{i0}}{z^2}|I_2|^2 + \frac{2\hbar\omega_0}{z}\mathrm{Re}(I_1 I_2)\right). \end{aligned} \tag{3.33}$$

In the zero-field limit, corresponding to $z \equiv 0$ and $I_2 \equiv 0$, the correction term F in (3.33), that is responsible for the laser-modified cross section, identically vanishes. To the best of our knowledge, such a closed expression for the laser-assisted hydrogen recombination was not given in the literature.

An explicit summation over the photon polarizations is performed as

$$\sum_{\lambda} \epsilon_{\mu}^{\lambda *} \epsilon_{\nu}^{\lambda} = \delta_{\mu\nu}, \tag{3.34}$$
$$\sum_{\lambda} (\vec{a} \cdot \vec{\epsilon}^{\lambda})^2 = a^2 (1 - \cos^2 \vartheta),$$

where ϑ is the angle between the vector $\vec{a}$, and the momentum of the outgoing photon $\vec{k}$.

The corresponding expressions for the integrals in eqs. (3.22) and (3.23) with an explicit summation over the photon polarizations are given by

$$\sum_{\lambda} |I_1|^2 = 2^6 \pi^2 \hbar^8 \frac{\xi^2 e^{-4\xi \mathrm{arccot}\xi}}{q^4 (1+\xi^2)^3} (1 - \cos^2 \theta), \tag{3.35}$$

$$\sum_{\lambda} |I_2|^2 = 2^6 \pi^2 \hbar^8 \frac{e^2 \xi^2}{\omega_0^2} \frac{e^{-4(1+\xi)\mathrm{arccot}\xi}}{q^6 (1+\xi^2)^5} \tag{3.36}$$
$$\times \left[\varepsilon_0^2 (1 - \cos^2 \phi)(1+\xi^2) - 4(\vec{\varepsilon}_0 \cdot \vec{e}_q)^2 (2+\xi^2) + 4(\vec{\varepsilon}_0 \cdot \vec{e}_q)^2 (4+\xi^2)(1 - \cos^2 \theta) \right],$$

and for the interference term we find

$$\sum_{\lambda} \mathrm{Re}(I_1 I_2) = 2^6 \pi^2 \hbar^8 \frac{e \xi^2}{\omega_0} \frac{e^{-2(1+2\xi)\mathrm{arccot}\xi}}{q^5 (1+\xi^2)^4} (\vec{\varepsilon}_0 \cdot \vec{e}_q)(4 \cos^2 \theta - 3), \tag{3.37}$$

where θ is the angle between the momentum of the incoming electron $\vec{q}$ and the momentum of the outgoing photon $\vec{k}$. The angle ϕ is formed by vectors $\vec{\varepsilon}_0$ and $\vec{k}$.

3.7 The soft photon approximation

The cross section given by eq. (3.33) is an exact result for the laser-assisted hydrogen recombination process under the used approximations for the electron and hydrogen laser-modified wave functions. To clarify the meaning of the obtained result we shall introduce a soft photon approximation. This allows one to reveal the meaning of each term in the expression for the cross section of the process given by (3.33). With this approximation the frequency of the emitted photon is independent of the number of the field harmonics L,

$$\hbar\omega = E_i - W_0 - L\hbar\omega_0 \simeq E_i - W_0. \tag{3.38}$$

In this approximation the partial "soft photon" cross section is given by

$$\frac{d\sigma_L^s}{d\Omega} = \frac{e^2 C_0^2}{8\pi^2 q(1-e^{-2\pi\xi})} \left(E_i - W_0\right)^3 \left|J_L(z)\right|^2 \left(|I_1|^2 + \frac{2L}{z}\mathrm{Re}(I_1 I_2) + \frac{L^2}{z^2}|I_2|^2\right). \tag{3.39}$$

Performing the summation (3.26) over L by means of the equalities (3.29)-(3.31) we obtain the following simple result:

$$\frac{d\sigma^s}{d\Omega} = \frac{e^2 C_0^2}{8\pi^2 q(1-e^{-2\pi\xi})} E_{i0}^3 \left(|I_1|^2 + \frac{|I_2|^2}{2}\right). \tag{3.40}$$

Here the first term $|I_1|^2$ corresponds to the standard laser-free recombination process whereas the second term $|I_2|^2$ is responsible for the field-modified electron (3.9) and

hydrogen (3.12) states. In the zero-field limit $I_2 \equiv 0$ and (3.40) recovers the standard field-free recombination cross section. We have to note that within the limits of the present approximation (3.38) the interference terms $\mathrm{Re}(I_1 I_2)$ are absent. In this and only this particular case does the square of the S-matrix (3.16) equal the sum of the squares of its terms.

3.8 Summary

In this chapter we have developed a new method that allows one to obtain an analytical cross section for the laser-assisted electron-ion collision. The standard S-matrix formalism is used for describing the atomic collision process. The S-matrix is constructed from the electron Coulomb-Volkov wave function in the combined Coulomb-laser field, and the hydrogen laser-perturbed state. By the aid of the Bessel generating function, the S-matrix is decomposed into an infinite series of the field harmonics.

We have introduced a new step to obtain the analytical expression for the cross section of the process. The main theoretical novelty is the application of the Plancherel theorem to the Bessel generating function. This allows one to obtain analytically the cross section of the laser-assisted hydrogen photo-recombination process. This process has been chosen in order to verify the proposed method. The field-enhancement coefficient is evaluated in an analytical way and the final expression for a laser-assisted hydrogen recombination process is presented by the sum of the field-free hydrogen cross section and the laser-assisted addition.

The developed method will allow one to reconsider a wide range of problems related to electron-ion collisions in an external field with the goal of obtaining analytical expressions for the cross sections of the corresponding scattering processes. The time-dependent problem

generated by the infinite series of the Coulomb-Volkov wave function is exactly separated from the spatial dependence and thus can be analytically solved by the proposed method.

Chapter 4

Nuclear Physics

In this chapter we present our results for the resonance width distribution in open quantum systems. Recent measurements of resonance widths for low-energy neutron scattering off heavy nuclei claim large deviations from the routinely used chi square, or the Porter-Thomas distribution. We propose a new "standard" width distribution based on the random matrix theory for a chaotic quantum system with a single open decay channel. Two methods of derivation lead to a single analytical expression that recovers, in the limit of very weak continuum coupling, the Porter-Thomas distribution for small widths of experimental interest. The parameter defining the result is the ratio of typical widths Γ to the energy level spacing D. Compared to the Porter-Thomas distribution, the new distribution suppresses small widths and increases the probabilities of larger widths. In the case of a neutron scattering with open multiple photon channels we derive the resonance width distribution which happens to be shifted compared to the Porter-Thomas distribution by an average photon width. The experimental data are very sensitive to a shift of the distribution and therefore the obtained results might be useful in comparison random matrix theory with the nuclear experimental data.

The results of this chapter are based on our paper,

GS and V. Zelevinsky, Phys. Rev. C **86**, 044602 (2012).

4.1 Introduction

Random matrix theory as a statistical approach for exploring properties of complex quantum systems was pioneered by Wigner and Dyson half a century ago [37]. This theory was successfully applied to excited states of complex nuclei and other mesoscopic systems [38–41], evaluating statistical fluctuations and correlations of energy levels and corresponding wave functions supposedly of "chaotic" nature.

The standard random matrix approach based on the Gaussian Orthogonal Ensemble (GOE) for systems with time-reversal invariance, and on the Gaussian Unitary Ensemble (GUE) if this invariance is violated, was formulated originally for *closed* systems with no coupling to the outside world. Although the practical studies of complex nuclei, atoms, disordered solids, or microwave cavities always require the use of reactions produced by external sources, the typical assumption was that such a probe at the resonance is sensitive to the specific components of the exceedingly complicated intrinsic wave function, one for each open reaction channel, and the resonance widths are measuring the weights of these components [42]. With the Gaussian distribution of independent amplitudes in a chaotic intrinsic wave function, the widths under this assumption are proportional to the squares of the amplitudes and as such can be described, for ν independent open channels, by the chi-square distribution with ν degrees of freedom. For low-energy elastic scattering of neutrons off heavy nuclei, where the interactions can be considered time-reversal invariant, one expects $\nu = 1$ that is usually called the Porter-Thomas distribution (PTD) [43],

$$\chi^2_\nu(x)\Big|_{\nu=1} = \left.\frac{e^{-x/2}x^{(\nu-2)/2}}{2^{\nu/2}\Gamma[\nu/2]}\right|_{\nu=1} = \frac{e^{-x/2}}{\sqrt{2\pi x}}, \tag{4.1}$$

where $\Gamma[z]$ is the gamma function.

Recent measurements [44,45] claimed that the neutron width distributions in low-energy neutron resonances on certain heavy nuclei are different from the PTD. As a rule, the fraction of greater widths is increased, while the fraction of narrow resonances is reduced which, being approximately presented with the aid of the same standard class of functions χ^2_ν, would require $\nu \neq 1$. The literature discussing the scattering and decay processes in chaotic systems, see for example [46–49] and references therein, does not provide a detailed description of the width distribution for the region of relatively small widths observed in low-energy neutron resonances.

There are various reasons for possible deviations from the simple statistical predictions [50–52]. First of all, the intrinsic dynamics, even in heavy nuclei, can be different from that in the GOE limit of many-body quantum chaos. If so, the detailed analysis of specific nuclei is required. As an example we can mention ^{232}Th, where for a long time a *sign problem* exists [53] concerning the resonances with strong enhancement of parity nonconservation in scattering of longitudinally polarized neutrons. The observed predominance of a certain sign of parity violating asymmetry contradicts to the statistical mechanism of the effect and may be related to the non-random coupling between quadrupole and octupole degrees of freedom [54]. The width distribution in the same nucleus reveals noticeable deviations from the PTD. The presence of a shell-model single-particle resonance serving as a doorway from the neutron capture to the compound nucleus can also make its footprint distorting the statistical pattern. Another (maybe related to the doorway resonance) effect can come from the changed energy dependence of the widths that is usually assumed to be proportional to $E^{\ell+1/2}$ for neutrons with orbital momentum ℓ. Finally, the situation is not strictly one-channel, since, along with elastic neutron scattering, many gamma-channels are open

as well. However, apart from structural effects, even in one-channel approximation, there exists a generic cause for the deviations from the PTD, since the applicability of the GOE is anyway violated by the *open* character of the system [55]. The appropriate modification of the GOE and PTD predictions, which should be applied before making specific conclusions, is our goal below.

The resonances are not the eigenstates of a Hermitian Hamiltonian, they are poles of the scattering matrix in the complex plane. Their *complex energies* $\mathcal{E} = E - i\Gamma/2$ can be rigorously described as eigenvalues of the *effective non-Hermitian Hamiltonian* [56]. As shown long ago, even for a single open channel, the statistical properties of the complex energies cannot be described by the GOE. The new dynamics is related to the interaction of intrinsic states through continuum. In the limit of strong coupling this leads to the overlapping resonances, Ericson fluctuations of cross sections, and sharp redistribution of widths similar to the phenomenon of *super-radiance*, see the review [57] and references therein. The control parameter of such restructuring is the ratio

$$\kappa = \frac{\pi\Gamma}{2D} \tag{4.2}$$

of typical widths, Γ, to the mean spacing between the resonances, D. In the region of low-energy neutron resonances, κ is still small but in order to correctly separate the general statistical effects from peculiar properties of individual nuclei we need to have at our disposal a generic width distribution that differs from the PTD as a function of the degree of openness.

4.2 Resonance width distribution

We need a practical tool that would allow one to compare an experimental output for an unstable quantum system with predictions of random matrix theory. We propose a new distribution function that is based, similar to the GOE, on the chaotic character of time-reversal invariant internal dynamics and corresponding decay amplitudes, but properly accounts for the continuum coupling through the effective non-Hermitian Hamiltonian. The numerical simulations for this Hamiltonian were described earlier [51, 58] but here we derive the analytical expression. In the typical case of nuclear applications, the introduced dimensionless parameter κ is bound from above by one. The super-radiant regime, $\kappa \geq 1$, can be of special interest, including such systems as microwave cavities, and in the considered framework the formal symmetry exists, $\kappa \to 1/\kappa$. At a large number of resonances and fixed number of open channels, after the super-radiant transition the broad state becomes a part of the background while the remaining "trapped" states return into the non-overlap regime. However, in heavy nuclei this transition hardly can be observed because earlier many new channels can be opened; in the modification of the PTD we see only precursors of this transition.

Our arguments will follow two different routes which lead to the equivalent results. The final formula for the statistical width distribution can be presented as

$$P(\Gamma) = C \frac{\exp\left[-\frac{N}{2\sigma^2}\Gamma(\eta-\Gamma)\right]}{\sqrt{\Gamma(\eta-\Gamma)}} \left(\frac{\sinh\left[\frac{\pi\Gamma}{2D}\frac{(\eta-\Gamma)}{\eta}\right]}{\frac{\pi\Gamma}{2D}\frac{(\eta-\Gamma)}{\eta}} \right)^{1/2} . \tag{4.3}$$

Here we consider $N \gg 1$ intrinsic states coupled to a single decay channel, for example, s-wave elastic neutron scattering. The parameter D is a mean energy spacing between the

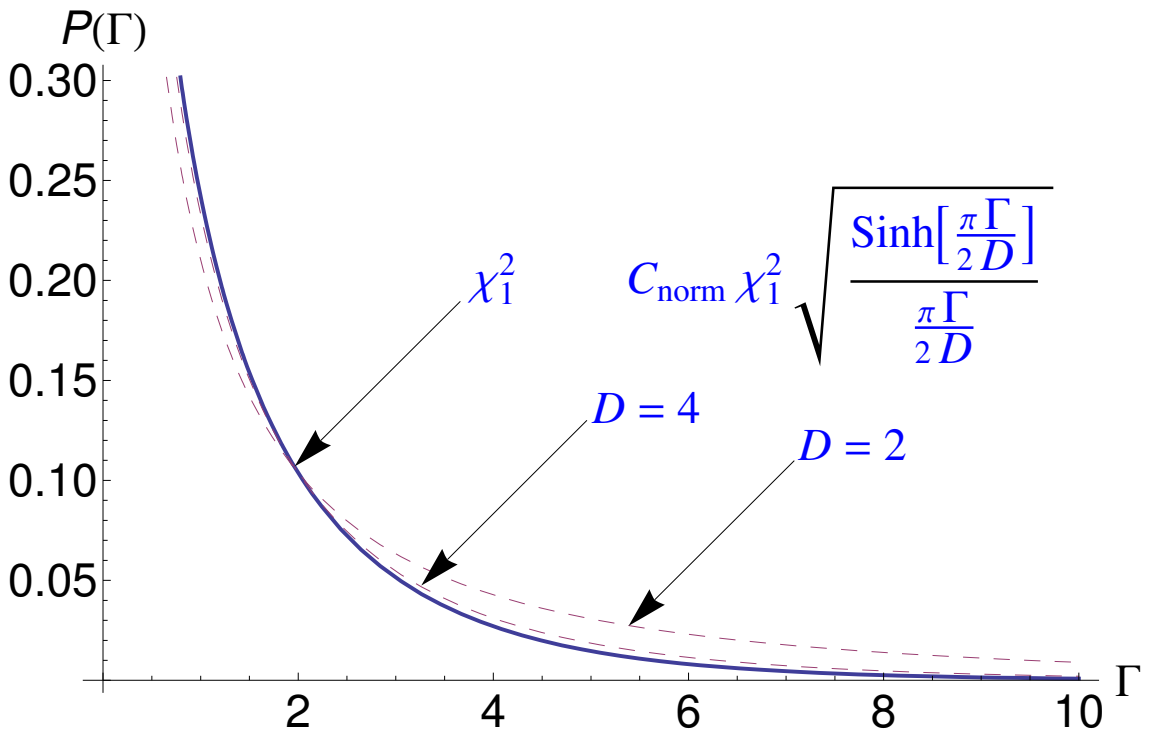

Figure 4.1: The proposed resonance width distribution according to eq. (4.3) with a single neutron channel in the practically important case $\eta \gg \Gamma$. The width Γ and mean level spacing D are measured in units of the mean value $\langle\Gamma\rangle$. "For interpretation of the references to color in this and all other figures, the reader is referred to the electronic version of this dissertation."

resonances, and C is a normalization constant. The quantity η is the total sum (the trace of the imaginary part of the effective non-Hermitian Hamiltonian that remains invariant in the transition to the biorthogonal set of its eigenfunctions) of all N widths; it appears as a parameter that fixes the starting ensemble distribution, see below eqs. (4.9) and (4.10). The possible values of widths are restricted from both sides, $0 < \Gamma < \eta$. The above mentioned symmetry $\kappa \to 1/\kappa$ is reflected in the symmetry $\Gamma \to (\eta - \Gamma)$ of a factor in eq. (4.3) but, as was already stated, our region of interest is at $\Gamma \ll \eta$. Another parameter, σ, determines the standard deviation of variable Γ evaluated consistently with the distribution

of eq. (4.3). In the practical region far away from the super-radiance we obtain

$$P(\Gamma) = C\chi_1^2(\Gamma) \left(\frac{\sinh \kappa}{\kappa} \right)^{1/2}, \tag{4.4}$$

where κ is a new dimensionless combination, eq. (4.2). The PTD is recovered in the limiting case $\kappa \to 0$ that corresponds to the approximation of an open quantum system by a closed one. The new element is the factor explicitly determined by the coupling strength κ. With growing continuum coupling the probability of larger widths increases. The distribution (4.3) for different ratios $\langle \Gamma \rangle / D$ is shown in Fig. 4.1.

The origin of the square root in the new factor is the linear energy level repulsion typical for the GOE spectral statistics. Indeed, in the complex plane, $\mathcal{E} = E - i\Gamma/2$, the distance between two poles $\mathcal{E}_m$ and $\mathcal{E}_n$ is $\sqrt{(E_m - E_n)^2 + (\Gamma_m - \Gamma_n)^2/4}$; after integration over all variables of other states we obtain a characteristic square root in the level repulsion, see below eq. (4.13) and the discussion after eq. (4.22).

4.3 Effective non-Hermitian Hamiltonian and scattering matrix

In order to come to the result (4.3), we start with the general description of complex energies $\mathcal{E} = E - i\Gamma/2$ in a system of N unstable states satisfying the GOE statistics inside the system and interacting with the single open channel through Gaussian random amplitudes. The general reaction theory [59] is constructed in terms of the elements of the scattering matrix in the space of open channels $a, b, ...$,

$$S^{ba}(E) = \delta^{ba} - iT^{ba}(E). \tag{4.5}$$

Within the formalism of the effective non-Hermitian Hamiltonian $\mathcal{H} = H - (i/2)W$, the T-matrix is defined as

$$T^{ba}(E) = \sum_{m,n=1}^{N} A_m^{b*} \left[\frac{1}{E - \mathcal{H}}\right]_{mn} A_n^a \tag{4.6}$$

in terms of the amplitudes A_n^a connecting an internal basis state n with an open channel a. Here we do not explicitly indicate the potential part of scattering that is not related to the internal dynamics of the compound nucleus. The anti-Hermitian part of the effective Hamiltonian is exactly represented by the sum over k open channels,

$$W_{mn} = \sum_{a=1}^{k} A_m^a A_n^{a*}, \tag{4.7}$$

where the amplitudes can be considered real in the case of time-reversal invariance. It is important that the factorized structure of the effective Hamiltonian guarantees the unitarity of the scattering matrix. The amplitudes A_n^a are assumed to be uncorrelated Gaussian quantities with zero mean and variance defined as $\overline{A_n^a A_{n'}^b} = \delta^{ab}\delta_{nn'}\eta/N$. The trace of the anti-Hermitian part of the effective Hamiltonian, $\eta = \mathrm{Tr}W$, i.e. the total sum of all N widths used in eq. (4.3), is a quantity invariant under orthogonal transformations of the intrinsic basis. The detailed discussion of the whole approach, numerous applications and relevant references can be found in the recent review article [57].

The simplest version of the R-matrix description uses instead of the amplitude T^{ba} its approximate form, where the denominator contains poles on the real energy axis corresponding to the eigenvalues of the Hermitian part H of the effective Hamiltonian. Then the continuum coupling occurs only at the entrance and exit points of the process while the influence of this coupling on the intrinsic dynamics of the compound nucleus is neglected (in general, the Hermitian part of the Hamiltonian, H, should also be renormalized by the off-shell contributions from the presence of the decay channels). Contrary to that, the full amplitude T^{ba}, eq. (4.6), accounts for this coupling during the entire process including the virtual excursions to the continuum and back from intrinsic states. The poles are the eigenvalues of the full effective Hamiltonian in the lower half of the complex energy plane. The experimental treatment corresponds to this full picture. According to the original experimental paper [44], the R-matrix code SAMMY [60] had been used in the experimental analysis where the relevant expression is given in the form

$$R_{cc'} = \sum_{\lambda} \frac{\gamma_{\lambda c}\gamma_{\lambda c'}}{E_\lambda - E - i\Gamma_\lambda/2}\delta_{JJ'}, \tag{4.8}$$

and the treatment included a careful segregation of s- and p-resonances, $J = J' = 1/2$ for an even target nucleus. In the notations of [60] λ represents a particular resonance, E_λ is the energy of the resonance. Here we can identify the intermediate states λ and their complex energies $E_\lambda - i\Gamma_\lambda/2$ with the eigenstates and complex eigenvalues of $\mathcal{H}$, while the numerator includes the amplitudes transformed to this new basis (under time-reversal invariance the scattering matrix is symmetric). In terms of the reduced width $\gamma^2_{\lambda c}$ and the penetration factor P_c, the partial width is $\Gamma_{\lambda c} = 2P_c\gamma^2_{\lambda c}$. Assuming a single channel and universal energy dependence of penetration factors, the statistics of the total widths is the same as that of $\gamma^2_{\lambda c}$.

4.4 From ensemble distribution to single width distribution

For a single-channel case, the *joint distribution* $P(\vec{E};\vec{\Gamma})$ of all complex energy poles has been rigorously derived in [55] under assumptions of the GOE intrinsic dynamics in the closed system and Gaussian distributed random decay amplitudes. The result is given by

$$P(\vec{E};\vec{\Gamma}) = C_N \prod_{m<n} \frac{(E_m - E_n)^2 + \frac{(\Gamma m - \Gamma n)^2}{4}}{\sqrt{(E_m - E_n)^2 + \frac{(\Gamma m + \Gamma n)^2}{4}}} \prod_n \frac{1}{\sqrt{\Gamma_n}}\, e^{-NF(\vec{E};\vec{\Gamma})}, \quad (4.9)$$

where the "free energy" F contains interactions of $N \gg 1$ complex poles in the interval $2a = ND$ of energies,

$$F(\vec{E};\vec{\Gamma}) = \frac{1}{a^2}\sum_n E_n^2 + \frac{1}{2a^2}\sum_{m<n}\Gamma_m\Gamma_n + \frac{1}{2\eta}\sum_n \Gamma_n. \quad (4.10)$$

For given N, this distribution contains two parameters, the semicircle radius a for the intrinsic dynamics and η characterizing the total trace of the imaginary part of the effective Hamiltonian.

Considering this free energy in the "mean-field" approximation, we see that the original mean value $\langle\Gamma\rangle_0 = \eta/N$ is substituted by $\langle\Gamma\rangle$ that is determined by the competition of two terms, $1/\langle\Gamma\rangle = 1/\langle\Gamma\rangle_0 + \langle\Gamma\rangle/4D^2$. The first product in front of $\exp(-NF)$ in eq. (4.9) substitutes the GOE level repulsion by the repulsion in the complex plane and interaction of the poles with their negative-Γ "images" [55]. The structure of this result guarantees that all widths Γ are positive. The formal difficulty with the distribution of eq. (4.9) is that it is *not an analytic function* of complex energies.

Our first step is to specify a single N-th pole $(E_N, \Gamma_N) \equiv (E, \Gamma)$ and, using the fact that the distribution ensures $\Gamma_n \geq 0$, return to the absolute values of the amplitudes, $\sqrt{\Gamma_n} = \xi_n$ for other roots. In this form we can apply the steepest descent method owing to a large parameter $N \gg 1$ and a *saddle point* inside the integration interval that was absent in the initial expression. Integration $\prod_{n=1}^{N-1} d\xi_n$ over all but one variable $\Gamma \equiv \Gamma_N = \xi_N^2$ leads to the following result for $P(\vec{E};\Gamma)$ as a function of multiple energy variables $\vec{E}$ and a single width variable Γ

$$P(\vec{E};\Gamma) = C_N \prod_{m<n} |E_m - E_n| \prod_n \sqrt{(E_n - E)^2 + \frac{\Gamma^2}{4}} \tag{4.11}$$
$$\times \exp\left[-\frac{N}{a^2}\left(\sum_n E_n^2 + E^2\right)\right] \frac{\exp\left[-\frac{N}{2\eta}\Gamma\right]}{\sqrt{\Gamma}} \left(\sqrt{\frac{2\pi}{N\left(\frac{\Gamma}{a^2} + \frac{1}{\eta}\right)}}\right)^{N-1}$$

Introducing new variables, $2a/N = D$ and $\lambda = \eta N$, we shall examine the behavior of one of the N-dependent factors in eq. (4.11) in the limit of $N \to \infty$,

$$\lim_{N\to\infty} \left[\frac{\exp\left[-\frac{N}{2\eta}\Gamma\right]}{\sqrt{\Gamma}} \left(1 + \frac{\lambda\Gamma}{a^2 N}\right)^{-\frac{N-1}{2}} \right] = \frac{\exp\left[-\frac{N}{2\eta}\Gamma\right]}{\sqrt{\Gamma}} \exp\left[-\frac{\lambda}{2a^2}\Gamma\right] \quad (4.12)$$

The scaling properties of the parameters η, a^2, and λ are as follows: $\eta \propto N$, a^2 and λ are both $\propto N^2$. As a result, the product of two exponents produces a well defined limit that brings in the desired dependence on the coupling strength κ.

The real energy distribution does not change much in an open system with a single decay channel being still, at finite but large N, close to a semicircle. We are working in the central region of the spectrum where the level density is approximately constant and the energy spectrum is close to equidistant (the maximum of the level spacing distribution is always at $s = \delta E/D \approx 1$ although the distribution in an open system changes at small spacings, $s < 1$, as we will comment later). With $E_n = E - nD$, we are able to perform an exact calculation of the product,

$$\begin{aligned} & C_N \prod_n \sqrt{(E_n - E)^2 + \frac{\Gamma^2}{4}} \qquad (4.13) \\ & = \widehat{C}_N \left(\prod_{n=1}^{N} \left[1 + \frac{\Gamma^2/4}{(nD)^2} \right] \right)_{N\to\infty}^{1/2} = \widehat{C}_N \left(\frac{\sinh\left[\frac{\pi}{2}\frac{\Gamma}{D}\right]}{\frac{\pi}{2}\frac{\Gamma}{D}} \right)^{1/2}, \end{aligned}$$

where we have used the famous `Euler formula`,

$$\frac{\sinh x}{x} = \prod_{k=1}^{\infty} \left[1 + \frac{x^2}{k^2\pi^2} \right]. \quad (4.14)$$

The width-independent factors will enter the normalization constant. Of course, the whole reasoning is valid in the limit $N \gg 1$. Finally, the width distribution for $\Gamma \ll \eta$ is represented by

$$P(\Gamma) = C \left(\frac{\sinh\left[\frac{\pi}{2}\frac{\Gamma}{D}\right]}{\frac{\pi}{2}\frac{\Gamma}{D}} \right)^{1/2} \frac{\exp\left[-\frac{N}{2\eta}\Gamma\right]}{\sqrt{\Gamma}} \exp\left[-\frac{\lambda}{2a^2}\Gamma\right]. \tag{4.15}$$

4.5 Doorway approach

As an alternative derivation, we will apply the *doorway approach* [38,61,62]. Here we use the eigenbasis of the imaginary part W of the effective non-Hermitian Hamiltonian, eq. (4.7). Due to the factorized nature of W dictated by unitarity [55], the number of its non-zero eigenvalues is equal to the number of open channels. In our case we have only one eigenvalue, the *doorway* $\varepsilon_0 - i\eta/2$, that has a non-zero width equal to the imaginary part η of the trace of the Hamiltonian. Remaining basis states are stable being driven by the Hermitian intrinsic Hamiltonian; its diagonalization produces their real energies ε_n. These states acquire the widths through the interaction with the doorway state; the corresponding matrix elements will be denoted h_n. In this basis, the effective Hamiltonian is represented as

$$\begin{pmatrix} \varepsilon_0 - \frac{i}{2}\eta & h_1 & h_2 & \cdots & h_N \\ h_1^* & \varepsilon_1 & 0 & \cdots & 0 \\ h_2^* & 0 & \varepsilon_2 & \cdots & 0 \\ \cdots & \cdots & \cdots & \cdots & \cdots \\ h_N^* & 0 & 0 & \cdots & \varepsilon_N \end{pmatrix}. \tag{4.16}$$

The complex eigenvalues $\mathcal{E} = E - i\Gamma/2$ are the roots of the secular equation,

$$\mathcal{E} = \varepsilon_0 - \frac{i}{2}\eta + \sum_{n=1}^{N} \frac{|h_n|^2}{\mathcal{E} - \varepsilon_n}, \tag{4.17}$$

that is equivalent to the set of coupled equations for real and imaginary parts,

$$E = \varepsilon_0 + \sum_{n=1}^{N} |h_n|^2 \frac{E - \varepsilon_n}{(E - \varepsilon_n)^2 + \Gamma^2/4}, \tag{4.18}$$

$$\Gamma = \frac{\eta}{1 + \sum_{n=1}^{N} \frac{|h_n|^2}{(E-\varepsilon_n)^2 + \Gamma^2/4}} \equiv f(\Gamma, E). \tag{4.19}$$

For the Gaussian distribution of the coupling matrix elements with $\langle |h|^2 \rangle = 2\sigma^2/N$ (this scaling was derived in [61]), we obtain

$$P(\Gamma) = \int_{-\infty}^{+\infty} \delta\left(\Gamma - f(\Gamma, E)\right) \exp\left[-\frac{N}{\sigma^2} \sum_{n=1}^{N} h_n^2\right] \prod_{n=1}^{N} dh_n. \tag{4.20}$$

The integration in (4.20) via the steepest descent method leads to eq. (4.3). In order to get this result we use a possibility to find a highest root $E = \varepsilon_N$ which we set as an origin relative to which the energies ε_n can be counted as $E = \varepsilon_N,\ \varepsilon_n = \varepsilon_N - nD$. An important intermediate step is the evaluation of the infinite product of the Lorentzian peaks

that can be simplified as

$$\left(\prod_{n=1}^{N-1}\left[1-\frac{\frac{\Gamma^2}{4}+(E-\varepsilon_N)^2}{\frac{\Gamma^2}{4}+(E-\varepsilon_n)^2}\right]\right)^{-1/2} \tag{4.21}$$
$$=\left(\prod_{n=1}^{N-1}\left[1-\frac{\frac{\Gamma^2}{4}}{\frac{\Gamma^2}{4}+(nD)^2}\right]\right)^{-1/2}=\left(\frac{\sinh\left[\frac{\pi}{2}\frac{\Gamma}{D}\right]}{\frac{\pi}{2}\frac{\Gamma}{D}}\right)^{+1/2}.$$

In a similar way one can analyze the resonance spacing distribution $P(s)$ along the real energy axis; spacings $s=\delta E/D$ are measured in units of their mean value D. As predicted in [55] and observed numerically in [58], the short-range repulsion disappears and the Wigner surmise with the standard linear preexponential factor s is substituted by the square root,

$$P(s)\propto\sqrt{s^2+4\frac{\langle\Gamma^2\rangle}{D^2}}\exp\left[-\text{const}\cdot s^2\right]. \tag{4.22}$$

At spacing $s\ll 1$, the probability behaves as $a+bs^2$ with the quadratic dependence on s that, similar to the GUE, mimics the violation of time-reversal invariance due to the open decay channel. The absence of short-range repulsion, $a\neq 0$ (the interaction through continuum, opposite to a normal Hermitian perturbation, repels widths and attracts real energies [63]), reflects the energy uncertainty of unstable states.

We demonstrated that two complementary approaches which reflect different physical aspects of the situation lead essentially to the equivalent (after identification of corresponding parameters) results which we prefer to write in the form (4.3). We expect that for other canonical ensembles the width distribution far from the super-radiance can be expressed by a similar formula with the function $(\sinh\kappa/\kappa)^{\beta/2}$, where the standard index of ensemble

is $\beta = 1$ for the GOE, $\beta = 2$ for the GUE, and $\beta = 4$ for the Gaussian Symplectic Ensemble. In the same way we expect the square root in eq. (4.22) to be substituted by the same power $\beta/2$.

The doorway approach naturally indicates the limits of the variable, $0 \leq \Gamma \leq \eta$. It has also an advantage of the possibility to generalize the answer taking into account explicitly the *rigidity* of the internal energy spectrum with fluctuations of level spacings around their mean value D [in our approximation, only this average value enters eq. (4.3)]. Another direction of generalization includes the possible influence of a single-particle resonance depending on a position of its centroid with respect to the considered interval of the resonance spectrum. In particular, that centroid may be located under threshold of our decay channel. In this case even the standard energy dependence of the widths can change as was mentioned long ago [61], see also [50]. The doorway state may or may not coincide with such a resonance so that the effective Hamiltonian (4.16) may contain two special states coupled with the "chaotic" background, one by intrinsic interactions and another one through the continuum.

4.6 Photon emission channels

The goal of this section is to estimate in the same spirit the influence of γ-channels on the resonance width distribution. Only a single open elastic neutron channel was taken into account in the analysis of data [44, 45]. The presence of even weak additional open channels changes the unitarity conditions. Examples of mutual influence of neutron and gamma channels are well known in the literature from long ago, see for example [64].

Generalizing the doorway description we allow now each intrinsic state to decay by gamma-emission which is always possible independently of the position of the neutron

threshold. In the simplest approximation, the effective non-Hermitian Hamiltonian is now represented by

$$\begin{pmatrix} \varepsilon_0 - \frac{i}{2}\eta & h_1 & h_2 & \cdots & h_N \\ h_1^* & \varepsilon_1 - \frac{i}{2}\gamma_1 & 0 & \cdots & 0 \\ h_2^* & 0 & \varepsilon_2 - \frac{i}{2}\gamma_2 & \cdots & 0 \\ \cdots & \cdots & \cdots & \cdots & \cdots \\ h_N^* & 0 & 0 & \cdots & \varepsilon_N - \frac{i}{2}\gamma_N \end{pmatrix}, \tag{4.23}$$

where we assumed that the intrinsic part of the matrix is pre-diagonalized and introduced γ_n as the widths for γ-channels.

Analogously to eq. (4.17), the complex energy eigenvalues $\mathcal{E} = E - \frac{i}{2}\Gamma$ are the roots of the secular equation,

$$\mathcal{E} = \varepsilon_0 - \frac{i}{2}\eta + \sum_{n=1}^{N} \frac{|h_n|^2}{\mathcal{E} - \left(\varepsilon_n - \frac{i}{2}\gamma_n\right)}, \tag{4.24}$$

equivalent to the set of coupled equations,

$$E = \varepsilon_0 + \sum_{n=1}^{N} |h_n|^2 \frac{E - \varepsilon_n}{(E-\varepsilon_n)^2 + (\Gamma - \gamma_n)^2/4}, \tag{4.25}$$

$$\Gamma = \frac{\eta + \sum_{n=1}^{N} |h_n|^2 \frac{\gamma_n}{(E-\varepsilon_n)^2 + (\Gamma-\gamma_n)^2/4}}{1 + \sum_{n=1}^{N} |h_n|^2 \frac{1}{(E-\varepsilon_n)^2 + (\Gamma-\gamma_n)^2/4}} \equiv g(\Gamma, E, \gamma). \tag{4.26}$$

The resonance width distribution for an open quantum system with γ-channels included is

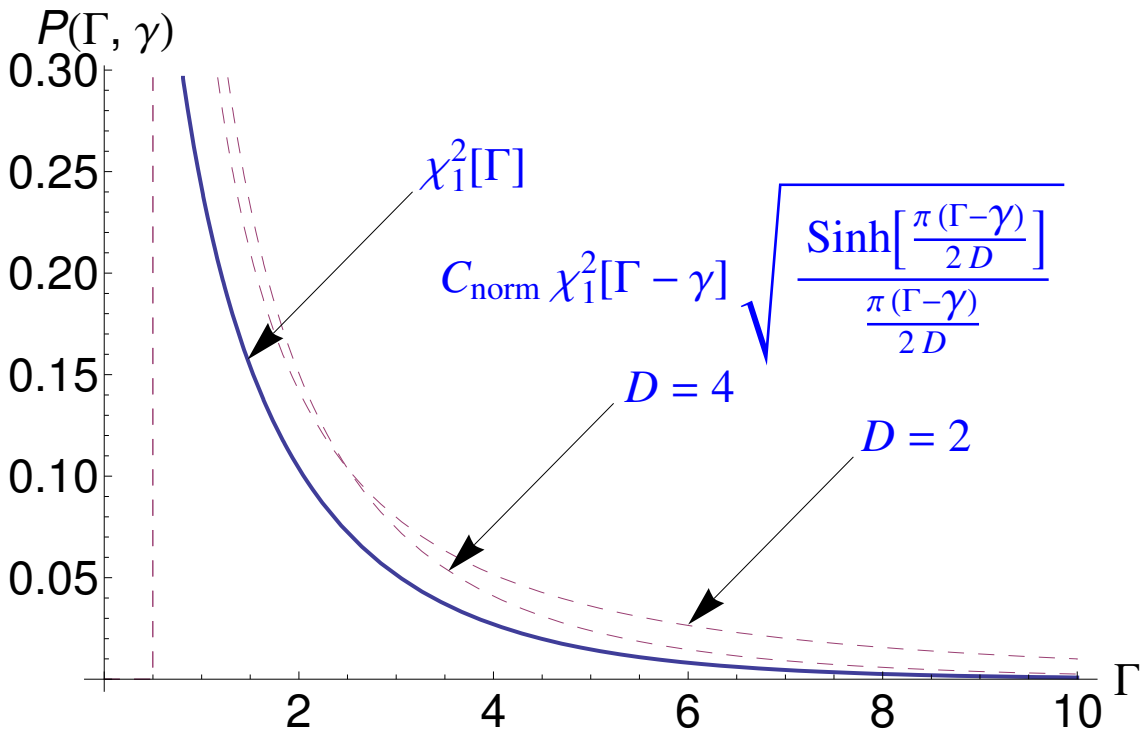

Figure 4.2: The proposed resonance width distribution according to eq. (4.28) with a single neutron channel and N gamma-channels in the practically important case $\eta \gg \Gamma$. The neutron width Γ, radiation width γ, and mean level spacing D are measured in units of the mean value $\langle\Gamma\rangle$.

given by

$$P(\Gamma,\gamma) = \int_{-\infty}^{+\infty} \delta\left(\Gamma - g(\Gamma, E, \gamma)\right) \exp\left[-\frac{N}{\sigma^2}\sum_{n=1}^{N} h_n^2\right] \prod_{n=1}^{N} dh_n. \qquad (4.27)$$

Estimating the gamma-widths by their average value, γ, and acting in the same manner as in the case of a single open channel we come to the final expression for the resonance width

distribution,

$$P(\Gamma,\gamma) = C\frac{(\eta-\gamma)}{\sqrt{(\Gamma-\gamma)(\eta-\Gamma)}} \tag{4.28}$$
$$\times \exp\left[-\frac{N}{2\sigma^2}(\Gamma-\gamma)(\eta-\Gamma)\right]\left(\frac{\sinh\left[\frac{\pi(\Gamma-\gamma)}{2D}\frac{(\eta-\Gamma)}{\eta}\right]}{\frac{\pi(\Gamma-\gamma)}{2D}\frac{(\eta-\Gamma)}{\eta}}\right)^{1/2},$$

that is shifted by $\Gamma \to (\Gamma-\gamma)$ compared to the previous result. The mentioned earlier symmetry between the ends of the distribution, $\Gamma = 0$ and $\Gamma = \eta$, would be substituted here by $\Gamma \to (\eta+\gamma)-\Gamma$. Thus, the effective influence of γ-channels on the resonance width distribution is reduced here to a shift of the whole distribution by a mean radiation width γ as seen in Fig. 4.2.

In the practical region far away from the super-radiance, $\Gamma \ll \eta$, we obtain

$$P(\Gamma,\gamma) = \chi_1^2\,(\Gamma-\gamma)\left(\frac{\sinh\left[\frac{\pi(\Gamma-\gamma)}{2D}\right]}{\frac{\pi(\Gamma-\gamma)}{2D}}\right)^{1/2}. \tag{4.29}$$

In order to extract the neutron width from the total resonance width, the treatment of the data has to be modified making in a sense an inverse shift. Of course, a more precise consideration should use a statistical distribution of the gamma widths.

4.7 Many-channel case

In the two-channel case the effective Hamiltonian is

$$\begin{pmatrix} \varepsilon_0 - \frac{i}{2}\eta_0 & h_1 & h_2 & h_3 & \cdots & h_N \\ h_1^* & \varepsilon_1 - \frac{i}{2}\eta_1 & v_2 & v_3 & \cdots & v_N \\ h_2^* & v_2^* & \varepsilon_2 & 0 & \cdots & 0 \\ \cdots & \cdots & \cdots & \cdots & \cdots & \cdots \\ h_N^* & v_N^* & 0 & 0 & \cdots & \varepsilon_N \end{pmatrix}. \tag{4.30}$$

It can be shown that the Schrödinger equation with Hamiltonian eq. (4.30) for complex eigenvalue $\mathcal{E}_\alpha = E_\alpha - \frac{i}{2}\Gamma_\alpha$ can be rewritten in terms of matrix

$$A = \begin{pmatrix} \sum_{k=2}^N \frac{h_k^2}{\varepsilon_k - \mathcal{E}_\alpha} + \mathcal{E}_\alpha - (\varepsilon_0 - \frac{i\eta_0}{2}) & h_1 - \sum_{k=2}^N \frac{h_k v_k}{\varepsilon_k - \mathcal{E}_\alpha} \\ h_1 - \sum_{k=2}^N \frac{h_k v_k}{\varepsilon_k - \mathcal{E}_\alpha} & \sum_{k=2}^N \frac{v_k^2}{\varepsilon_k - \mathcal{E}_\alpha} + \mathcal{E}_\alpha - (\varepsilon_1 - \frac{i\eta_1}{2}) \end{pmatrix} \tag{4.31}$$

namely the secular equation for the Hamiltonian eq. (4.30) is equivalent to

$$\det A = 0. \tag{4.32}$$

We shall note that in the general case dimension of the corresponding matrix A is equal to the number of open channels, i.e. number of rows (or columns) k with random variables in the original Hamiltonian (see *Appendix B*).

Following the general procedure we get the equation for the width,

$$\Gamma = \frac{\frac{E(\eta_0+\eta_1)}{2} - \frac{\varepsilon_1\eta_0+\varepsilon_0\eta_1}{2}}{\left[E - \frac{\varepsilon_0+\varepsilon_1}{2} - \sum_k \frac{v_k^2\varepsilon_0+h_k^2\varepsilon_1}{2\left(\frac{\Gamma^2}{4}+(E-\varepsilon_k)^2\right)} + \sum_k \frac{E(v_k^2+h_k^2)}{2\left(\frac{\Gamma^2}{4}+(E-\varepsilon_k)^2\right)}\right]}$$
$$\equiv f(\Gamma, h_k, v_k). \tag{4.33}$$

By averaging the width Γ, eq. (4.33), over the set of random variables h_n and v_n we get the width distribution,

$$P(\Gamma) = \int_{-\infty}^{+\infty} \delta\left(\Gamma - f(\Gamma, h_n, v_n)\right)$$
$$\times \exp\left[-\frac{N}{\sigma^2}\sum_{n=1}^{N} h_n^2\right] \prod_{n=1}^{N} dh_n \exp\left[-\frac{N}{\sigma^2}\sum_{n=1}^{N} v_n^2\right] \prod_{n=1}^{N} dv_n. \tag{4.34}$$

Introducing $k = 2$ dimensional spherical coordinates

$$r_N^2 \equiv v_N^2 + h_N^2 \tag{4.35}$$

and taking into account

$$V_k(R) = \frac{\pi^{\frac{k}{2}}}{\Gamma\left[\frac{k}{2}+1\right]} R^k, \tag{4.36}$$
$$dV_k(R) = \frac{\pi^{\frac{k}{2}}}{\Gamma\left[\frac{k}{2}+1\right]} k R^{k-1} dR \simeq C_k R^{k-1} dR,$$

we obtain

$$P(\Gamma) = \int_{-\infty}^{+\infty} \prod_{n=1}^{N-1} dh_n \prod_{n=1}^{N-1} dv_n \delta\left(\Gamma - f(\Gamma, h_n, v_n)\right) \tag{4.37}$$
$$\times \exp\left[-\frac{N}{\sigma^2}\sum_{n=1}^{N-1} h_n^2\right] \exp\left[-\frac{N}{\sigma^2}\sum_{n=1}^{N-1} v_n^2\right] \exp\left[-N\frac{r_N^2}{\sigma^2}\right] \frac{\pi^{\frac{k}{2}}}{\Gamma\left[\frac{k}{2}+1\right]} k r_N^{k-1} dr_N.$$

The Dirac δ-function produces a derivative in the denominator which behaves as

$$\left|\frac{d\Gamma}{dr_N}\right| = C\frac{r_N}{\sum_{i=1}^{k}\eta_i/k}. \tag{4.38}$$

After applying the steepest descent method and in the particular case $k = 2$ after smoke clears we have

$$P(\Gamma) = C\exp\left[-\frac{N}{2\sigma^2}\Gamma\left(\frac{\eta_0+\eta_1}{2} - \Gamma\right)\right] \times \phi\left(\frac{\Gamma}{D}\right), \tag{4.39}$$

which, except for the factor $\phi\left(\Gamma/D\right)$, is nothing but $\chi_k^2\left[\Gamma\left(\frac{\eta_0+\eta_1}{2} - \Gamma\right)\right]$ distribution in case of $k = 2$ open channels. The factor $\phi\left(\Gamma/D\right)$ is evaluated by means of the Euler formula and is given in terms of the sum of partial width η,

$$\eta = \frac{\sum_{i=1}^{k}\eta_i}{k}, \tag{4.40}$$

and the number of open channels k,

$$\phi\left(\frac{\Gamma}{D}\right) = \left(\frac{\sinh\left[\frac{\pi\Gamma}{2D}\frac{(\eta-\Gamma)}{\eta}\right]}{\frac{\pi\Gamma}{2D}\frac{(\eta-\Gamma)}{\eta}}\right)^{\frac{k}{2}}. \tag{4.41}$$

In the general case of k open channels the width distribution is

$$P(\Gamma) = C \exp\left[-\frac{N}{2\sigma^2}\Gamma\left(\eta-\Gamma\right)\right]\left(\Gamma\left(\eta-\Gamma\right)\right)^{\frac{k-2}{2}}\left(\frac{\sinh\left[\frac{\pi\Gamma}{2D}\frac{(\eta-\Gamma)}{\eta}\right]}{\frac{\pi\Gamma}{2D}\frac{(\eta-\Gamma)}{\eta}}\right)^{\frac{k}{2}}. \quad (4.42)$$

4.8 Conclusion

In this chapter we proposed a new resonance width distribution for an open quantum system based on chaotic intrinsic dynamics and coupling of states with the same quantum numbers to the common decay channel. Two approximate methods lead to an equivalent analytical expression for the width distribution that does not belong to the class of chi-square distributions with the only parameter ν traditionally used in the analysis of data. In the limit of vanishing openness and return to a closed system we recover the standard PTD. The new result depends on the ratio (4.2) of the width to the mean level spacing, $\kappa \sim \Gamma/D$, that regulates the strength of the continuum coupling. The deviations from the PTD grow with κ up to the critical strength $\kappa \sim 1$, when the broad "super-radiant" state becomes essentially the part of the background, while the remaining "trapped" states return to the weak coupling regime. This physics was repeatedly discussed previously, especially in relation to quantum signal transmission through mesoscopic devices [57,65], but it is outside of our interest here.

In the practical region of low-energy neutron resonances, the effects predicted here are relatively small. Although at small κ the derived neutron width distribution supports an experimental trend, the final judgment can be made only after the presence of gamma-channels was accounted for. We have to attract the attention of experimentalists to the fact

that the data should be analyzed with the aid of the distribution that does not belong to the routinely used chi-square class; gamma channels should be included into consideration. We can also mention that the result agrees with numerical simulations [51] for the full many-resonance distribution function (4.9). Using the suggested distribution as a new reference point, one can ascribe the remaining deviations to the specific features of individual systems (level densities, single-particle structure in a given energy region, shape transformations, energy dependence of the widths etc.). Unfortunately, we still do not have experimental tests for the full distribution (4.9). Although in nuclear physics it is hard to make such a detailed analysis for higher energies and greater degree of resonance overlap, the systems with tunable chaos, such as microwave cavities, acoustic blocks, or even elastomechanical devices [66], seem to provide appropriate tools for such studies.

Chapter 5

Cosmology

In this chapter we present analytical solution for time evolution of the gravitational wave damping in the early Universe due to freely streaming neutrinos in both early-time and late-time limit, as well as for the general case. In the extreme cases of early-time and late-time limits, the solution is represented by a convergent series of spherical Bessel functions of even order, which is not the case for the general solution. The derivation was possible with the help of a new compact formula for the convolution of spherical Bessel functions of integer order.

The results of this chapter are based on our work,
GS, arXiv:1204.1384 (2012).

5.1 Introduction

Thorough analysis of cosmic microwave background (CMB) radiation provides a unique test for the standard inflationary cosmological model [67–72]. While scalar fluctuations of CMB serve as an invaluable source for exploring density of matter and radiation and large-scale structure of the universe [73–78], observations of tensor fluctuations of CMB open a window for searching after a signature of gravitational waves [79–82].

The CMB observations done by Wilkinson Microwave Anisotropy Probe (WMAP) [83]

generally support theoretical predictions based on the standard inflationary cosmological model. The detailed analysis of the experimental data provides more and more accurate values [84–86] for the most valuable cosmological parameters, such as baryon density, total matter density, Hubble constant, and age of the Universe.

Independently of WMAP measurements, there is a long quest for a direct observation of cosmological gravitational waves [87]. The specially designed for this task Laser Interferometer Gravitational Wave Observatory (LIGO) puts a major effort in this experimental challenge [88]. A direct observation of cosmological gravitational waves would serve as a decisive test for validity of the Einstein general theory of relativity in the same way as the Michelson - Morley experiment served as a major proof for the Einstein special theory of relativity.

In this chapter we analyze the problem of gravitational wave damping in the early Universe due to freely streaming neutrinos in both early and late-time regime. The exact solution in the early-time limit is given by a convergent series of spherical Bessel functions of even order. In this limit the solution is independent of dimensionless parameter of momentum Q. The neutrino source perturbation does not change the qualitative behavior of the homogeneous gravitational wave damping solution but effectively changes its amplitude from unity to the corresponding asymptotic value.

The late-time limit solution is represented by a convergent series of spherical Bessel functions of even order and is Q-independent for large values of Q. Thus the prediction made by S. Weinberg concerning the Q-independent solution for the gravitational wave damping given by a series of even spherical Bessel functions is valid in both early and late-time limit.

S. Weinberg's predictions fails in the general case where we were able to construct the

solution in terms of an infinite series of the product of spherical Bessel function and reciprocal sum of the time parameter u and the parameter Q. Even though for large Q-values the series coefficients of the proposed solution are Q-independent, the solution for the gravitational wave damping depends on Q-value, and in general is represented by a linear combination of both even and odd spherical Bessel functions.

The constructed solution for the general case was possible due the nontrivial equality for the differential operator of the gravitational wave damping problem which upon its action onto the trial function returns the exact sum of its action onto the function in the early and late-time limits, which we consider as the main result of the present investigation.

5.2 Fluctuations in General Relativity

In this section we are interested in the Einstein field equation for the traceless and divergenceless part of the metric perturbation tensor $h_{ij}(\mathbf{x}, t)$ for the metric tensor $g_{\mu\nu}$, defined as

$$\begin{aligned} g_{00} &= -1, \\ g_{i0} &= 0, \\ g_{ij}(\mathbf{x}, t) &= a^2(t)\delta_{ij} + h_{ij}(\mathbf{x}, t), \end{aligned} \tag{5.1}$$

where $a(t)$ is the `Robertson--Walker` scale factor, which measures the expansion rate of the Universe.

In the subsequent section we derive the kinetic Boltzmann equation for the neutrino energy-momentum tensor π_{ij}^{T} which will be given in terms of the metric perturbation tensor

$h_{ij}(\mathbf{x},t)$. Finally we obtain the integro-differential equation for the metric perturbation $h_{ij}(\mathbf{x},t)$ which we subsequently build solution for.

The `Einstein` field equation,

$$R_{\mu\nu} = -8\pi G S_{\mu\nu}, \tag{5.2}$$

is given in terms of the `Ricci` tensor $R_{\mu\nu}$,

$$R_{\mu\nu} = \frac{\partial \Gamma^{\lambda}_{\lambda\mu}}{\partial x^{\nu}} - \frac{\partial \Gamma^{\lambda}_{\mu\nu}}{\partial x^{\lambda}} + \Gamma^{\lambda}_{\mu\sigma}\Gamma^{\sigma}_{\nu\lambda} - \Gamma^{\lambda}_{\mu\nu}\Gamma^{\sigma}_{\lambda\sigma}, \tag{5.3}$$

the shifted energy-momentum tensor $S_{\mu\nu}$,

$$S_{\mu\nu} = T_{\mu\nu} - \frac{1}{2} g_{\mu\nu} g^{\rho\sigma} T_{\rho\sigma}, \tag{5.4}$$

and `Newton` gravitational constant G. Here we have introduced the field $\Gamma^{\lambda}_{\mu\nu}$ known as the affine connection,

$$\Gamma^{\lambda}_{\mu\nu} = \frac{1}{2} g^{\lambda\rho} \left[\frac{\partial g_{\rho\mu}}{\partial x^{\nu}} + \frac{\partial g_{\rho\nu}}{\partial x^{\mu}} - \frac{\partial g_{\mu\nu}}{\partial x^{\rho}} \right]. \tag{5.5}$$

Below we introduce the unperturbed metrics and energy-momentum tensor which we label by a horizontal bar.

First we introduce the unperturbed Robertson–Walker metrics,

$$\begin{aligned} \overline{g}_{00} &= -1, \\ \overline{g}_{i0} &= \overline{g}_{0i} = 0, \\ \overline{g}_{ij}(t) &= a^2(t)\delta_{ij}, \end{aligned} \tag{5.6}$$

and the unperturbed energy-momentum tensor that is given in terms of energy density $\overline{\rho}$ and pressure $\overline{p}$,

$$\begin{aligned} \overline{T}_{00} &= \overline{\rho}, \\ \overline{T}_{i0} &= \overline{T}_{0i} = 0, \\ \overline{T}_{ij} &= \delta_{ij}\overline{p}. \end{aligned} \tag{5.7}$$

This parametrization ensures the existence of a local inertial Cartesian reference frame in which a moving perfect fluid is isotropic.

In terms of the velocity four-vector $\overline{u}_\mu$ that is defined in the co-moving inertial reference frame,

$$\begin{aligned} \overline{u}^0 &= 1, \\ \overline{u}^i &= 0, \end{aligned} \tag{5.8}$$

the unperturbed energy-momentum tensor can be conveniently written as

$$\overline{T}_{\mu\nu} = \overline{p}\,\overline{g}_{\mu\nu} + (\overline{p} + \overline{\rho})\,\overline{u}_\mu \overline{u}_\nu. \tag{5.9}$$

In *Appendix C* we derive the fundamental `Friedmann` equations which are given in terms of the unperturbed density $\overline{\rho}$ and pressure $\overline{p}$,

$$\overline{\rho} = \frac{3}{8\pi G}\left(\frac{\dot{a}^2}{a^2}\right), \tag{5.10}$$

$$\overline{p} = -\frac{1}{8\pi G}\left(\frac{2\ddot{a}}{a} + \frac{\dot{a}^2}{a^2}\right). \tag{5.11}$$

Therefore for the trace of the unperturbed energy-momentum tensor we have

$$\overline{T}^{\lambda}{}_{\lambda} = 4\overline{p} - (\overline{\rho} + \overline{p}) = 3\overline{p} - \overline{\rho} = -\frac{3}{4\pi G}\left(\frac{\ddot{a}}{a} + \frac{\dot{a}^2}{a^2}\right). \tag{5.12}$$

The perturbation to the shifted energy-momentum tensor, $\delta S_{\mu\nu}$, in the Einstein field equation (5.2) comes from perturbation to the energy momentum tensor $\delta T_{\mu\nu}$, perturbation to its trace, $\delta T^{\lambda}{}_{\lambda}$, and perturbation to the metrics $h_{\mu\nu}$,

$$\delta S_{\mu\nu} = \delta T_{\mu\nu} - \frac{1}{2}\overline{g}_{\mu\nu}\delta T^{\lambda}{}_{\lambda} - \frac{1}{2}h_{\mu\nu}\overline{T}^{\lambda}{}_{\lambda}. \tag{5.13}$$

Taking into account metrics (5.1), the components of the tensor $\delta S_{\mu\nu}$ are

$$\delta S_{jk} = \delta T_{jk} - \frac{a^2}{2}\delta_{jk}\delta T^{\lambda}{}_{\lambda} + \frac{3}{8\pi G}\left(\frac{\ddot{a}}{a} + \frac{\dot{a}^2}{a^2}\right)h_{jk}, \tag{5.14}$$

$$\delta S_{j0} = \delta T_{j0} + \frac{3}{8\pi G}\left(\frac{\ddot{a}}{a} + \frac{\dot{a}^2}{a^2}\right)h_{j0}, \tag{5.15}$$

$$\delta S_{00} = \delta T_{00} + \frac{1}{2}\delta T^{\lambda}{}_{\lambda} + \frac{3}{8\pi G}\left(\frac{\ddot{a}}{a} + \frac{\dot{a}^2}{a^2}\right)h_{00}. \tag{5.16}$$

Then the Einstein equation (5.2) for space-space components is

$$-8\pi G\left(\delta T_{jk}-\frac{a^2}{2}\delta_{jk}\delta T^{\lambda}{}_{\lambda}+\frac{3}{8\pi G}\left(\frac{\ddot{a}}{a}+\frac{\dot{a}^2}{a^2}\right)h_{jk}\right)=\delta R_{jk} \tag{5.17}$$

with the perturbation to the `Ricci` tensor

$$\begin{aligned}\delta R_{jk}=&-\frac{1}{2}\partial_j\partial_k h_{00}-(2\dot{a}^2+a\ddot{a})\delta_{jk}h_{00}-\frac{1}{2}a\dot{a}\delta_{jk}\dot{h}_{00} \\ &+\frac{1}{2a^2}\left(\nabla^2 h_{jk}-\partial_i\partial_j h_{ik}-\partial_i\partial_k h_{ij}+\partial_j\partial_k h_{ii}\right) \\ &-\frac{1}{2}\ddot{h}_{jk}+\frac{\dot{a}}{2a}(\dot{h}_{jk}-\delta_{jk}\dot{h}_{ii})+\left(\frac{\dot{a}^2}{a^2}\right)(-2h_{jk}+\delta_{jk}h_{ii})+\frac{\dot{a}}{a}\delta_{jk}\partial_i h_{i0} \\ &+\frac{1}{2}(\partial_j\dot{h}_{k0}+\partial_k\dot{h}_{j0}+\frac{\dot{a}}{2a}(\partial_j h_{k0}+\partial_k h_{j0}).\end{aligned} \tag{5.18}$$

The next step is to introduce the most general parametrization for the metrics perturbation,

$$h_{ij}=a^2\left[A\delta_{ij}+\frac{\partial^2 B}{\partial x^i\partial x^j}+\frac{\partial C_i}{\partial x^j}+\frac{\partial C_j}{\partial x^i}+D_{ij}\right], \tag{5.19}$$

$$h_{i0}=a\left[\frac{\partial F}{\partial x^i}+G_i\right], \tag{5.20}$$

$$h_{00}=-E. \tag{5.21}$$

For the traceless and divergenceless tensor perturbation,

$$\frac{\partial D_{ij}}{\partial x^i}=0, \tag{5.22}$$

$$D_{ii}=0, \tag{5.23}$$

$$D_{ij}=D_{ji}, \tag{5.24}$$

we are left only with

$$h_{ij} = a^2 D_{ij}, \tag{5.25}$$

while all other terms contribute only to scalar and vector perturbations. As a consequence, the metrics perturbation tremendously simplifies to

$$\begin{aligned} &3\left(\frac{\ddot{a}}{a} + \frac{\dot{a}^2}{a^2}\right) h_{jk} + \delta R_{jk} = \frac{1}{2a^2}\nabla^2 h_{jk} - \frac{1}{2}\ddot{h}_{jk} + \frac{\dot{a}}{2a}\dot{h}_{jk} + \left(\frac{3\ddot{a}}{a} + \frac{\dot{a}^2}{a^2}\right) h_{jk} \\ &= \frac{1}{2}\nabla^2 D_{jk} - \frac{a}{2}\left(3\dot{a}\dot{D}_{jk} + a\ddot{D}_{jk}\right). \end{aligned} \tag{5.26}$$

The most general perturbation to the energy-momentum tensor can be written as

$$\delta T_{ij} = \overline{p} h_{ij} + a^2\left[\delta_{ij}\delta p + \partial_i\partial_j \pi^S + \partial_i \pi_j^V + \partial_j \pi_i^V + \pi_{ij}^T\right], \tag{5.27}$$

$$\delta T_{i0} = \overline{p} h_{i0} - (\overline{\rho} + \overline{p})\left(\partial_i \delta u + \delta u_i^V\right), \tag{5.28}$$

$$\delta T_{00} = -\overline{\rho} h_{00} + \delta\rho. \tag{5.29}$$

where π^S, π_j^V, and π_{ij}^T are the scalar, vector and tensor perturbations, correspondingly. For the perturbation to the energy-momentum tensor $\delta T_{\mu\nu}$, there is only a single term π_{ij}^T, which satisfies the traceless and divergenceless conditions,

$$\frac{\partial \pi_{ij}^T}{\partial x^i} = 0, \tag{5.30}$$

$$\pi_{ii}^T = 0, \tag{5.31}$$

$$\pi_{ij}^T = \pi_{ji}^T. \tag{5.32}$$

The explicit form of the tensor perturbation π_{ij}^T will be found from the kinetic `Boltzmann`

equation in the subsequent section.

Finally we arrive at the desirable Einstein field equation for the metrics perturbation mode D_{jk} [89],

$$\nabla^2 D_{jk} - a^2 \ddot{D}_{jk} - 3a\dot{a}\dot{D}_{jk} = -16\pi G a^2 \pi^T_{jk}. \tag{5.33}$$

The obtained equation governs the metric perturbation tensor D_{jk} that is driven by the energy-momentum tensor perturbation π^T_{jk}.

5.3 Boltzmann equation for neutrinos

In this section our main interest is to obtain the neutrino energy-momentum tensor perturbation π^T_{jk} from the Boltzmann equation. Following S. Weinberg [89] we argue that the velocity of cold dark matter and baryonic plasma is too slow to make a contribution to anisotropic inertia tensor. Therefore the only contributions to the anisotropic inertia tensor are due to photons and neutrinos. Photons, however, have a short mean free time before the era of recombination [89], and therefore their contribution to the anisotropic inertia tensor is relatively small. As the result, we are left with neutrinos, which we assume to be massless, that represent the main source for perturbation to the anisotropic inertia tensor.

First we define the neutrino distribution function in the phase space as

$$n_\nu(\mathbf{x}, \mathbf{p}, t) \equiv \sum_r \left[\prod_{i=1}^{3} \delta\left(x^i - x^i_r(t)\right) \prod_{i=1}^{3} \delta\left(p^i - p^i_r(t)\right) \right], \tag{5.34}$$

where r labels a neutrino trajectory. From the momentum definition

$$p_r^\mu = \frac{dx_r^\mu}{du_r}, \tag{5.35}$$

where we used a scalar quantity u that specifies position along the particle trajectory, we obtain

$$\dot{x}_r^i = \frac{p_r^i}{p_r^0}. \tag{5.36}$$

The space-time trajectory satisfies the geodesic equation

$$\frac{d^2 x_r^\lambda}{du_r^2} + \Gamma_{\mu\nu}^\lambda(x_r)\frac{dx_r^\mu}{du_r}\frac{dx_r^\nu}{du_r} = 0, \tag{5.37}$$

which together with the affine connection (5.5) given in the components by

$$\Gamma_{ij}^k = \frac{1}{2}g^{kl}\left(\frac{\partial g_{li}}{\partial x^j} + \frac{\partial g_{lj}}{\partial x^i} - \frac{\partial g_{ij}}{\partial x^l}\right), \tag{5.38}$$

$$\Gamma_{i0}^j = \frac{1}{2}g^{jk}\dot{g}_{ki}, \tag{5.39}$$

$$\Gamma_{ij}^0 = \frac{1}{2}\dot{g}_{ij}, \tag{5.40}$$

defines the rate of the momentum change,

$$\dot{p}_{ri} = \frac{1}{2p_r^0}p_r^j p_r^k \left(\frac{\partial g_{jk}}{\partial x^i}\right)_{\mathbf{x}=\mathbf{x}_r}. \tag{5.41}$$

The neutrino number density is conserved, which can be expresses as

$$\frac{dn_\nu}{dt} = \frac{\partial n_\nu}{\partial t} + \frac{\partial n_\nu}{\partial x^i}\frac{p^i}{p^0} + \frac{\partial n_\nu}{\partial p_i}\frac{p^j p^k}{2p^0}\frac{\partial g_{jk}}{\partial x^i} = 0, \tag{5.42}$$

where we we have introduced the standard notations,

$$p^i = g^{ij}(\mathbf{x},t)p_j, \tag{5.43}$$
$$p^0 = \sqrt{g^{ij}(\mathbf{x},t)p_i p_j}.$$

Our goal is to derive the kinetic Boltzmann equation in the first order in metrics and density perturbation, $\delta g_{ij}(\mathbf{x},t)$ and $\delta n_\nu(\mathbf{x},t)$, correspondingly. In the following we denote an arbitrary perturbation to the metrics as

$$g_{ij}(\mathbf{x},t) = a^2(t)\delta_{ij} + \delta g_{ij}(\mathbf{x},t). \tag{5.44}$$

For the perturbation of the neutrino density we have

$$n_\nu(\mathbf{x},t) = \overline{n}_\nu[a(t)p] + \delta n_\nu(\mathbf{x},t), \tag{5.45}$$
$$\overline{n}_\nu(p) = \frac{1}{(2\pi)^3}\frac{1}{\exp\left[\frac{p}{a(t)}\frac{1}{k\overline{T}(t)}\right]+1}. \tag{5.46}$$

Then the Boltzmann equation for neutrinos to the first order in perturbations reads

$$\frac{\partial\delta n_\nu(\mathbf{x},\mathbf{p},t)}{\partial t} + \frac{\partial\delta n_\nu(\mathbf{x},\mathbf{p},t)}{\partial x^i}\frac{p_i}{a(t)p} \tag{5.47}$$
$$+\frac{\overline{n}'_\nu(p)}{2p}\frac{\partial}{\partial t}\left(a^2(t)\delta g^{ij}(\mathbf{x},t)\right)p_i p_j + \frac{\overline{n}'_\nu(p)}{2p}\frac{\partial}{\partial x^k}\left(a^2(t)\delta g^{ij}(\mathbf{x},t)\right)p_i p_j\frac{p_k}{a(t)p}$$
$$+\overline{n}'_\nu(p)\frac{p_i p_j p_k}{2a^3(t)p^2}\frac{\partial}{\partial x^k}\left(\delta g_{ij}(\mathbf{x},t)\right) = 0,$$

where

$$\overline{n}'_\nu(p) = \frac{\partial \overline{n}_\nu(p)}{\partial p}. \tag{5.48}$$

Up to the first order the inverse metric tensor is

$$g^{ij} = \frac{1}{a^2}\delta_{ij} - \frac{1}{a^4}\delta g_{ij}, \tag{5.49}$$

and we can greatly simplify the Boltzmann equation due to the following cancellation:

$$\begin{aligned} &\frac{\overline{n}'_\nu(p)}{2p}\frac{\partial}{\partial x^k}\left(a^2(t)\delta g^{ij}(\mathbf{x},t)\right)p_i p_j \frac{p_k}{a(t)p} + \overline{n}'_\nu(p)\frac{p_i p_j p_k}{2a^3(t)p^2}\frac{\partial}{\partial x^k}\left(\delta g_{ij}(\mathbf{x},t)\right) \\ &= \left(-\frac{1}{a^2(t)}\right)\overline{n}'_\nu(p)\frac{p_i p_j p_k}{2a(t)p^2}\frac{\partial}{\partial x^k}\left(\delta g_{ij}(\mathbf{x},t)\right) + \overline{n}'_\nu(p)\frac{p_i p_j p_k}{2a^3(t)p^2}\frac{\partial}{\partial x^k}\left(\delta g_{ij}(\mathbf{x},t)\right) = 0. \end{aligned} \tag{5.50}$$

Therefore we are left with

$$\frac{\partial \delta n_\nu(\mathbf{x},\mathbf{p},t)}{\partial t} + \frac{\partial \delta n_\nu(\mathbf{x},\mathbf{p},t)}{\partial x^i}\frac{p_i}{a(t)p} = \frac{\overline{n}'_\nu(p)}{2p}p_i p_j \frac{\partial}{\partial t}\left(\frac{1}{a^2(t)}\delta g_{ij}(\mathbf{x},t)\right). \tag{5.51}$$

Introducing the tensor perturbation

$$\delta g_{ij}(\mathbf{x},t) = h_{ij}(\mathbf{x},t) = a^2 D_{ij}(\mathbf{x},t), \tag{5.52}$$

and the unit vector along the momentum

$$\widehat{p_i} = \frac{p_i}{p}, \tag{5.53}$$

$$p \equiv \sqrt{p_i p_i}, \tag{5.54}$$

we arrive at the Boltzmann equation in the coordinate space,

$$\frac{\partial \delta n_\nu(\mathbf{x},\mathbf{p},t)}{\partial t} + \frac{\partial \delta n_\nu(\mathbf{x},\mathbf{p},t)}{\partial x^i}\frac{\widehat{p}_i}{a(t)} = \frac{1}{2}p\overline{n}'_\nu(p)\widehat{p}_i\widehat{p}_j\dot{D}_{ij}(\mathbf{x},t). \tag{5.55}$$

The next step is to introduce a dimensionless intensity perturbation $J(\mathbf{x},\widehat{p},t)$,

$$a^4(t)\overline{\rho}_\nu(t)J(\mathbf{x},\widehat{p},t) \equiv N_\nu \int_0^\infty \delta n_\nu(\mathbf{x},\mathbf{p},t)p^3 dp d^2\widehat{p}, \tag{5.56}$$

$$\overline{\rho}_\nu(t) \equiv \frac{N_\nu}{a^4(t)}\int_0^\infty dp\overline{n}_\nu(p)4\pi p^3. \tag{5.57}$$

Multiplying the Boltzmann equation (5.55) by $p^3 dp d^2\widehat{p}$ with subsequent integration over momentum p and performing integration by parts, we obtain for the right hand side

$$\begin{aligned}&\frac{1}{2}\widehat{p}_i\widehat{p}_j\dot{D}_{ij}(\mathbf{x},t)\int_0^\infty dp\overline{n}'_\nu(p)4\pi p^4 = -2\widehat{p}_i\widehat{p}_j\dot{D}_{ij}(\mathbf{x},t)\int_0^\infty dp\overline{n}_\nu(p)4\pi p^3 \\ &= -2\widehat{p}_i\widehat{p}_j\dot{D}_{ij}(\mathbf{x},t)\overline{\rho}_\nu(t)\frac{a^4(t)}{N_\nu}.\end{aligned} \tag{5.58}$$

As the result, the Boltzmann equation for the dimensionless neutrino density $J(\mathbf{x},\widehat{p},t)$ is [89]

$$\frac{\partial J(\mathbf{x},\widehat{p},t)}{\partial t} + \frac{\widehat{p}_i}{a(t)}\frac{\partial J(\mathbf{x},\widehat{p},t)}{\partial x^i} = -2\widehat{p}_i\widehat{p}_j\dot{D}_{ij}(\mathbf{x},t). \tag{5.59}$$

5.4 Momentum representation

Now we have all the tools we need to build the solution of the Boltzmann equation for the neutrino density. We introduce a stochastic amplitude for the single non-decaying mode with the wave number $\mathbf{q}$ and helicity λ,

$$\beta(\mathbf{q}, \lambda), \tag{5.60}$$

together with its local correlation,

$$\langle \beta(\mathbf{q}, \lambda) \beta^*(\mathbf{q}', \lambda') \rangle = \delta_{\lambda\lambda'} \delta^3 \left(\mathbf{q} - \mathbf{q}' \right). \tag{5.61}$$

Also we need the polarization tensor

$$e_{ij}(\widehat{q}, \lambda), \tag{5.62}$$

satisfying the traceless and divergenceless conditions automatically,

$$e_{ii} = 0, \tag{5.63}$$

$$q_i e_{ij} = 0. \tag{5.64}$$

In the following we transform the obtained Boltzmann equation (5.59) into the momentum representation.

First we need to introduce the notion of helicity, labeled by λ. The wave propagating in the direction $\widehat{k}$ is said to have a helicity λ if it bears an angular momentum $\hbar\lambda$ in the direction of flight. The traceless and divergenceless conditions for the metric perturbation

tensor in the momentum representation D^q_{ij} are

$$D^q_{ij} = D^q_{ji}, \tag{5.65}$$

$$D^q_{ii} = 0, \tag{5.66}$$

$$q_i D^q_{ij} = q_j D^q_{ij} = 0. \tag{5.67}$$

Under the rotation by an angle θ, the metric perturbation tensor in the momentum representation D^q_{ij} transforms as

$$D^q_{11} \mp D^q_{12} \longrightarrow e^{i\lambda\theta}\left[D^q_{11} \mp D^q_{12}\right], \tag{5.68}$$

$$\lambda = \pm 2.$$

Further we introduce the Fourier representation for the metric perturbation tensor $D_{ij}(\mathbf{x}, t)$,

$$D_{ij}(\mathbf{x}, t) = \sum_{\lambda=\pm 2} \int d^3q \exp\left(i\mathbf{qx}\right)\beta(\mathbf{q}, \lambda) e_{ij}(\widehat{q}, \lambda) D_q(t), \tag{5.69}$$

the Fourier representation for the anisotropic inertia tensor $\pi^T_{ij}(\mathbf{x}, t)$,

$$\pi^T_{ij}(\mathbf{x}, t) = \sum_{\lambda=\pm 2} \int d^3q \exp\left(i\mathbf{qx}\right)\beta(\mathbf{q}, \lambda) e_{ij}(\widehat{q}, \lambda) \pi^T_q(t), \tag{5.70}$$

and the Fourier representation for dimensionless neutrino density function $J(\mathbf{x}, \widehat{p}, t)$,

$$J(\mathbf{x}, \widehat{p}, t) = \sum_{\lambda=\pm 2} \int d^3q \exp\left(i\mathbf{qx}\right)\beta(\mathbf{q}, \lambda) e_{ij}(\widehat{q}, \lambda) \widehat{p}_i \widehat{p}_j J_q(q, \widehat{p} \cdot \widehat{q}, t). \tag{5.71}$$

As the result, the momentum representation of the Boltzmann equation (5.59) for the neutrino density $J_q(q, \widehat{p}\cdot\widehat{q}, t)$ becomes the first-order differential equation,

$$\dot{J}_q(q, \widehat{p}\cdot\widehat{q}, t) + i\widehat{p}\cdot\widehat{q}\frac{q}{a(t)}J_q(q, \widehat{p}\cdot\widehat{q}, t) = -2\dot{D}_q(t). \tag{5.72}$$

Performing a simple algebra with an integrating factor,

$$\begin{aligned} &\exp\left[-iq\widehat{p}\cdot\widehat{q}\int_{t_0}^{t}\frac{dt''}{a(t'')}\right]\int_{t_0}^{t}dt'\exp\left[iq\widehat{p}\cdot\widehat{q}\int_{t_0}^{t'}\frac{dt''}{a(t'')}\right]\dot{D}_q(t') \qquad (5.73)\\ &=\int_{t_0}^{t}dt'\exp\left[-iq\widehat{p}\cdot\widehat{q}\int_{t'}^{t}\frac{dt''}{a(t'')}\right]\dot{D}_q(t'), \end{aligned}$$

we obtain the solution of the Boltzmann equation for the neutrino density,

$$J_q(q, \widehat{p}\cdot\widehat{q}, t) = -2\int_{t_0}^{t}dt'\exp\left[-iq\widehat{p}\cdot\widehat{q}\int_{t'}^{t}\frac{dt''}{a(t'')}\right]\dot{D}_q(t'). \tag{5.74}$$

5.5 Perturbations to the energy-momentum tensor

In this section we shall find the neutrino stress-energy tensor in the momentum representation $\pi_q^T(t)$. The first-order perturbations to the energy-momentum tensor are

$$\delta T^i{}_j = \frac{1}{a^4(t)} \int \left(\prod_{k=1}^{3} dp_k \right) \delta n_\nu(\mathbf{x}, \mathbf{p}, t) \frac{p_i p_j}{p}, \tag{5.75}$$

$$\delta T^0{}_j = \frac{1}{a^4(t)} \int \left(\prod_{k=1}^{3} dp_k \right) \delta n_\nu(\mathbf{x}, \mathbf{p}, t) p_j, \tag{5.76}$$

$$\delta T^0{}_0 = \frac{1}{a^4(t)} \int \left(\prod_{k=1}^{3} dp_k \right) \delta n_\nu(\mathbf{x}, \mathbf{p}, t) p. \tag{5.77}$$

For our purpose we need only the tensor part $\delta T^i{}_j$ that can be simplified as

$$\delta T^i{}_j = \frac{1}{a^4(t)} \int \left(\prod_{k=1}^{3} dp_k \right) a^2(t) \delta n_\nu(\mathbf{x}, \mathbf{p}, t) p \widehat{p}_i \widehat{p}_j. \tag{5.78}$$

Recalling the definition of the dimensionless intensity perturbation $J(\mathbf{x}, \widehat{p}, t)$, eq. (5.56), we obtain for the tensor perturbation $\delta T^i{}_j$

$$\begin{aligned} &\delta T^i{}_j = \\ &= \frac{1}{a^4(t)} \int \left(\prod_{k=1}^{3} dp_k \right) \delta n_\nu(\mathbf{x}, \mathbf{p}, t) p \widehat{p}_i \widehat{p}_j = \overline{\rho}_\nu(t) \int \frac{d^2\widehat{p}}{4\pi} J(\mathbf{x}, \widehat{p}, t) \widehat{p}_i \widehat{p}_j \\ &= \overline{\rho}_\nu(t) \sum_{\lambda=\pm 2} \int d^3q \exp(i\mathbf{q}\mathbf{x}) \beta(\mathbf{q}, \lambda) e_{kl}(\widehat{q}, \lambda) \int \frac{d^2\widehat{p}}{4\pi} \widehat{p}_i \widehat{p}_j \widehat{p}_k \widehat{p}_l J_q(q, \widehat{p} \cdot \widehat{q}, t). \end{aligned} \tag{5.79}$$

The algebra of the polarization tensor $e_{kl}(\widehat{q})$ simplifies the task,

$$\int d^2\widehat{p}\ f(\widehat{p}\cdot\widehat{q})\widehat{p}_i\widehat{p}_k e_{jk}(\widehat{q}) = \frac{1}{2}e_{ij}(\widehat{q})\int d^2\widehat{p}\ f(\widehat{p}\cdot\widehat{q})\left(1-(\widehat{p}\cdot\widehat{q})^2\right), \quad (5.80)$$

$$\int d^2\widehat{p}\ f(\widehat{p}\cdot\widehat{q})\widehat{p}_i\widehat{p}_j\widehat{p}_k\widehat{p}_l e_{kl}(\widehat{q}) = \frac{1}{4}e_{ij}(\widehat{q})\int d^2\widehat{p}\ f(\widehat{p}\cdot\widehat{q})\left(1-(\widehat{p}\cdot\widehat{q})^2\right)^2. \quad (5.81)$$

As the result we have for the tensor perturbation

$$\delta T^i{}_j = \overline{\rho}_\nu(t)\sum_{\lambda=\pm 2}\int d^3q \exp\left(i\mathbf{qx}\right)\beta(\mathbf{q},\lambda)e_{ij}(\widehat{q}) \quad (5.82)$$
$$\times\frac{1}{4}\int\frac{d^2\widehat{p}}{4\pi}\ \left(1-(\widehat{p}\cdot\widehat{q})^2\right)^2 J_q(q,\widehat{p}\cdot\widehat{q},t),$$

and with the obtained earlier solution of the Boltzmann equation for the neutrino density $J_q(q,\mu,t)$, eq. (5.74), we have

$$\delta T^i{}_j = \overline{\rho}_\nu(t)\sum_{\lambda=\pm 2}\int d^3q \exp\left(i\mathbf{qx}\right)\beta(\mathbf{q},\lambda)e_{ij}(\widehat{q}) \quad (5.83)$$
$$\times\left(\frac{-2}{4}\right)\int\frac{d^2\widehat{p}}{4\pi}\ \left(1-(\widehat{p}\cdot\widehat{q})^2\right)^2\int_{t_0}^{t}dt'\exp\left[-iq(\widehat{p}\cdot\widehat{q})\int_{t'}^{t}\frac{dt''}{a(t'')}\right]\dot{D}_q(t').$$

In the obtained expression for the tensor perturbation we can perform the surface integration

$$I(u)\equiv\int\frac{d^2\widehat{p}}{4\pi}\ \left(1-(\widehat{p}\cdot\widehat{q})^2\right)^2\exp\left[-iq(\widehat{p}\cdot\widehat{q})\int_{t'}^{t}\frac{dt''}{a(t'')}\right]. \quad (5.84)$$

Introducing the time variable u and the angle variable s,

$$u = q \int_{t'}^{t} \frac{dt''}{a(t'')}, \tag{5.85}$$

$$s = (\widehat{p} \cdot \widehat{q}), \tag{5.86}$$

and, owing to the azimuthal symmetry,

$$d^2\widehat{p} = 2\pi ds, \tag{5.87}$$

we express the surface integral $I(u)$ in terms of spherical Bessel functions $j_n(u)$,

$$\begin{aligned} I(u) &= \int_{-1}^{1} \frac{ds}{2} \left(1 - s^2\right)^2 \exp\left[-ius\right] \\ &= \left(-\frac{8}{u^5}\right) \left[3u\cos u + \left(u^2 - 3\right)\sin u\right] \\ &= 8\frac{j_2(u)}{u^2} = 8\left(\frac{1}{15}j_0(u) + \frac{2}{21}j_2(u) + \frac{1}{35}j_4(u)\right). \end{aligned} \tag{5.88}$$

Finally the tensor perturbation simplifies to

$$\delta T^i{}_j = \sum_{\lambda=\pm 2} \int d^3q \exp\left(i\mathbf{qx}\right)\beta(\mathbf{q},\lambda)e_{ij}(\widehat{q}) \tag{5.89}$$

$$\times(-4)\overline{\rho}_\nu(t) \int_{t_0}^{t} dt' K\left(q\int_{t'}^{t} \frac{dt''}{a(t'')}\right)\dot{D}_q(t'),$$

with the kernel

$$K(u) \equiv \frac{1}{15}j_0(u) + \frac{2}{21}j_2(u) + \frac{1}{35}j_4(u). \tag{5.90}$$

Recalling the momentum representation of the anisotropic inertia tensor $\pi^T_{ij}(\mathbf{x}, t)$, eq. (5.70), we arrive at the neutrino stress-energy tensor in the momentum representation

$$\pi^T_q(t) = -4\overline{\rho}_\nu(t) \int_0^t dt' K \left(q \int_{t'}^t \frac{dt''}{a(t'')} \right) \dot{D}_q(t'). \tag{5.91}$$

In terms of the time variable u it looks like [89]

$$\pi^T_q(u) = -4\overline{\rho}_\nu(u) \int_0^u dU K\left(u - U\right) D'_q(U), \tag{5.92}$$

which is nothing but the convolution integral of the kernel $K(u)$, eq. (5.90), and the time derivative of the metrics perturbation $D_q(u)$.

5.6 Gravitational wave damping

The Einstein field equation for the tensor perturbation is given by eq. (5.33). Recalling the Fourier representations for the metric perturbation tensor $D_{ij}(\mathbf{x},t)$, eq. (5.69), and for the anisotropic inertia tensor $\pi^T_{ij}(\mathbf{x},t)$, eq. (5.70), we obtain the gravitational wave damping equation in the momentum representation

$$\ddot{D}_q(t)+\frac{3\dot{a}}{a}\dot{D}_q(t)+\frac{q^2}{a^2}D_q(t)=-64\pi G\overline{\rho}_\nu(t)\int_0^t dt' K\left(q\int_{t'}^t\frac{dt''}{a(t'')}\right)\dot{D}_q(t'), \tag{5.93}$$

where the kernel $K(u)$ is given by (5.90). In terms of the time variable u, eq. (5.85), the left hand side of the gravitational wave equation transforms as

$$\begin{aligned}&\ddot{D}_q(t)+\frac{3\dot{a}}{a}\dot{D}_q(t)+\frac{q^2}{a^2}D_q(t) \\ &=\left(\frac{q}{a(u)}\right)^2\left[D''_q(u)+2\left(\frac{a'(u)}{a(u)}\right)D'_q(u)+D_q(u)\right].\end{aligned} \tag{5.94}$$

As the result, we obtain the gravitational wave equation entirely in terms of the variable u,

$$\begin{aligned}&D''(u)+2\left(\frac{a'(u)}{a(u)}\right)D'(u)+D(u) \\ &=-64\pi G\left(\frac{a(u)}{q}\right)^2\overline{\rho}_\nu(u)\int_0^u dU K\left(u-U\right)D'(U).\end{aligned} \tag{5.95}$$

In terms of the `Hubble` expansion rate,

$$H(t)=\frac{\dot{a}(t)}{a(t)}, \tag{5.96}$$

and the time variable u, the Friedmann equation for the unperturbed energy density $\overline{\rho}$ becomes

$$\overline{\rho} = \frac{3}{8\pi G} H^2(t) = \frac{3}{8\pi G} \left(\frac{\dot{a}^2(t)}{a^2(t)} \right) = \frac{3}{8\pi G} \left(\frac{q}{a(u)} \frac{a'(u)}{a(u)} \right)^2, \tag{5.97}$$

and therefore the energy-momentum prefactor in eq. (5.95) can be expressed as

$$\begin{aligned} & -64\pi G \left(\frac{a(u)}{q} \right)^2 \overline{\rho}_\nu(u) \\ & = -64\pi G \left(\frac{a(u)}{q} \right)^2 H^2(t) \frac{\overline{\rho}_\nu(u)}{\overline{\rho}} \frac{3}{8\pi G} = -24 \frac{\overline{\rho}_\nu(u)}{\overline{\rho}} \left(\frac{a'(u)}{a(u)} \right)^2. \end{aligned} \tag{5.98}$$

Finally we obtain the gravitational wave equation

$$D''(u) + 2 \left(\frac{a'(u)}{a(u)} \right) D'(u) + D(u) = -24 \frac{\overline{\rho}_\nu(u)}{\overline{\rho}} \left(\frac{a'(u)}{a(u)} \right)^2 \int_0^u dU K\,(u - U)\, D'(U). \tag{5.99}$$

The unperturbed equilibrium neutrino and photon energy density, $\overline{\rho}_\nu(u)$ and $\overline{\rho}_\gamma(u)$, correspondingly, define the ratio

$$f_\nu(0) \equiv \frac{\overline{\rho}_\nu(u)}{\overline{\rho}} = \frac{\overline{\rho}_\nu}{\overline{\rho}_\nu + \overline{\rho}_\gamma} = \frac{3 \left(\frac{7}{8} \right) \left(\frac{4}{11} \right)^{4/3}}{1 + 3 \left(\frac{7}{8} \right) \left(\frac{4}{11} \right)^{4/3}} \simeq 0.40523, \tag{5.100}$$

which we refer to *Appendix D* for details.

It is convenient to use the dimensionless quantity

$$\begin{aligned} & y \equiv \frac{a(t)}{a_{eq}}, \\ & a_{eq} = a(t = t_{eq}), \end{aligned} \tag{5.101}$$

where t_{eq} is the time of matter-radiation equality, which will be discussed in the next section.

Introducing Q as the ratio of the wave number to its value at the time of matter-radiation equality,

$$\begin{aligned} Q &= \sqrt{2}\frac{q}{q_{eq}}, \\ q_{eq} &= a_{eq}H_{eq}, \end{aligned} \tag{5.102}$$

and owing to

$$\frac{du}{dy} = \frac{Q}{\sqrt{1+y}}, \tag{5.103}$$

we obtain

$$\begin{aligned} &(1+y)\frac{d^2D(y)}{dy^2} + \left(\frac{2(1+y)}{y} + \frac{1}{2}\right)\frac{dD(y)}{dy} + Q^2D(y) \\ &= -\frac{24f_\nu(0)}{y^2}\int_0^y K\left(2Q\left(\sqrt{1+y} - \sqrt{1+y'}\right)\right)\frac{dD(y')}{dy'}dy'. \end{aligned} \tag{5.104}$$

With the change of variable

$$y = \frac{u(u+4Q)}{4Q^2}, \tag{5.105}$$

we may rewrite the obtained equation in a more convenient form,

$$\begin{aligned} &\frac{d^2D(u)}{du^2} + \left(\frac{4(u+2Q)}{u(u+4Q)}\right)\frac{dD(u)}{du} + D(u) \\ &= -24f_\nu(0)\left(\frac{4Q}{u(u+4Q)}\right)^2\int_0^u K(u-U)\frac{dD(U)}{dU}dU, \end{aligned} \tag{5.106}$$

with the kernel $K(u)$ given by eq. (5.90), and the initial conditions

$$D(0) = 1, \tag{5.107}$$
$$\left.\frac{dD(u)}{du}\right|_{u=0} = 0.$$

5.7 Matter-radiation equality

Matter-radiation equality corresponds to moment at which ratio of the co-moving wavenumber q to the expansion rate a becomes equal to the Hubble expansion rate H,

$$\frac{q}{a(t)} = H(t), \tag{5.108}$$
$$t \equiv t_{eq}. \tag{5.109}$$

By integrating eq. (5.108) over time we can express the matter-radiation equality in terms of the time variable u,

$$u(t_{eq}) = q\int_0^{t_{eq}} \frac{dt'}{a(t')} = \int_0^{t_{eq}} H(t')dt' = \int_0^{t_{eq}} \frac{\dot{a}(t')}{a(t')}dt' = \ln\left[\frac{a(t_{eq})}{a(0)}\right] \tag{5.110}$$

The early-time limit, $u \ll Q$, that corresponds to the long wavelengths, or equivalently to the lower-bound wavenumbers $q \ll q_{eq}$, while the late-time limit, $u \gg Q$, that is referred to the short wavelengths, corresponds to the upper-bound wavenumbers $q \gg q_{eq}$.

In order to find the value for q_{eq} we must recall the black-body spectrum, which is formulated in terms of the number density of photons $n_T(\nu)$ being in equilibrium with

matter at a temperature T,

$$n_T(\nu)d\nu = \frac{8\pi\nu^2 d\nu}{\exp\left(\frac{2\pi\hbar\nu}{kT}\right) - 1}, \tag{5.111}$$

with Planck constant $\hbar$ and Boltzmann constant k. The energy density of the black body radiation is

$$\rho(T) = \int_0^\infty 2\pi\hbar\nu n_T(\nu)d\nu = a_B T^4, \tag{5.112}$$

$$a_B = \frac{4\sigma}{c} = \frac{8\pi^5 k^4}{15(2\pi\hbar c)^3}, \tag{5.113}$$

where σ is the Stefan-Boltzmann constant,

$$\sigma = \frac{2\pi^5 k^4 c}{15(2\pi\hbar c)^3}. \tag{5.114}$$

The maximum of the black-body radiation at the present moment corresponds to the temperature $T_{\gamma 0}$,

$$T_{\gamma 0} = 2.725 \text{ K}, \tag{5.115}$$

which specifies the energy density at the present moment,

$$\rho_0 = a_B T_{\gamma 0}^4. \tag{5.116}$$

For sake of convenience we introduce the Hubble constant H_0,

$$H_0 = \frac{\dot{a}(t_0)}{a(t_0)}, \tag{5.117}$$

in units of $100\ \frac{\text{km}}{\text{s Mpc}}$ and denote it as h,

$$h = H_0 \times \left(100 \frac{\text{km}}{\text{s Mpc}}\right)^{-1}. \tag{5.118}$$

In the general case the critical energy density ρ is given by the Friedmann equation and it consists of a mixture of vacuum energy, non-relativistic matter, and radiation,

$$\rho = \frac{3}{8\pi G} H_0^2 \left[\Omega_\Lambda + \Omega_M \left(\frac{a_0}{a}\right)^3 + \Omega_R \left(\frac{a_0}{a}\right)^4\right], \tag{5.119}$$

where present date quantities are labeled by a zero index. The present values for energy density of vacuum, non-relativistic matter, and radiation are given by

$$\rho_{\Lambda 0} = \frac{3}{8\pi G} H_0^2 \Omega_\Lambda, \tag{5.120}$$

$$\rho_{M0} = \frac{3}{8\pi G} H_0^2 \Omega_M, \tag{5.121}$$

$$\rho_{R0} = \frac{3}{8\pi G} H_0^2 \Omega_R, \tag{5.122}$$

and according to the general Friedmann equation we have constraint for some of Ω-ratios,

$$\Omega_\Lambda + \Omega_M + \Omega_R + \Omega_K = 1, \tag{5.123}$$

$$\Omega_K \equiv -\frac{K}{(a_0 H_0)^2}, \tag{5.124}$$

where K is the curvature constant. Owing to eqs. (5.119) and (5.116) we get the expansion

rate for the radiation-dominated universe filled by photons and neutrinos, we have

$$H(t) = \frac{\dot{a}(t)}{a(t)} = H_0\sqrt{\Omega_R \frac{T^4}{T_{\gamma 0}^4}} = 2.1 \times 10^{-20}\ \mathrm{s}^{-1}\frac{T^2}{T_{\gamma 0}^2}. \tag{5.125}$$

Now we introduce the ratio of the photon and neutrino mass density to the total mass density $\rho_{M0} = \Omega_M \rho_0$,

$$\frac{\rho_{R0}}{\rho_{M0}} = \frac{\Omega_R}{\Omega_M} = 4.15 \times 10^{-5}\frac{1}{\Omega_M h^2}. \tag{5.126}$$

The redshift of the matter-radiation equality is

$$1 + z_{eq} = \frac{\Omega_M}{\Omega_R} = \frac{\Omega_M h^2}{4.15 \times 10^{-5}}. \tag{5.127}$$

During the radiation-dominated era we get the expansion rate

$$H(t) = 2.1 \times 10^{-20}\ (1+z)^2 \mathrm{s}^{-1}. \tag{5.128}$$

At the matter-radiation equality, the matter energy density is larger then the radiation energy density, and as the result Hubble constant acquires additional $\sqrt{2}$,

$$\begin{aligned} \frac{q_{eq}}{a_{eq}} &= H_{eq} = \sqrt{2} \times 2.1 \times 10^{-20}\ (1+z_{eq})^2 \mathrm{s}^{-1} \\ &= 1.72 \times 10^{-11} (\Omega_M h^2)^2 \mathrm{s}^{-1}, \end{aligned} \tag{5.129}$$

which corresponds to the critical wavelength λ_0,

$$\lambda_0 = 2\pi\frac{a_0}{q_{eq}} = 2\pi\frac{a_{eq}}{q_{eq}}(1+z_{eq}) = 85(\Omega_M h^2)^{-1}\mathrm{Mpc}. \tag{5.130}$$

5.8 Late-time evolution of the gravitational wave damping

In the late-time regime, $u \gg Q \gg 1$, the general eq. (5.106) simplifies into

$$u^4\left(\frac{d^2D(u)}{du^2} + \frac{4}{u}\frac{dD(u)}{du} + D(u)\right) = \alpha\int_0^u K(u-U)\frac{dD(U)}{dU}dU, \tag{5.131}$$

where

$$\alpha \equiv -24 f_\nu(0)(4Q)^2. \tag{5.132}$$

Below we present the analytical solution for eq. (5.131) together with boundary conditions (5.107).

We need to find a specific function that would "absorb" all derivatives d/du and all powers of u in the left hand side of eq. (5.131). For the differential operator that appears in the left hand side of eq. (5.131),

$$L = u^4\left(\frac{d^2}{du^2} + \frac{4}{u}\frac{d}{du} + 1\right), \tag{5.133}$$

these conditions can be satisfied with the function

$$f_n(u) = \frac{n(n+3)}{2n-1}[j_{n-2}(u)+j_n(u)] + \frac{(n-2)(n+1)}{2n+3}[j_n(u)+j_{n+2}(u)], \tag{5.134}$$

where $j_n(u)$ is the spherical Bessel function of the order n.

Applying the differential operator (5.133) to the function (5.134) we obtain a single spherical Bessel function

$$L[f_n(u)] = n(n-2)(n+1)(n+3)(2n+1)j_n(u) \tag{5.135}$$

which is exactly what we are looking for.

Here we shall note that the functions $f_n(u)$, eq. (5.134), are not eigenfunctions of the differential operator L, eq. (5.133), as one can see from eq. (5.135). However, the system of spherical Bessel functions forms a complete set and therefore one can decompose any function f_n in a linear combination of those. The differential operator L is linear and therefore its action onto a sum of spherical Bessel functions returns a sum of those. We will see that the right hand side of eq. (5.131) can be represented by a series of spherical Bessel functions. As a result we will have to identify coefficients in front of each spherical Bessel function. Each of these coefficients is evaluated by the orthogonal property of spherical Bessel functions and therefore determined uniquely.

Therefore we can look for the solution of eq. (5.131) in terms of the expansion

$$D(u) = \sum_{n=0}^{\infty} c_n \left(\frac{n(n+3)}{2n-1}[j_{n-2}(u) + j_n(u)] + \frac{(n-2)(n+1)}{2n+3}[j_n(u) + j_{n+2}(u)] \right). \tag{5.136}$$

The left hand side of eq. (5.131) transforms into

$$\sum_{n=0}^{\infty} n(n-2)(n+1)(n+3)(2n+1)c_n j_n(u). \tag{5.137}$$

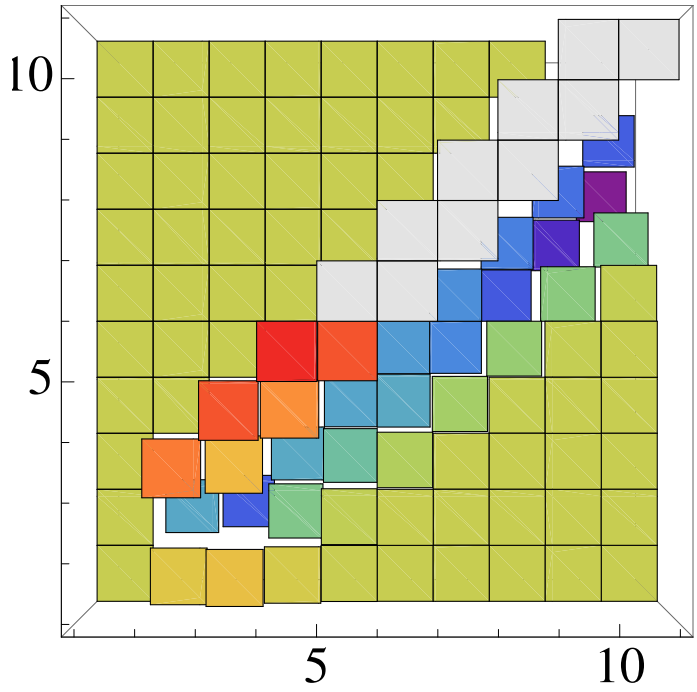

Figure 5.1: Graphical representation for the upper but one triangular structure of the matrix $B_{2k,2l}$, eq. (70). The matrix indices l and k define a position of the matrix element in the xy-plane, while along z-axis we plot its value.

The regular at the origin solution for the homogeneous part of eq. (5.131),

$$D_0''(u) + \frac{4}{u} D_0'(u) + D_0(u) = 0, \tag{5.138}$$

is the sum of the two spherical Bessel functions,

$$D_0(u) = j_0(u) + j_2(u). \tag{5.139}$$

The homogenous part $D_0(u)$ of the general solution $D(u)$ can be already seen as a linear combination of the first two terms in the expansion (5.136) for $n = 0$ and $n = 2$.

The right hand side of eq. (5.131) is represented by the convolution of the kernel (5.90) with the first derivative of the unknown function $D(u)$ which we are looking for in terms

of the series (5.136). We must have a mathematical tool that relates a convolution of spherical Bessel functions to a series of those. In *Appendix E* we prove a useful formula for the convolution of spherical Bessel functions, that is not presented in the mathematical literature:

$$J_{n,m}(u) \equiv \int_0^u dU j_m(u-U) j_n(U) = \tag{5.140}$$
$$= \frac{4(-i)^{n+m}}{2i} \sum_{l=0}^{\infty} (2l+1) i^l j_l(u)$$
$$\times \left(\sum_{\substack{L=|l-m| \\ L-n-1\geq 0}}^{L=l+m} \frac{\langle l,0,m,0|L,0\rangle^2}{L+L^2-n(1+n)} + \sum_{\substack{L=|l-n| \\ m-L-1\geq 0}}^{L=l+n} \frac{\langle l,0,n,0|L,0\rangle^2}{L+L^2-m(1+m)} \right),$$

where $\langle l,0,m,0|L,0\rangle$ are the Clebsch-Gordan coefficients.

The right hand side of eq. (5.131) is

$$\alpha \int_0^u K(u-U) \frac{dD(U)}{dU} dU = \alpha \sum_{\substack{l=0 \\ l\in \text{even}}}^{\infty} j_l(u) \sum_{\substack{k=0 \\ k\in \text{even}}}^{l+2} B_{k,l} c_k. \tag{5.141}$$

By the aid of eq. (5.140) matrix $B_{k,l}$ is generated by the convolution of the first derivative of the function $D(u)$,

$$D'(u) = \tag{5.142}$$
$$= \sum_n c_n \left(j_{n-3}(u) \frac{(-2+n)n(3+n)}{(-3+2n)(-1+2n)} + j_{n-1}(u) \frac{n\left(-3-4n+n^2\right)}{(-3+2n)(3+2n)} \right.$$
$$\left. + j_{n+1}(u) \frac{(-1-n)\left(2+6n+n^2\right)}{(-1+2n)(5+2n)} + j_{n+3}(u) \frac{(-1-n)(-2+n)(3+n)}{(3+2n)(5+2n)} \right),$$

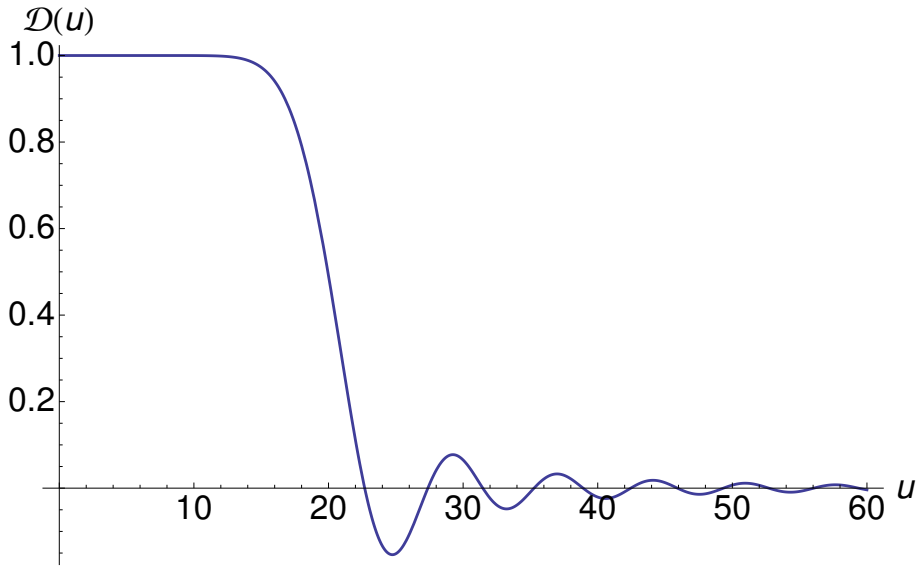

Figure 5.2: Late-time evolution of the gravitational wave damping $D(u)$ in the early Universe.

with the kernel (5.90) and for integer $k \in [0, 10]$ and $l \in [0, 10]$ is given by eq. (70) in *Appendix F*.

We should notice an unpleasant feature of the matrix of coefficients (70): the first row up to a factor $k = -5$ is identical to the second row. This is a direct response to the symmetry of the introduced function $f_n(u)$, eq. (5.178). The functions $f_n(u)$ for $n = 0$ and $n = 2$ are exactly the same up to the factor $k = -5$,

$$f_0(u) = -\frac{2}{3}(j_0(u) + j_2(u)), \qquad (5.143)$$
$$f_2(u) = \frac{10}{3}(j_0(u) + j_2(u)).$$

Therefore the rank of the matrix (70) is $\texttt{Rank}[B] = N - 1$. This is a real obstacle because it leads to inconsistency with the boundary conditions. Indeed, the boundary conditions

(5.107) are met if we set

$$-\frac{2}{3}c_0 + \frac{10}{3}c_2 = 1. \tag{5.144}$$

On the other hand, the linear dependence of the matrix is equivalent to

$$-\frac{2}{3}c_0 + \frac{10}{3}c_2 = 0. \tag{5.145}$$

In order to avoid this unpleasant feature we can start summation in the series (5.136) from $n = 2$ instead of $n = 0$ which is equivalent to setting

$$c_0 \equiv 0, \tag{5.146}$$

and thus the boundary conditions (5.107) are met if we set

$$c_2 = \frac{3}{10}. \tag{5.147}$$

Absence of the $j_2(u)$ term in the left hand side of eq. (5.137) leads to a restriction on the first coefficients in eq. (5.141)

$$-\frac{1}{3}c_2 + \frac{4}{15}c_4 = 0. \tag{5.148}$$

Finally we get the system of linear equations for even integers $n \geq 0$,

$$n(n-2)(n+1)(n+3)(2n+1)c_n = \alpha \sum_{\substack{k=0 \\ k\in\text{even}}}^{n+2} B_{k,n}c_k \tag{5.149}$$

that returns the solution (for even n and k)

$$c_{n+2} = \frac{n(n-2)(n+1)(n+3)(2n+1)c_n - \alpha \sum^{n}_{\substack{k=0 \\ k\in\text{even}}} B_{k,n}c_k}{\alpha B_{n+2,n}}. \quad (5.150)$$

In the limit $Q \gg 1$ and owing to $\alpha \equiv -24 f_\nu(0)(4Q)^2$ we have the Q-independent solution

$$c_{n+2} = -\frac{\sum^{n}_{\substack{k=0 \\ k\in\text{even}}} B_{k,n}c_k}{B_{n+2,n}}, \quad (5.151)$$

and therefore for $n \in [0, 9]$ we have

$$c_{2n} = \left\{0, \frac{3}{10}, \frac{3}{8}, \frac{5}{16}, \frac{35}{128}, \frac{63}{256}, \frac{231}{1024}, \frac{429}{2048}, \frac{6435}{32768}, \frac{12155}{65536}\right\} \quad (5.152)$$

which completes our series solution (5.136).

5.9 Early-time evolution of the gravitational wave damping

In this section we rederive the known solution [92] for the graviational wave damping in the early-time limit, $u \ll Q$. In this limit eq. (5.106) becomes

$$u^2\left(\frac{d^2D(u)}{du^2} + \frac{2}{u}\frac{dD(u)}{du} + D(u)\right) = \beta \int_0^u K(u-U)\frac{dD(U)}{dU}dU, \quad (5.153)$$

where

$$\beta \equiv -24 f_\nu(0). \tag{5.154}$$

We shall present the analytical solution for eq. (5.153) together with boundary conditions (5.107). Recalling the differential equation for the spherical Bessel function $j_n(u)$,

$$u^2 \left(\frac{d^2 j_n(u)}{du^2} + \frac{2}{u} \frac{d j_n(u)}{du} + j_n(u) \right) - n(n+1) j_n(u) = 0, \tag{5.155}$$

we will look for a solution in terms of a series of spherical Bessel functions

$$D(u) = \sum_{n=0}^{\infty} c_n j_n(u). \tag{5.156}$$

The left hand side of eq. (5.153) transforms into

$$\sum_{n=0}^{\infty} n(n+1) c_n j_n(u). \tag{5.157}$$

The right hand side of eq. (5.153) is represented by the convolution of the kernel (5.90) with the first derivative of the unknown function $D(u)$ which we are looking for in terms of a series (5.156).

The right hand side of eq. (5.153) is

$$\beta \sum_{\substack{l=0 \\ l \in \text{even}}}^{\infty} j_l(u) \sum_{\substack{k=0 \\ k \in \text{even}}}^{l} F_{k,l} c_k, \tag{5.158}$$

where the matrix $F_{k,l}$ is obtained by the convolution of the kernel (5.90) with the first

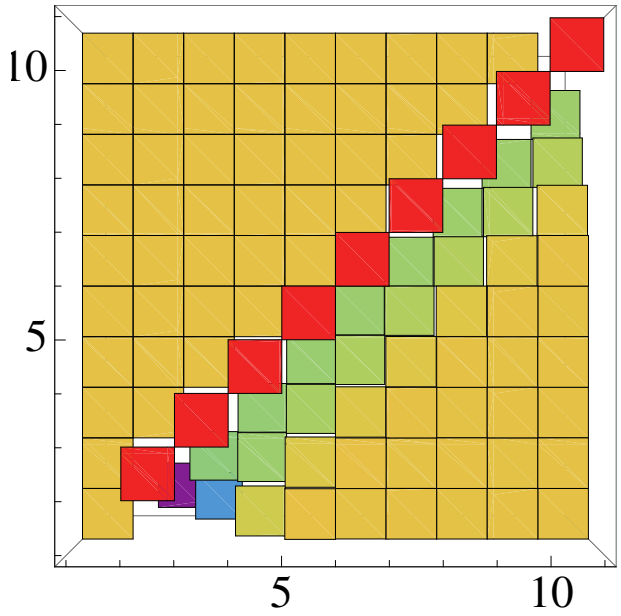

Figure 5.3: Graphical representation for the upper triangular structure of the matrix $F_{2k,2l}$, eq. (72). The matrix indices l and k define the position of the matrix element in the xy-plane, while along z-axe we plot its value.

derivative of the spherical Bessel function,

$$\frac{dj_n(u)}{du} = \frac{n}{2n+1} j_{n-1}(u) - \frac{n+1}{2n+1} j_{n+1}(u), \tag{5.159}$$

and for integer $k \in [0, 10]$ and $l \in [0, 10]$ is given in the *Appendix G*.

Combination of eq. (5.158) and eq. (5.153) leads to the set of linear equations,

$$n(n+1)c_n = \beta \sum_{\substack{k=0 \\ k\in\text{even}}}^{n} F_{k,n} c_k, \tag{5.160}$$

which returns a convergent solution (for even n and k) [92]

$$c_n = \frac{\beta \sum_{\substack{k=0 \\ k\in\text{even}}}^{n-2} F_{k,n} c_k}{n(n+1) - \beta F_{nn}}. \tag{5.161}$$

The boundary conditions (5.107) are met if we set

$$c_0 = 1. \tag{5.162}$$

The values for the coefficients c_{2k} in the proposed series (5.156) are

$$\begin{aligned} c_2 &= \frac{5\beta}{2(-90+\beta)}, \\ c_4 &= \frac{27\left(-40\beta+\beta^2\right)}{8(-300+\beta)(-90+\beta)}, \\ c_6 &= \frac{13\left(-756000\beta-60960\beta^2+469\beta^3\right)}{1680(-630+\beta)(-300+\beta)(-90+\beta)}, \end{aligned} \tag{5.163}$$

and the corresponding numerical values of the coefficients $\{c_{2k}\}$ for integer $k \in [0, 10]$ are:

$$\Big\{1.00, 2.43807 \times 10^{-1}, 5.28424 \times 10^{-2}, 6.13545 \times 10^{-3}, 2.97534 \times 10^{-4}, 6.16273 \times 10^{-5},$$
$$-4.99866 \times 10^{-6}, 2.33661 \times 10^{-6}, -8.58529 \times 10^{-7}, 3.76664 \times 10^{-7}, -1.79692 \times 10^{-7}\Big\}.$$

The asymptotic expansion for large argument $u \gg 1$ of spherical Bessel function,

$$\lim_{u\to\infty}\left[j_n(u)\right] = \frac{\cos\left[u - \frac{\pi}{2}(n+1)\right]}{u}, \tag{5.164}$$

defines value of the amplitude [92]

$$A_0 \equiv \sum_{k=0}^{k=10} (-1)^k c_{2k} = 0.803127, \tag{5.165}$$

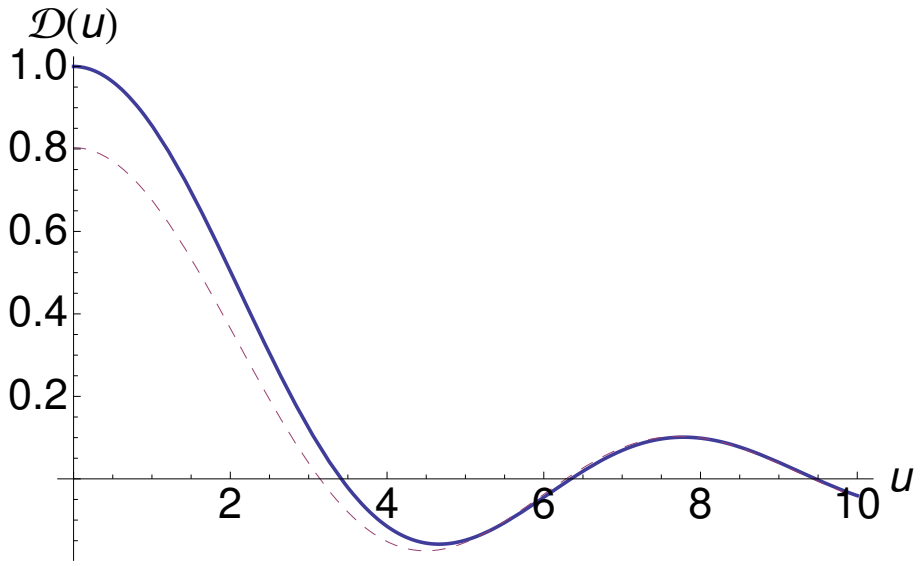

Figure 5.4: Damping of gravitational wave as a function of conformal time u in the early-time limit. Solid line corresponds to the exact solution of the gravitational wave damping in the early-time limit and dashed line is the approximate solution, $A_0 j_0(u)$, eq. (5.166).

and the solution in the early-time limit has an asymptotic form

$$D(u) = A_0 j_0(u). \tag{5.166}$$

Here we have got a numerical value for A_0 that differs from S. Weinberg's [89, 90] value by about 0.065%. The solution (5.166) is the *asymptotic* one, which could not be the exact solution for the problem (5.153). Indeed, the differential operator on the left hand side of eq. (5.153), being applied to (5.166) returns *identical zero*, which of course is inconsistent with the perturbation presented by the right hand side of eq. (5.153). The exact solution is given by an infinite linear combination of spherical Bessel functions (5.156) with coefficients (5.164) and asymptotically approaches (5.166). In other words, the perturbation on the right hand side of eq. (5.153) does not change the behavior of the homogeneous solution eq. (5.153) but effectively changes the amplitude A_0 from unity to the value given by (5.165).

To summarize, the series solution (5.156) with the coefficients (5.164) for the damping

of gravitational wave as a function of conformal time u in the early-time limit is shown in Fig. 5.4. We note the *strict* upper triangular structure of matrix $F_{2k,2l}$ that guarantees the convergent solution for eq. (5.153) in the early-time limit. In this limit the anisotropic inertia tensor $h_{ij}(t)$ never exceeds by absolute magnitude unity and therefore can be treated as a small perturbation to the metric (5.1). Therefore in the limit $u \ll Q$ the problem (5.153) leads to damping of a gravitational wave independently of the Q value.

5.10 General solution for the gravitational wave damping

In this section we would like to build the solution for the general gravitational equation

$$(u(u+4Q))^2\left(\frac{d^2D(u)}{du^2}+\left(\frac{4(u+2Q)}{u(u+4Q)}\right)\frac{dD(u)}{du}+D(u)\right) \tag{5.167}$$
$$=-24f_\nu(0)(4Q)^2\int_0^u K(u-U)\frac{dD(U)}{dU}dU.$$

Here we define the differential operator

$$L\equiv(u(u+4Q))^2\left(\frac{d^2}{du^2}+\frac{4(u+2Q)}{u(u+4Q)}\frac{d}{du}+1\right), \tag{5.168}$$

and consider the function

$$f_n(u)=\frac{n(3+n)j_{n-1}(u)}{4Q+u}+\frac{(-2+n)(1+n)j_{n+1}(u)}{4Q+u}, \tag{5.169}$$

then we have equality

$$L[f_n(u)]=4Q\left[(-1+n)n^2(3+n)j_{n-1}(u)+(-2+n)(1+n)^2(2+n)j_{n+1}(u)\right]$$
$$+(-2+n)n(1+n)(3+n)(1+2n)j_n(u). \tag{5.170}$$

We shall explain the meaning of the obtained eq. (5.170).

First we consider the early-time limit that simplifies the differential operator eq. (5.168)

into

$$\lim_{u\ll Q}[L]\equiv L_0=(4Qu)^2\left(\frac{d^2}{du^2}+\frac{2}{u}\frac{d}{du}+1\right), \tag{5.171}$$

and the trial function eq. (5.169) reduces to

$$\lim_{u\ll Q}[f_n(u)]\equiv f_n^0(u)=\frac{n(3+n)}{4Q}j_{n-1}(u)+\frac{(-2+n)(1+n)}{4Q}j_{n+1}(u). \tag{5.172}$$

By acting the operator (5.171) on the function (5.172) we obtain

$$\begin{aligned} &L_0[f_n^0(u)]= \\ &=4Q\left[(-1+n)n^2(3+n)j_{n-1}(u)+(-2+n)(1+n)^2(2+n)j_{n+1}(u)\right] \end{aligned} \tag{5.173}$$

that exactly coincides with the square brackets (5.170).

Repeating the analogous procedure in the late-time limit, we obtain for the operator (5.168),

$$\lim_{u\gg Q}[L]\equiv L_1=u^4\left(\frac{d^2}{du^2}+\frac{4}{u}\frac{d}{du}+1\right), \tag{5.174}$$

and for the function (5.169),

$$\begin{aligned} &\lim_{u\gg Q}[f_n(u)]\equiv f_n^1(u)=\frac{n(3+n)j_{n-1}(u)}{u}+\frac{(-2+n)(1+n)j_{n+1}(u)}{u} \\ &=\frac{n(n+3)}{2n-1}[j_{n-2}(u)+j_n(u)]+\frac{(n-2)(n+1)}{2n+3}[j_n(u)+j_{n+2}(u)], \end{aligned} \tag{5.175}$$

we arrive at the identity

$$L_1[f_n^1(u)] = (-2+n)n(1+n)(3+n)(1+2n)j_n(u), \tag{5.176}$$

that exactly coincides with a single term outside of the square brackets (5.170).

Thus we have proved a nontrivial equality

$$L[f_n(u)] = L_0[f_n^0(u)] + L_1[f_n^1(u)], \tag{5.177}$$

which means that action of the general operator L, eq. (5.169), onto the trial function $f_n(u)$, eq. (5.170), returns the *exact* sum of its action onto the function in the early-time, $L_0[f_n^0(u)]$, and the late-time, $L_1[f_n^1(u)]$, limits.

As the result of the obtained eq. (5.177) we will be looking for a solution in terms of a series

$$D(u) = \sum_{n=0}^{+\infty} c_n \left(\frac{n(3+n)j_{n-1}(u)}{4Q+u} + \frac{(-2+n)(1+n)j_{n+1}(u)}{4Q+u} \right). \tag{5.178}$$

Naturally we have to integrate the right hand side eq. (5.167) for arbitrary n,

$$-24 f_\nu(0)(4Q)^2 \int_0^u K(u-U) \frac{d}{dU} \left[\frac{n(3+n)j_{n-1}(U)}{4Q+U} + \frac{(-2+n)(1+n)j_{n+1}(U)}{4Q+U} \right] dU. \tag{5.179}$$

We can break the integral (5.179) into two parts,

$$\int_0^u \longrightarrow \int_0^{u_0} + \int_{u_0}^u, \tag{5.180}$$

bearing in mind that $u_0 \ll Q$. This procedure separates the early-time limit, representing the first integral, from the late-time limit of the second integral

In the early-time limit eq. (5.179) reduces to

$$-24 f_\nu(0)(4Q) \times \int_0^u K(u-U) \frac{d}{dU} \left[n(3+n) j_{n-1}(U) + (-2+n)(1+n) j_{n+1}(U) \right], \tag{5.181}$$

while in the late-time limit it corresponds to

$$-24 f_\nu(0)(4Q)^2 \int_0^u K(u-U) \times \frac{d}{dU} \left[\frac{n(n+3)}{2n-1} [j_{n-2}(U) + j_n(U)] + \frac{(n-2)(n+1)}{2n+3} [j_n(U) + j_{n+2}(U)] \right] dU. \tag{5.182}$$

Recalling the convolution integral formula (5.140) we will be able to transform the Einstein field equation (5.167) into a set of linear equations.

After breaking the integral into two parts eq. (5.167) transforms into

$$\begin{aligned} &\sum_{n=0}^{+\infty} c_n \left[(4Q) \left\{ (-1+n) n^2 (3+n) j_{n-1}(u) + (-2+n)(1+n)^2 (2+n) j_{n+1}(u) \right\} \right. \\ &\left. + (-2+n) n (1+n)(3+n)(1+2n) j_n(u) \right] = -24 f_\nu(0)(4Q)^2 \\ &\times \left(\left\{ \sum_{n=0}^{+\infty} c_n \int_0^u K(u-U) \frac{d}{dU} \left[\frac{n(3+n) j_{n-1}(U) + (-2+n)(1+n) j_{n+1}(U)}{4Q} \right] dU \right\} \right. \\ &- \sum_{n=0}^{+\infty} c_n \int_0^u K(u-U) \\ &\left. \times \frac{d}{dU} \left[\frac{n(n+3)}{2n-1} [j_{n-2}(U) + j_n(U)] + \frac{(n-2)(n+1)}{2n+3} [j_n(U) + j_{n+2}(U)] \right] dU \right). \end{aligned} \tag{5.183}$$

The early-time limit case that corresponds to the equation formed by the terms inside the curly brackets,

$$\sum_{n=0}^{+\infty} c_n \left[(-1+n)n^2(3+n)j_{n-1}(u) + (-2+n)(1+n)^2(2+n)j_{n+1}(u)\right] = \tag{5.184}$$
$$-24 f_\nu(0) \sum_{n=0}^{+\infty} c_n \int_0^u K(u-U)\frac{d}{dU}\left[n(3+n)j_{n-1}(U) + (-2+n)(1+n)j_{n+1}(U)\right] dU,$$

exactly reproduces the solution for the early-time evolution of the gravitational wave, and the late-time limit evolution represented by the differential equation formed by the terms outside the curly brackets,

$$\sum_{n=0}^{+\infty} c_n \left[(-2+n)n(1+n)(3+n)(1+2n)j_n(u)\right] = -24 f_\nu(0)(4Q)^2 \tag{5.185}$$
$$\times \sum_{n=0}^{+\infty} c_n \int_0^u K(u-U)$$
$$\times \frac{d}{dU}\left[\frac{n(n+3)}{2n-1}[j_{n-2}(U) + j_n(U)] + \frac{(n-2)(n+1)}{2n+3}[j_n(U) + j_{n+2}(U)]\right] dU,$$

exactly reconstructs the late-time evolution of the gravitational wave.

5.11 Evaluation of the convolution integrals

Here we shall calculate the convolution integrals in the right hand side of eq. (5.183). The first integral is

$$-24 f_\nu(0)(4Q) \sum_{n=0}^{+\infty} c_n \int_0^u K(u-U) \tag{5.186}$$
$$\times \frac{d}{dU}\left[n(3+n) j_{n-1}(U) + (-2+n)(1+n) j_{n+1}(U)\right] dU$$
$$= -24 f_\nu(0)(4Q) \left[\sum_{l=0}^{\infty} j_{2l}(u) \sum_{k=0}^{l} A_{2k+1,2l} c_{2k+1} + \sum_{l=0}^{\infty} j_{2l+1}(u) \sum_{k=0}^{l+1} A_{2k,2l+1} c_{2k}\right],$$

where the matrices $A_{2k+1,2l}$ and $A_{2k,2l+1}$ are obtained by the convolution of the kernel $K(u)$ given by eq. (5.90) with the first derivative of the function

$$\frac{d}{dU}\left[n(3+n) j_{n-1}(U) + (-2+n)(1+n) j_{n+1}(U)\right] = \tag{5.187}$$
$$= j_{n-2}(U)\left(\frac{(-1+n)n(3+n)}{-1+2n}\right) + j_n(U)\left(-\frac{(1+2n)\left(-2+5n+5n^2\right)}{(-1+2n)(3+2n)}\right)$$
$$+ j_{n+2}(U)\left(-\frac{(-2+n)(1+n)(2+n)}{3+2n}\right),$$

and for integer $k \in [0, 10]$ and $l \in [0, 10]$ are given in *Appendix H*.

The second integral that constitutes the right hand side eq. (5.183) is (without the factor

$-24 f_\nu(0)(4Q)^2)$

$$\sum_{n=0}^{+\infty} c_n \int_0^u K(u-U) \times \frac{d}{dU}\left[\frac{n(n+3)}{2n-1}[j_{n-2}(U)+j_n(U)]+\frac{(n-2)(n+1)}{2n+3}[j_n(U)+j_{n+2}(U)]\right] dU = \left[\sum_{l=0}^{\infty} j_{2l}(u)\sum_{k=0}^{l+1} B_{2k,2l}c_{2k} + \sum_{l=0}^{\infty} j_{2l+1}(u)\sum_{k=0}^{l+1} B_{2k+1,2l+1}c_{2k+1}\right], \tag{5.188}$$

where the matrices $B_{2k,2l}$ and $B_{2k+1,2l+1}$ are obtained by the convolution of the kernel $K(u)$ (5.90) with the first derivative of the function

$$\frac{d}{dU}\left[\frac{n(n+3)}{2n-1}[j_{n-2}(U)+j_n(U)]+\frac{(n-2)(n+1)}{2n+3}[j_n(U)+j_{n+2}(U)]\right] = j_{n-3}(U)\left(\frac{(-2+n)n(3+n)}{(-3+2n)(-1+2n)}\right) + j_{n-1}(U)\left(\frac{n\left(-3-4n+n^2\right)}{(-3+2n)(3+2n)}\right) + j_{n+1}(U)\left(-\frac{(1+n)\left(2+6n+n^2\right)}{(-1+2n)(5+2n)}\right) + j_{n+3}(U)\left(-\frac{(-2+n)(1+n)(3+n)}{(3+2n)(5+2n)}\right), \tag{5.189}$$

and for integer $k \in [0,10]$ and $l \in [0,10]$ are given in *Appendix F*.

Finally eq. (5.183) can be written as a set of linear equations

$$\sum_n n(n+1)j_n(u) \times [(4Q)n(n-3)c_{n-1} + (n+3)(n-2)(2n+1)c_n + (4Q)(n+1)(n+4)c_{n+1}] = -24 f_\nu(0)(4Q)\left[\sum_{l=0}^{\infty} j_{2l}(u)\sum_{k=0}^{l} A_{2k+1,2l}c_{2k+1} + \sum_{l=0}^{\infty} j_{2l+1}(u)\sum_{k=0}^{l+1} A_{2k,2l+1}c_{2k}\right] -24 f_\nu(0)(4Q)^2\left[\sum_{l=0}^{\infty} j_{2l}(u)\sum_{k=0}^{l+1} B_{2k,2l}c_{2k} + \sum_{l=0}^{\infty} j_{2l+1}(u)\sum_{k=0}^{l+1} B_{2k+1,2l+1}c_{2k+1}\right]. \tag{5.190}$$

Specifying even spherical Bessel functions in eq. (5.190) leads to

$$2n(1+2n)\left[(4Q)2n(-3+2n)c_{-1+2n}+(-2+2n)(3+2n)(1+4n)c_{2n}+\right. \tag{5.191}$$
$$\left.(4Q)(1+2n)(4+2n)c_{1+2n}\right]j_{2n}(u)+$$
$$+\left(24f_\nu(0)(4Q)j_{2n}(u)\sum_{k=0}^{n}A_{2k+1,2n}c_{2k+1}+24f_\nu(0)(4Q)^2j_{2n}(u)\sum_{k=0}^{n+1}B_{2k,2n}c_{2k}\right)=0,$$

which returns the recurrence relation for even coefficients

$$c_{2n+2}=-\frac{1}{24f_\nu(0)(4Q)^2B_{2n+2,2n}}\times\{2n(1+2n)[(4Q)2n(-3+2n)c_{-1+2n}$$
$$+(-2+2n)(3+2n)(1+4n)c_{2n}+(4Q)(1+2n)(4+2n)c_{1+2n}]+$$
$$+\left(24f_\nu(0)(4Q)\sum_{k=0}^{n}A_{2k+1,2n}c_{2k+1}+24f_\nu(0)(4Q)^2\sum_{k=0}^{n}B_{2k,2n}c_{2k}\right)\Bigg\} \tag{5.192}$$

Orthogonality between odd spherical Bessel functions in eq. (5.190) returns

$$(1+2n)(2+2n)\left[(4Q)(-2+2n)(1+2n)c_{2n}+\right. \tag{5.193}$$
$$\left.(-1+2n)(4+2n)(1+2(1+2n))c_{1+2n}+(4Q)(2+2n)(5+2n)c_{2+2n}\right]j_{1+2n}(u)+$$
$$+\left(24f_\nu(0)(4Q)j_{2n+1}(u)\sum_{k=0}^{n+1}A_{2k,2n+1}c_{2k}+\right.$$
$$\left.24f_\nu(0)(4Q)^2j_{2n+1}(u)\sum_{k=0}^{n+1}B_{2k+1,2n+1}c_{2k+1}\right)=0,$$

that leads to the recurrence relation for the odd coefficients,

$$c_{2n+3} = -\frac{1}{24 f_\nu(0)(4Q)^2 B_{2n+3,2n+1}} \{(1+2n)(2+2n)\,[(4Q)(-2+2n)(1+2n)c_{2n}+$$
$$+(-1+2n)(4+2n)(1+2(1+2n))c_{1+2n} + (4Q)(2+2n)(5+2n)c_{2+2n}] +$$
$$+\left(24 f_\nu(0)(4Q)\sum_{k=0}^{n+1} A_{2k,2n+1}c_{2k} + 24 f_\nu(0)(4Q)^2 \sum_{k=0}^{n} B_{2k+1,2n+1}c_{2k+1}\right)\Bigg\}. \quad (5.194)$$

As we see the coefficients of the general solution depend on the value of the parameter Q. However, in both early-time and late-time limits the parameter $Q \gg 1$, and we return to the Q-independent coefficient values found in the late-time regime, eq. (5.152). Even though the coefficient c_k become Q-independent, the series solution given by (5.178) still depends on Q-value, and in general is represented by a combination of even and odd spherical Bessel functions. This is the main conclusion of the general solution of gravitational wave damping which is in a contradiction with the prediction made by S. Weinberg [89] concerning the behavior of gravitational wave damping in the early Universe.

5.12 Conclusion

We have analyzed the problem of gravitational wave damping in the early Universe due to freely streaming neutrinos in both early-time and late-time limits. The derivation was possible with the help of a new compact formula for the convolution of spherical Bessel functions of integer order.

The exact solution in the early-time limit is given by a convergent series of spherical Bessel functions of even order with Q-independent coefficients. The neutrino source perturbation does not change the qualitative behavior of the homogeneous gravitational wave damping solution but effectively changes its amplitude from unity to the corresponding asymptotic value.

As in the early-time limit, the late-time limit solution is represented by a convergent series of spherical Bessel functions of even order and is Q-independent for large values of Q. Thus the prediction made by S. Weinberg concerning the Q-independent solution for the gravitational wave damping given by a series of even spherical Bessel functions is valid in both early-time and late-time limits.

S. Weinberg's predictions fails in the general case where we were able to construct the solution in terms of an infinite series of the product of spherical Bessel function and inverse time parameter u shifted by the value of Q parameter. Even though for large Q-values the coefficients of the proposed solution are Q-independent, the solution for the gravitational wave damping depends on Q-value, and in general is represented by a linear combination of even and odd spherical Bessel functions.

The constructed solution for the general case was possible due the nontrivial equality for the differential operator of the gravitational wave damping problem which upon its action

onto the trial function returns the exact sum of its action onto the function in the early-time and late-time limits, which we consider as the main result of the present investigation.

Thus we conclude that the problem of gravitational wave damping in the early Universe due to freely streaming neutrinos is completely solved in an analytical way in both early and late-time limits, and in the general time case.

Chapter 6

Conclusions

In this Thesis we exposed our results in atomic physics, nuclear physics, and cosmology presented in the quantum scattering language and unified within the framework of the scattering matrix formalism. Basic governing principles, such as conservation laws and detailed balance principle, unitarity and gauge invariance of the scattering matrix were given special attention throughout the Thesis.

In the *Atomic Physics* chapter we presented the calculation of the axial anomaly contribution to parity nonconservation (PNC) in atoms. The main result is the prediction of the emission of an electric photon by the magnetic dipole which has not been observed yet. The probability of this process is very small but the non-zero result is important from theoretical point of view.

The Ward identities were imposed on the S-matrix *before* the calculation of the loop integral. This allowed us to express the divergent integrals in terms of the convergent ones and thus obtain the gauge-invariant expression for the S-matrix. We emphasize the vital difference between the axial anomaly contribution to the PNC effects and the impossibility for the real Z-boson of spin $J = 1$ to decay into two *real* photons, the result known as the Landau-Yang theorem. The difference is in the virtual photon that connects the triangular graph of the axial anomaly with the electron atomic transition, e.g., $6s - 7s$ transition in cesium, that contributes to the nonzero axial anomaly S-matrix. We have shown that one can see the impact of the axial anomaly in atomic physics through the parity violation in

atoms.

The chapter on *Quantum Optics* was devoted to the electron laser-assisted scattering process off an arbitrary central potential. Here we introduced a new method that allowed us to obtain an analytical cross section for the electron-ion collision in a laser field. For the illustration of the general method we performed a calculation for the hydrogen laser-assisted recombination.

The S-matrix of the scattering process was constructed from the electron Coulomb-Volkov wave function in the combined Coulomb-laser field and the hydrogen perturbed state. By the aid of the Bessel generating function, the S-matrix was decomposed into an infinite series of the field harmonics. The new step that resulted in a closed analytical expression for the cross section of the process was the Plancherel theorem application to the Bessel generating function. This allowed us to sum the infinite series of Bessel functions and as the result obtain the cross section of the laser-assisted hydrogen photo-recombination process in a closed form.

In the *Nuclear Physics* chapter we investigated the resonance width distribution for low-energy neutron scattering off heavy nuclei. We used the language of Random Matrix Theory for describing the nuclear scattering process. Random Matrix Theory that based on the unitarity of scattering matrix was originally formulated for closed quantum systems. The unstable complex nucleus is an open quantum system, where the intrinsic dynamics has to be supplemented by the coupling of chaotic internal states through the continuum. In our work we proposed a new width distribution based on random matrix theory and the doorway approach for a chaotic quantum system with a single decay channel. The revealed statistics of the width distribution exhibits distinctive properties that are characteristically different from the regularities shared by closed quantum systems. The obtained results directly relate

the Porther-Thomas distribution for multiple narrow nuclear resonances to a resonance, collectivized by the coherent coupling of intrinsic states through the continuum, a nuclear analog of the Dicke superradiant phenomena in quantum optics.

In the *Cosmology* chapter our main object of investigation was the space-time metric perturbed by the stress-energy tensor of neutrino scattering in the early Universe. We have analyzed the problem of gravitational wave damping in the early Universe due to freely streaming neutrinos in both early-time and late-time limits.

The Einstein field equation was derived for the traceless and divergenceless tensor component of the metrics perturbation. The energy-momentum tensor that governs the neutrino scattering in the early Universe was derived from the kinetic Boltzmann equation. In the linearized Boltzmann equation neutrinos interact through the metrics perturbation. As the result, the solution of the Boltzmann equation is given in terms of the tensor component of the metrics perturbation. Finally we arrived at the intergo-differential Einstein field equation for the tensor component of the metrics perturbation which we subsequently built solution for.

The Einstein field equation for the tensor component of the metrics perturbation $D(u)$ is given in terms of the time parameter u and the dimensionless wavenumber Q. The obtained equation we analyzed in two extreme cases, the early-time limit, $u \ll Q$, that corresponds to the lower-bound wavenumbers $q \ll q_{eq}$, and the late-time limit, $u \gg Q$, that is referred to the upper-bound wavenumbers $q \gg q_{eq}$. In these cases we were able to build the exact solution in terms of a convergent series of spherical Bessel functions of even order with Q-independent coefficients. In the early-time limit, the neutrino source perturbation does not change the qualitative behavior of the homogeneous gravitational wave damping solution but effectively changes its amplitude from unity to the corresponding asymptotic value. As

in the early-time limit, the late-time limit solution is represented by a convergent series of spherical Bessel functions of even order and is Q-independent for large values of Q.

Based on the obtained solutions in the extreme cases, we were able to construct the solution for the general time case due the nontrivial equality for the differential operator of the gravitational wave damping problem. Its action onto the trial function returns the exact sum of its action onto the function in the early-time and late-time limits. Even though for large Q-values the coefficients of the proposed solution are Q-independent, the general solution for the gravitational wave damping depends on the parameter Q, being represented by a linear combination of the product of the spherical Bessel function and the inverse sum of time variable u shifted the parameter Q.

Thus we conclude that the problem of gravitational wave damping in the early Universe due to freely streaming neutrinos is completely solved in an analytical way in both early and late-time limits, and in the general time case.

Here we would like to stress that the found property of the general differential operator is the property of the Einstein field equation for the traceless and divergenceless tensor component of the metrics perturbation that is independent of the specific form of the energy-momentum tensor. This means that the developed technique can be equally applied for the tensor perturbations obtained from the kinetic Boltzmann equation for photons or non-relativistic matter. We thus hope that the developed method would be helpful for the corresponding calculations.

APPENDICES

A Electron wave function behavior near the nucleus

Suppose we have the field of the nucleus

$$U(r) = -\frac{Z}{r}, \tag{1}$$

and we would like to find the behavior of the electron wave function in the region close to the nucleus,

$$r \sim \frac{1}{Z}. \tag{2}$$

The semiclassical description in the region

$$\frac{1}{Z} \ll r \ll 1 \tag{3}$$

is valid due to small variation of the wavelength,

$$\frac{d}{dr}\left(\frac{1}{p}\right) \sim \frac{d}{dr}\left(\frac{1}{\sqrt{|U|}}\right) \sim \frac{1}{\sqrt{rZ}} \ll 1. \tag{4}$$

For the spherically symmetrical semiclassical wave function we obtain

$$|\psi(r)| \sim \frac{1}{r\sqrt{p}} \sim \frac{1}{r\sqrt[4]{|U|}} \sim \frac{1}{Z^{1/4}r^{3/4}}, \tag{5}$$

$$\left|\psi\left(r = \frac{1}{Z}\right)\right| \sim Z^{1/2}, \tag{6}$$

$$\left|\frac{d^2}{dr^2}\left[\psi\left(r = \frac{1}{Z}\right)\right]\right| \sim \frac{1}{Z^{1/4}r^{11/4}} \sim Z^{5/2}. \tag{7}$$

Finally the probability to find an electron in the region close to the nucleus in a nonrelativistic limit is

$$W \sim |\psi(r)|^2 \, r^3 \sim \frac{1}{Z^2}. \tag{8}$$

B Secular equation in the general case

The secular equation for the rotationally invariant Hamiltonian

$$\begin{pmatrix}
\varepsilon_0 - \frac{i}{2}\eta_0 & h_1 & h_2 & h_3 & h_4 & \cdots & h_N \\
h_1^* & \varepsilon_1 - \frac{i}{2}\eta_1 & v_2 & v_3 & v_4 & \cdots & v_N \\
h_2^* & v_2^* & \varepsilon_2 - \frac{i}{2}\eta_2 & l_3 & l_4 & \cdots & l_N \\
h_3^* & v_3^* & l_3^* & \varepsilon_3 & 0 & \cdots & 0 \\
\cdots & \cdots & \cdots & \cdots & \cdots & \cdots & \cdots \\
h_N^* & v_N^* & l_N^* & 0 & 0 & \cdots & \varepsilon_N
\end{pmatrix} \tag{9}$$

can be written in terms of the matrix

$$A = \tag{10}$$
$$= \begin{pmatrix}
\frac{h_k^2}{\varepsilon_k - \mathcal{E}_\alpha} + \mathcal{E}_\alpha - (\varepsilon_0 - \frac{i\eta_0}{2}) & h_1 - \frac{h_k v_k}{\varepsilon_k - \mathcal{E}_\alpha} & h_2 - \frac{h_k l_k}{\varepsilon_k - \mathcal{E}_\alpha} \\
h_1 - \frac{h_k v_k}{\varepsilon_k - \mathcal{E}_\alpha} & \frac{v_k^2}{\varepsilon_k - \mathcal{E}_\alpha} + \mathcal{E}_\alpha - (\varepsilon_1 - \frac{i\eta_1}{2}) & v_2 - \frac{v_k l_k}{\varepsilon_k - \mathcal{E}_\alpha} \\
h_2 - \frac{h_k l_k}{\varepsilon_k - \mathcal{E}_\alpha} & v_2 - \frac{v_k l_k}{\varepsilon_k - \mathcal{E}_\alpha} & \frac{l_k^2}{\varepsilon_k - \mathcal{E}_\alpha} + \mathcal{E}_\alpha - (\varepsilon_2 - \frac{i\eta_2}{2})
\end{pmatrix},$$

and is given by

$$\det A = 0. \tag{11}$$

C Friedmann equations

In this Appendix we give a detailed derivation of the fundamental Friedmann equation.

We start from the Ricci tensor that in components looks like,

$$R_{ij} = \frac{\partial \Gamma^k_{ki}}{\partial x^j} - \left[\frac{\partial \Gamma^k_{ij}}{\partial x^k} + \frac{\partial \Gamma^0_{ki}}{\partial t}\right] + \left[\Gamma^0_{ik}\Gamma^k_{j0} + \Gamma^k_{i0}\Gamma^0_{jk} + \Gamma^l_{ik}\Gamma^k_{jl}\right] - \left[\Gamma^k_{ij}\Gamma^l_{kl} + \Gamma^0_{ij}\Gamma^l_{0l}\right], \tag{12}$$

$$R_{00} = \frac{\partial \Gamma^i_{i0}}{\partial t} + \Gamma^i_{0j}\Gamma^j_{0i}. \tag{13}$$

First we separate the spatial-spatial part of the Ricci tensor, $\widetilde{R}_{ij}$,

$$\widetilde{R}_{ij} = \frac{\partial \Gamma^k_{ki}}{\partial x^j} - \frac{\partial \Gamma^k_{ij}}{\partial x^k} + \Gamma^l_{ik}\Gamma^k_{jl} - \Gamma^k_{ij}\Gamma^l_{kl}. \tag{14}$$

On the other hand the spatial part of the spherically symmetric and isotropic metrics is given by

$$\widetilde{g}_{ij} = \delta_{ij} + K\frac{x^i x^j}{1 - K\mathbf{x}^2}, \tag{15}$$

$$\widetilde{g}_{ij}\big|_{\mathbf{x}=0} = \delta_{ij}, \tag{16}$$

where K is the curvature constant. We note that the spatial components of the 4D affine connections Γ^k_{ij} are proportional to the affine connection calculated in the 3D from the spatial part of the metric tensor $\widetilde{g}_{ij}$,

$$\Gamma^k_{ij} = K x^k \widetilde{g}_{ij}. \tag{17}$$

Further we calculate the spatial Ricci tensor at $\mathbf{x} = 0$,

$$\widetilde{R}_{ij}\Big|_{\mathbf{x}=0} = \frac{\partial \Gamma^k_{ki}}{\partial x^j} - \frac{\partial \Gamma^k_{ij}}{\partial x^k} = K\delta_{ij} - 3K\delta_{ij} = -2K\delta_{ij}. \tag{18}$$

Recalling the metrics (15) we reconstruct the spatial Ricci tensor for every point,

$$\widetilde{R}_{ij} = -2K\widetilde{g}_{ij}, \tag{19}$$

which is valid for all spatial coordinate systems.

The space-time components of the affine connections appearing in the Ricci tensor,

$$\begin{aligned}
&\frac{\partial \Gamma^0_{ij}}{\partial t} = \widetilde{g}_{ij}\frac{d}{dt}(a\dot{a}), \\
&\frac{\partial \Gamma^i_{i0}}{\partial t} = 3\frac{d}{dt}\left(\frac{\dot{a}}{a}\right), \\
&\Gamma^0_{ik}\Gamma^k_{j0} = \widetilde{g}_{ij}\dot{a}^2, \\
&\Gamma^0_{ij}\Gamma^l_{0l} = 3\widetilde{g}_{ij}\dot{a}^2, \\
&\Gamma^i_{0j}\Gamma^j_{i0} = 3\left(\frac{\dot{a}}{a}\right)^2.
\end{aligned} \tag{20}$$

As the result, we have for the Ricci tensor,

$$\begin{aligned}
R_{ij} &= \widetilde{R}_{ij} - \left[\widetilde{g}_{ij}\frac{d}{dt}(a\dot{a})\right] + \left[2\widetilde{g}_{ij}\dot{a}^2\right] - \left[3\widetilde{g}_{ij}\dot{a}^2\right] \qquad (21) \\
&= \widetilde{R}_{ij} - 2\dot{a}^2\widetilde{g}_{ij} - a\ddot{a}\widetilde{g}_{ij}, \\
R_{00} &= 3\frac{d}{dt}\left(\frac{\dot{a}}{a}\right) + 3\left(\frac{\dot{a}}{a}\right)^2 = 3\frac{\ddot{a}}{a}. \qquad (22)
\end{aligned}$$

Recalling the space-space components of the Ricci tensor eq. (18), we arrive at the final

expression for the Ricci tensor,

$$R_{ij} = -\left[2K + 2\dot{a}^2 + a\ddot{a}\right]\widetilde{g}_{ij}. \tag{23}$$

The energy-momentum tensor is given in terms of energy density ρ and pressure p,

$$\begin{aligned} T_{00} &= \rho, \\ T_{i0} &= T_{0i} = 0, \\ T_{ij} &= a^2 p \widetilde{g}_{ij}. \end{aligned} \tag{24}$$

Therefore the shifted energy-momentum tensor $S_{\mu\nu}$,

$$S_{\mu\nu} = T_{\mu\nu} - \frac{1}{2} g_{\mu\nu} T^{\lambda}{}_{\lambda}, \tag{25}$$

in components looks like

$$S_{ij} = T_{ij} - \frac{1}{2}\widetilde{g}_{ij} a^2 T^{\lambda}{}_{\lambda} = a^2 p \widetilde{g}_{ij} - \frac{1}{2}\widetilde{g}_{ij} a^2 (3p - \rho) = \frac{1}{2}(\rho - p) a^2 \widetilde{g}_{ij}, \tag{26}$$

$$S_{00} = T_{00} + \frac{1}{2} T^{\lambda}{}_{\lambda} = \rho + \frac{1}{2}(3p - \rho) = \frac{1}{2}(3p + \rho). \tag{27}$$

Finally the Einstein equations are,

$$-\left[2K + 2\dot{a}^2 + a\ddot{a}\right]\widetilde{g}_{ij} = -4\pi G(\rho - p) a^2 \widetilde{g}_{ij}, \tag{28}$$

$$3\frac{\ddot{a}}{a} = -4\pi G(3p + \rho). \tag{29}$$

Simple algebra leads to the fundamental Friedmann equations,

$$\rho = \frac{3}{8\pi G}\left(\frac{\dot{a}^2}{a^2} + \frac{K}{a^2}\right), \tag{30}$$

$$p = -\frac{1}{8\pi G}\left(\frac{2\ddot{a}}{a} + \frac{\dot{a}^2}{a^2} + \frac{K}{a^2}\right), \tag{31}$$

In the case when we can neglect the curvature constant term K, Friedmann equations simplify to

$$\rho = \frac{3}{8\pi G}\left(\frac{\dot{a}^2}{a^2}\right) = \frac{3}{8\pi G}H^2, \tag{32}$$

$$p = -\frac{1}{8\pi G}\left(\frac{2\ddot{a}}{a} + \frac{\dot{a}^2}{a^2}\right). \tag{33}$$

D Energy density for fermions and bosons in the early Universe

We start form the number density $n(p)$ for fermions, $n^{+f}(p,T)$, and bosons, $n_{-b}(p,T)$, with the rest mass m, momentum p, with number of spin states, or the number of independent polarization states g,

$$n^{\pm}(p,T) = g\frac{4\pi p^2}{(2\pi\hbar)^3}\frac{1}{\exp\left[\frac{\sqrt{p^2+m^2}}{kT}\right] \pm 1}. \tag{34}$$

The energy, pressure and entropy density are given in terms of the number density $n(p)$ by

$$\rho(T) = \int_0^\infty dp\ n(p,T)\sqrt{p^2+m^2}, \tag{35}$$

$$p(T) = \int_0^\infty dp\ n(p,T)\frac{p^2}{3\sqrt{p^2+m^2}}, \tag{36}$$

$$s(T) = \frac{1}{T}\int_0^\infty dp\ n(p,T)\left(\sqrt{p^2+m^2}+\frac{p^2}{3\sqrt{p^2+m^2}}\right). \tag{37}$$

For massless particles we obtain

$$\rho^{\pm}(T) = \int_0^\infty dp\ g\frac{4\pi p^3}{(2\pi\hbar)^3}\frac{1}{\exp\left[\frac{p}{kT}\right]\pm 1}. \tag{38}$$

In order to perform the momentum integration in eq. (38) we employ the standard integrals,

$$\int_0^\infty \frac{z^{2n-1}}{e^z+1} = \frac{2^{2n-1}-1}{2n}\pi^{2n}B_n, \tag{39}$$

$$\int_0^\infty \frac{z^{2n-1}}{e^z-1} = \frac{(2\pi)^{2n}}{4n}\pi^{2n}B_n, \tag{40}$$

given in terms of the Bernoulli numbers B_n. Thus we obtain the massless fermion and boson contribution to the energy density,

$$\rho^{-}(T) = \frac{g}{2}a_B T^4, \tag{41}$$

$$\rho^{+}(T) = \frac{7g}{16}a_B T^4 = \frac{7}{8}\rho^{-}(T) \tag{42}$$

where we used the earlier introduced notation,

$$a_B = \frac{4\sigma}{c} = \frac{8\pi^5 k^4}{15(2\pi\hbar c)^3}. \tag{43}$$

For the entropy density of photons, electrons and positrons,

$$\begin{aligned} s(T) &= \frac{4}{3} a_B T^3 \\ &+ \frac{2\times 2}{T}\int_0^\infty dp\ \frac{4\pi p^2}{(2\pi\hbar)^3}\frac{1}{\exp\left[\frac{\sqrt{p^2+m_e^2}}{kT}\right]+1}\left(\sqrt{p^2+m_e^2}+\frac{p^2}{3\sqrt{p^2+m_e^2}}\right). \end{aligned} \tag{44}$$

In terms of the dimensionless parameter,

$$x = \frac{m_e}{kT}, \tag{45}$$

the entropy density (44) is given in terms of the function $F(x)$.

$$\begin{aligned} F(x) &= \\ &= 1 + \frac{45}{2\pi^4}\int_0^\infty dy\ y^2 \frac{1}{\exp\left[\sqrt{y^2+x^2}\right]+1}\left(\sqrt{y^2+x^2}+\frac{y^2}{3\sqrt{y^2+x^2}}\right), \end{aligned} \tag{46}$$

with its asymptotic behavior,

$$F(0) = \frac{11}{4}, \tag{47}$$

$$\lim_{x\to\infty} F(x) = 1. \tag{48}$$

As the result, the contribution of photons, electrons and positrons to the entropy density is,

$$s(T) = \frac{4}{3} a_B T^3 F\left(\frac{m_e}{kT}\right) \tag{49}$$

The condition of thermal equilibrium can be expressed in term of entropy as,

$$s(T)a^3 = \text{const.} \tag{50}$$

Applying the thermal equilibrium condition in the limit that corresponds to the neutrino temperature, $kT_\nu \gg m_e$, and to the photon temperature, $kT \ll m_e$, we get,

$$T_\nu = T\left(\frac{F\left(m_e/kT\right)}{F\left(m_e/kT_\nu\right)}\right)^{1/3} = T\left(\frac{11}{4}\right)^{-1/3}. \tag{51}$$

Finally the photon, neutrino, and antineutrino contribution to the energy density is,

$$\rho(T) = a_B T^4 + \left(3 \times 2 \times \frac{7}{16}\right) a_B T_\nu^4 = a_B T^4 + a_B T^4 \left(3 \times 2 \times \frac{7}{16}\right)\left(\frac{4}{11}\right)^{4/3}. \tag{52}$$

As the result, we obtain the ratio of neutrino energy density to the total neutrino and photon energy density,

$$f_\nu(0) = \frac{\rho_\nu}{\rho_\gamma + \rho_\nu} = \frac{3\left(\frac{7}{8}\right)\left(\frac{4}{11}\right)^{4/3}}{1 + 3\left(\frac{7}{8}\right)\left(\frac{4}{11}\right)^{4/3}} \simeq 0.40523. \tag{53}$$

E Convolution integral of spherical Bessel functions

Here we derive the convolution integral (5.140) of spherical Bessel functions for integer orders n, m. Theoretical efforts for such a convolution integral were put forward in [92] but here we report a new compact formula that has a clear exchange symmetry ($n \longleftrightarrow m$) and can be readily applied for practical calculations.

Starting with the integral

$$J_{n,m}(u) \equiv \int_0^u dU j_m(u-U) j_n(U), \tag{54}$$

we prove eq. (5.140). First, we represent a spherical Bessel function as a Fourier transformation of the Legendre polynomial $P_n(z)$,

$$j_n(u) = \frac{(-i)^n}{2} \int_{-1}^{1} ds \exp(ius) P_n(s). \tag{55}$$

Substitution of (55) into (54) leads to

$$\begin{aligned} J_{n,m}(u) &= \frac{(-i)^{n+m}}{4} \int_{-1}^{1} ds \int_{-1}^{1} dt \exp(iut) P_m(s) P_n(t) \int_0^u dU \exp(iUs - iUt) \\ &= \frac{(-i)^{n+m}}{4i} \int_{-1}^{1} ds \int_{-1}^{1} dt P_m(s) P_n(t) \frac{\exp(ius) - \exp(iut)}{(s-t)}. \end{aligned} \tag{56}$$

Now we employ the Legendre function of the second kind $Q_n(z)$ defined as

$$Q_n(z) = \frac{1}{2} \int_{-1}^{1} dz' \frac{P_n(z')}{z - z'}. \tag{57}$$

Performing the integrations over t and s we obtain

$$\frac{(-i)^{n+m}}{4i}\int_{-1}^{1}ds\int_{-1}^{1}dtP_m(s)P_n(t)\frac{\exp(ius)-\exp(iut)}{(s-t)} \tag{58}$$
$$=\frac{(-i)^{n+m}}{2i}\int_{-1}^{1}dt\exp(iut)\left[P_n(t)Q_m(t)+P_m(t)Q_n(t)\right].$$

Further we reincarnate spherical Bessel functions by decomposing plane waves in terms of Legendre polynomials

$$\exp(iut)=\sum_{l=0}^{\infty}(2l+1)i^l j_l(u)P_l(t), \tag{59}$$

which leads to

$$\frac{(-i)^{n+m}}{2i}\int_{-1}^{1}dt\exp(iut)\left[P_n(t)Q_m(t)+P_m(t)Q_n(t)\right] \tag{60}$$
$$=\frac{(-i)^{n+m}}{2i}\sum_{l=0}^{\infty}(2l+1)i^l j_l(u)\int_{-1}^{1}dtP_l(t)\left[P_n(t)Q_m(t)+P_m(t)Q_n(t)\right].$$

The angular momentum coupling simplifies the product of Legendre polynomials,

$$P_l(x)P_m(x)=\sum_{L=|l-m|}^{L=l+m}\langle l,0,m,0|L,0\rangle^2 P_L(x), \tag{61}$$

in terms of the Clebsch - Gordan coefficients $\langle l,0,m,0|L,0\rangle$. Introducing

$$W_{m-1}(z)=2\sum_{k=0}^{[\frac{m-1}{2}]}\frac{(m-2k-1)}{(2k+1)(m-k)}P_{m-2k-1}(z), \tag{62}$$

and using the analog of eq. (61),

$$P_l(z)Q_m(z) = \sum_{L=|l-m|}^{L=l+m} \langle l,0,m,0|L,0\rangle^2 \left(Q_L(z) + W_{L-1}(z)\right) - P_l(z)W_{m-1}(z), \quad (63)$$

we come to

$$\begin{aligned}
&\int_{-1}^{1} dt P_l(t)\left[P_n(t)Q_m(t) + P_m(t)Q_n(t)\right] \quad (64)\\
&= \int_{-1}^{1} dt \left[P_n(t)\underbrace{P_l(t)Q_m(t)}_{I} + \underbrace{P_l(t)P_m(t)}_{II}Q_n(t)\right]\\
&= \int_{-1}^{1} dt \left[P_n(t)\left(\sum_{L=|l-m|}^{L=l+m} \langle l,0,m,0|L,0\rangle^2 \left(Q_L(t) + W_{L-1}(t)\right) - P_l(t)W_{m-1}(t)\right)\right.\\
&\left. + \sum_{L=|l-m|}^{L=l+m} \langle l,0,m,0|L,0\rangle^2 P_L(t)Q_n(t)\right],
\end{aligned}$$

where in the first term we have decomposed the product $P_l(t)Q_m(t)$, whereas in the second term we decomposed the product $P_l(t)P_m(t)$. Using the parity identity,

$$\int_{-1}^{1} dt P_n(t)Q_L(t) = -\int_{-1}^{1} dt P_L(t)Q_n(t), \quad (65)$$

we obtain

$$\begin{aligned}
&\int_{-1}^{1} dt P_l(t)\left[P_n(t)Q_m(t) + P_m(t)Q_n(t)\right] \quad (66)\\
&= \int_{-1}^{1} dt \left[P_n(t)\left(\sum_{L=|l-m|}^{L=l+m} \langle l,0,m,0|L,0\rangle^2 W_{L-1}(t) - P_l(t)W_{m-1}(t)\right)\right].
\end{aligned}$$

Therefore

$$\int_{-1}^{1} dt \sum_{L=|l-m|}^{L=l+m} \langle l,0,m,0|L,0\rangle^2 P_n(t) W_{L-1}(t) \tag{67}$$
$$= \int_{-1}^{1} dt \sum_{L=|l-m|}^{L=l+m} \langle l,0,m,0|L,0\rangle^2 \sum_{k=0}^{[(L-1)/2]} \frac{2L-4k-1}{(2k+1)(L-k)} P_{L-2k-1}(t) P_n(t)$$
$$= 4 \sum_{\substack{L=|l-m| \\ L-n-1\geq 0}}^{L=l+m} \frac{\langle l,0,m,0|L,0\rangle^2}{L+L^2-n(1+n)}.$$

On the other hand,

$$\int_{-1}^{1} dt P_l(t) W_{m-1}(t) P_n(t) \tag{68}$$
$$= \int_{-1}^{1} dt \sum_{k=0}^{[(m-1)/2]} \frac{2m-4k-1}{(2k+1)(m-k)} P_{m-2k-1}(t) P_l(t) P_n(t)$$
$$= \int_{-1}^{1} dt \sum_{k=0}^{[(m-1)/2]} \frac{2m-4k-1}{(2k+1)(m-k)} P_{m-2k-1}(t) \sum_{L=|l-n|}^{L=l+n} \langle l,0,n,0|L,0\rangle^2 P_L(t)$$
$$= -4 \sum_{\substack{L=|l-n| \\ m-L-1\geq 0}}^{L=l+n} \frac{\langle l,0,n,0|L,0\rangle^2}{L+L^2-m(1+m)}.$$

Thus, the identity (5.140) is demonstrated,

$$\int_{-1}^{1} dt \sum_{L=|l-m|}^{L=l+m} \langle l,0,m,0|L,0\rangle^2 P_n(t) W_{L-1}(t) - \int_{-1}^{1} dt P_n(t) P_l(t) W_{m-1}(t)$$
$$= 4 \sum_{\substack{L=|l-m| \\ L-n-1\geq 0}}^{L=l+m} \frac{\langle l,0,m,0|L,0\rangle^2}{L+L^2-n(1+n)} + 4 \sum_{\substack{L=|l-n| \\ m-L-1\geq 0}}^{L=l+n} \frac{\langle l,0,n,0|L,0\rangle^2}{L+L^2-m(1+m)}. \tag{69}$$

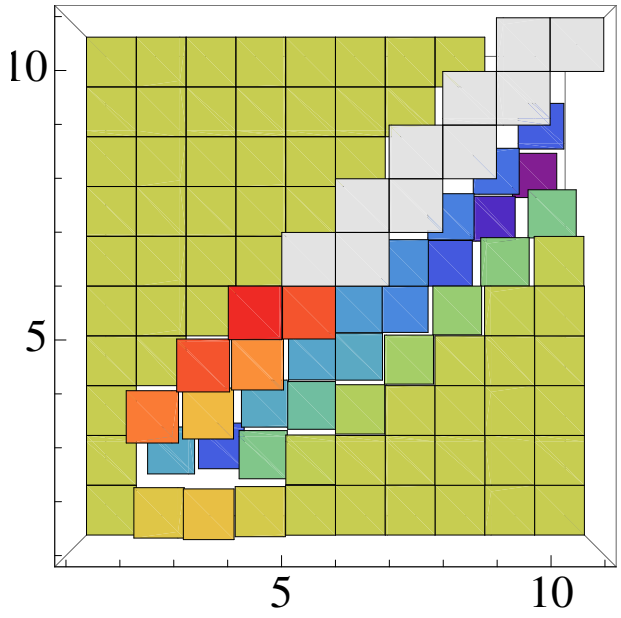

Figure 1: Graphical representation for the upper but one triangular structure of the matrix $B_{2k,2l}$. The matrix indices l and k define a position of the matrix element in the xy-plane, while along z-axe we plot its value.

F Convolution matrices in the late-time limit

$$B_{2k,2l} \equiv \tag{70}$$

$$\begin{pmatrix}
0 & \frac{1}{15} & \frac{1}{10} & \frac{13}{350} & \frac{17}{4900} & -\frac{1}{3780} & \frac{1}{19404} & -\frac{29}{1981980} & \frac{1}{193050} \\
0 & -\frac{1}{3} & -\frac{1}{2} & -\frac{13}{70} & -\frac{17}{980} & \frac{1}{756} & -\frac{5}{19404} & \frac{29}{396396} & -\frac{1}{38610} \\
0 & \frac{4}{15} & \frac{7}{55} & -\frac{5671}{17325} & -\frac{10523}{44100} & -\frac{733}{13860} & -\frac{1453}{640332} & -\frac{29}{77297220} & \frac{173}{5855850} \\
0 & 0 & \frac{18}{55} & \frac{793}{3465} & -\frac{3013}{8820} & -\frac{13507}{41580} & -\frac{2077}{23716} & -\frac{1247}{220220} & \frac{353}{1351350} \\
0 & 0 & 0 & \frac{88}{225} & \frac{68323}{209475} & -\frac{6611}{17955} & -\frac{1343}{3234} & -\frac{3652637}{30060030} & -\frac{4375681}{491891400} \\
0 & 0 & 0 & 0 & \frac{26}{57} & \frac{1661}{3933} & -\frac{81703}{204930} & -\frac{4520839}{8918910} & -\frac{39881}{257400} \\
0 & 0 & 0 & 0 & 0 & \frac{12}{23} & \frac{74315}{143451} & -\frac{244553}{567567} & -\frac{302161}{504504} \\
0 & 0 & 0 & 0 & 0 & 0 & \frac{238}{405} & \frac{701017}{1142505} & -\frac{2355893}{5077800} \\
0 & 0 & 0 & 0 & 0 & 0 & 0 & \frac{304}{465} & \frac{11539}{16275}
\end{pmatrix}$$

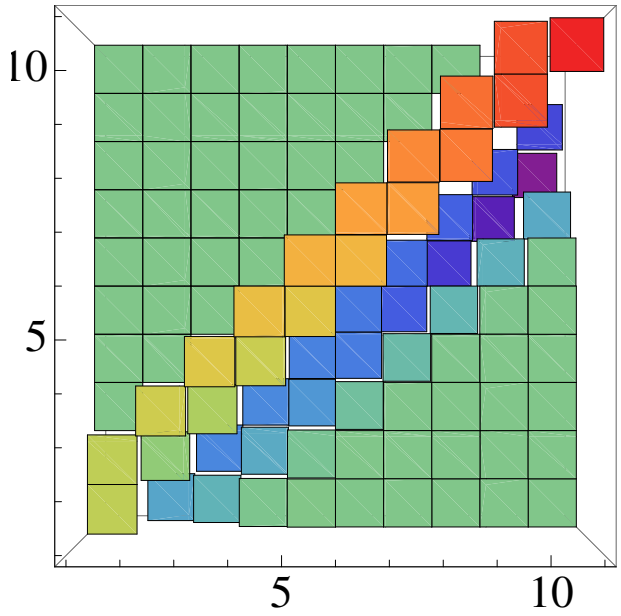

Figure 2: Graphical representation for the upper but one triangular structure of the matrix $B_{2k+1,2l+1}$. The matrix indices l and k define a position of the matrix element in the xy-plane, while along z-axe we plot its value.

$$B_{2k+1,2l+1} \equiv \tag{71}$$

$$\begin{pmatrix}
\frac{6}{25} & -\frac{17}{75} & -\frac{11}{70} & -\frac{23}{1470} & \frac{95}{15876} & -\frac{5543}{4365900} & \frac{10463}{23123100} & -\frac{713}{3567564} & \frac{28343}{281582730} \\
\frac{6}{25} & \frac{47}{675} & -\frac{91}{270} & -\frac{127}{630} & -\frac{19}{540} & -\frac{161}{326700} & -\frac{439}{3303300} & \frac{589}{11042460} & -\frac{2039}{93860910} \\
0 & \frac{8}{27} & \frac{440}{2457} & -\frac{9509}{28665} & -\frac{7429}{26460} & -\frac{102373}{1455300} & -\frac{9913}{2484300} & \frac{589}{4471740} & \frac{5}{1085994} \\
0 & 0 & \frac{14}{39} & \frac{1289}{4641} & -\frac{13655}{38556} & -\frac{507449}{1372140} & -\frac{898553}{8588580} & -\frac{2368307}{324648324} & \frac{152875}{394215822} \\
0 & 0 & 0 & \frac{36}{85} & \frac{4009}{10710} & -\frac{6638}{17325} & -\frac{126901}{275275} & -\frac{4156573}{30060030} & -\frac{611515}{58402344} \\
0 & 0 & 0 & 0 & \frac{22}{45} & \frac{529}{1125} & -\frac{9433}{22750} & -\frac{116219}{210210} & -\frac{4553149}{26546520} \\
0 & 0 & 0 & 0 & 0 & \frac{208}{375} & \frac{14358}{25375} & -\frac{1907}{4263} & -\frac{9211}{14280} \\
0 & 0 & 0 & 0 & 0 & 0 & \frac{18}{29} & \frac{93031}{140679} & -\frac{226529}{471240} \\
0 & 0 & 0 & 0 & 0 & 0 & 0 & \frac{68}{99} & \frac{11087}{14652}
\end{pmatrix}$$

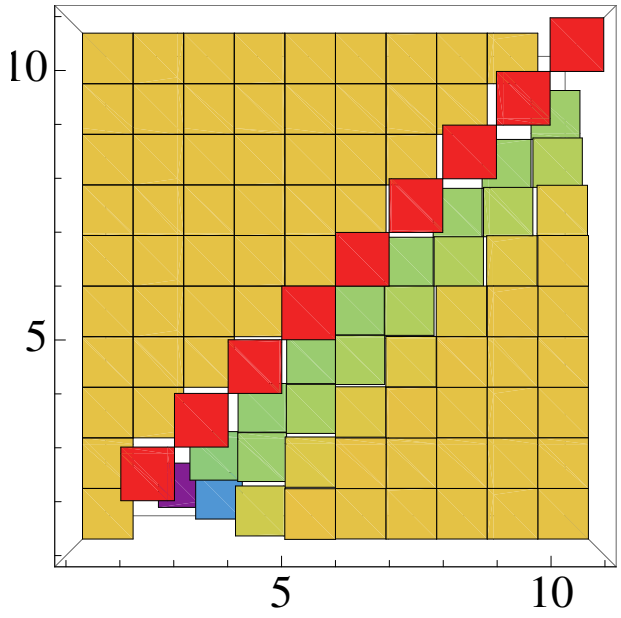

Figure 3: Graphical representation for the upper triangular structure of the matrix $F_{2k,2l}$, eq. (72). The matrix indices l and k define the position of the matrix element in the xy-plane, while along z-axe we plot its value.

G Convolution matrix in the early-time limit

$$F_{2k,2l} \equiv \tag{72}$$

$$\begin{pmatrix}
0 & -\frac{1}{6} & -\frac{1}{10} & -\frac{13}{900} & \frac{17}{11025} & -\frac{1}{2520} & \frac{25}{174636} & -\frac{29}{463320} & \frac{1}{32175} \\
0 & \frac{1}{15} & -\frac{1}{20} & -\frac{13}{315} & -\frac{17}{2520} & \frac{1}{1260} & -\frac{1}{4536} & \frac{29}{343035} & -\frac{1}{25740} \\
0 & 0 & \frac{1}{15} & -\frac{143}{3150} & -\frac{221}{6300} & -\frac{41}{7560} & \frac{85}{137214} & -\frac{551}{3243240} & \frac{163}{2509650} \\
0 & 0 & 0 & \frac{1}{15} & -\frac{17}{392} & -\frac{17}{525} & -\frac{18715}{3841992} & \frac{8207}{15057900} & -\frac{23}{156156} \\
0 & 0 & 0 & 0 & \frac{1}{15} & -\frac{19}{450} & -\frac{5}{162} & -\frac{2850091}{624323700} & \frac{59}{117117} \\
0 & 0 & 0 & 0 & 0 & \frac{1}{15} & -\frac{115}{2772} & -\frac{145}{4851} & -\frac{12247}{2802800} \\
0 & 0 & 0 & 0 & 0 & 0 & \frac{1}{15} & -\frac{261}{6370} & -\frac{319}{10920} \\
0 & 0 & 0 & 0 & 0 & 0 & 0 & \frac{1}{15} & -\frac{341}{8400} \\
0 & 0 & 0 & 0 & 0 & 0 & 0 & 0 & \frac{1}{15}
\end{pmatrix}$$

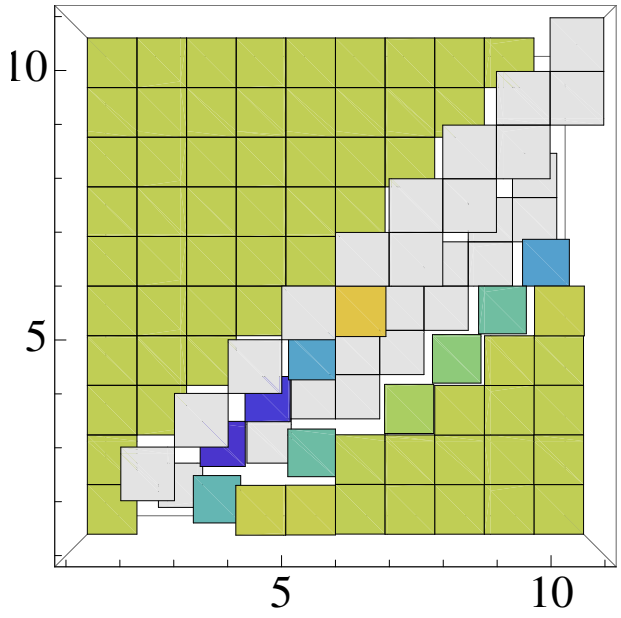

Figure 4: Graphical representation for the upper triangular structure of the matrix $A_{2k+1,2l}$. The matrix indices l and k define the position of the matrix element in the xy-plane, while along z-axe we plot its value.

H Convolution Matrices in the early-time limit

$$A_{2k+1,2l} \equiv \tag{73}$$

$$\begin{pmatrix}
0 & -\frac{4}{5} & -\frac{3}{10} & \frac{13}{525} & \frac{289}{14700} & -\frac{1}{315} & \frac{59}{58212} & -\frac{1247}{2972970} & \frac{1}{4950} \\
0 & \frac{6}{5} & -\frac{19}{30} & -\frac{208}{225} & -\frac{1649}{6300} & -\frac{1}{135} & -\frac{409}{274428} & \frac{1073}{1274130} & -\frac{1103}{2509650} \\
0 & 0 & \frac{8}{3} & -\frac{194}{315} & -\frac{19261}{8820} & -\frac{3779}{4725} & -\frac{10985}{174636} & \frac{158891}{52702650} & -\frac{17}{319410} \\
0 & 0 & 0 & \frac{14}{3} & -\frac{31}{84} & -\frac{178}{45} & -\frac{144125}{91476} & -\frac{39079907}{270540270} & \frac{2305}{234234} \\
0 & 0 & 0 & 0 & \frac{36}{5} & \frac{8}{75} & -\frac{1235}{198} & -\frac{44836523}{17342325} & -\frac{130891}{520520} \\
0 & 0 & 0 & 0 & 0 & \frac{154}{15} & \frac{73}{90} & -\frac{258796}{28665} & -\frac{5359}{1400} \\
0 & 0 & 0 & 0 & 0 & 0 & \frac{208}{15} & \frac{1282}{735} & -\frac{17259}{1400} \\
0 & 0 & 0 & 0 & 0 & 0 & 0 & 18 & \frac{2441}{840} \\
0 & 0 & 0 & 0 & 0 & 0 & 0 & 0 & \frac{68}{3}
\end{pmatrix}$$

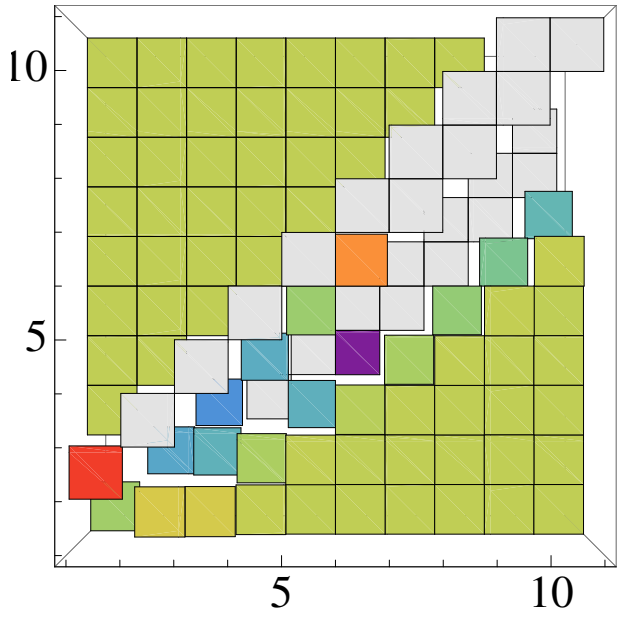

Figure 5: Graphical representation for the upper triangular structure of the matrix $A_{2k,2l+1}$. The matrix indices l and k define the position of the matrix element in the xy-plane, while along z-axe we plot its value.

$$A_{2k,2l+1} \equiv \tag{74}$$

$$\begin{pmatrix}
-\frac{2}{15} & \frac{1}{9} & \frac{22}{225} & \frac{5}{294} & -\frac{19}{9450} & \frac{23}{41580} & -\frac{2}{9555} & \frac{31}{326700} & -\frac{35}{722007} \\
\frac{2}{3} & -\frac{5}{9} & -\frac{22}{45} & -\frac{25}{294} & \frac{19}{1890} & -\frac{23}{8316} & \frac{2}{1911} & -\frac{31}{65340} & \frac{175}{722007} \\
0 & \frac{28}{15} & -\frac{49}{75} & -\frac{73}{49} & -\frac{1577}{3150} & -\frac{4853}{152460} & \frac{177}{385385} & \frac{8587}{18404100} & -\frac{1069}{3128697} \\
0 & 0 & \frac{18}{5} & -\frac{383}{735} & -\frac{5681}{1890} & -\frac{882947}{762300} & -\frac{580796}{5780775} & \frac{4061}{660660} & -\frac{509}{722007} \\
0 & 0 & 0 & \frac{88}{15} & -\frac{151}{945} & -\frac{87193}{17325} & -\frac{154003}{75075} & -\frac{5855497}{30060030} & \frac{217787}{15459444} \\
0 & 0 & 0 & 0 & \frac{26}{3} & \frac{71}{165} & -\frac{492}{65} & -\frac{134571}{42350} & -\frac{33633}{106964} \\
0 & 0 & 0 & 0 & 0 & 12 & \frac{341}{273} & -\frac{4681}{441} & -\frac{252625}{55692} \\
0 & 0 & 0 & 0 & 0 & 0 & \frac{238}{15} & \frac{3617}{1575} & -\frac{8671}{612} \\
0 & 0 & 0 & 0 & 0 & 0 & 0 & \frac{304}{15} & \frac{911}{255}
\end{pmatrix}$$

BIBLIOGRAPHY

BIBLIOGRAPHY

[1] M. A. Bouchiat and C. C. Bouchiat, Physics Letters B, **48**, 111 (1974).

[2] C. S. Wood, S. C. Bennet, D. Cho, B. P. Masterson, J. L. Roberts, C. E. Tanner and C. E. Wieman, Science **275**, 1759 (1997).

[3] A. Schafer, G. Soff, P. Indelicato, B. Muller, and W. Greiner, Phys. Rev. A **40**, 7362 (1989).

[4] R. W. Dunford, Phys. Rev. A **54**, 3820 (1996).

[5] L. N. Labzowsky, A. V. Nefiodov, G. Plunien, G. Soff, R. Marrus and D. Liesen, Phys. Rev. A **63**, 054105 (2001).

[6] M. Zolotorev and D. Budker, Phys. Rev. Lett. **78**, 4717 (1997).

[7] M. Y. Kuchiev and V. V. Flambaum, Phys. Rev. Lett. **89**, 283002 (2002).

[8] A. I. Milstein, O. P. Sushkov and I. S. Terekhov, Phys. Rev. Lett. **89**, 283003 (2002).

[9] V. M. Shabaev, K. Pachucki, I. I. Tupitsyn and V. A. Yerokhin, Phys. Rev. Lett. **94**, 213002 (2005).

[10] V. V. Flambaum and J. S. M. Ginges, Phys. Rev. A **72** , 052115 (2005).

[11] J. Sapirstein, K. Pachucki, A. Vietta and K. T. Cheng, Phys. Rev. A **67**, 052110 (2003).

[12] I. Bednyakov, L. Labzowsky, G. Plunien, G. Soff and V. Karasiev, Phys. Rev. A **61**, 012103 (1999).

[13] S. Weinberg, *The Quantum Theory of Fields, Vol. 2. Modern Applications* (Cambridge University Press, Cambridge, UK, 2000).

[14] S. Adler, Phys. Rev. **177**, 2426 (1969);
J. S.Bell and R. Jackiw, Nuovo Cimento A **60**, 47, (1969).

[15] I. B. Khriplovich, *Parity Noncoservation in Atomic Phenomena* (Gordon and Breach, London, 1991).

[16] L. Rosenberg, Phys. Rev. **129**, 2786 (1963); M.L. Laursen and M.A. Samuel, Z. Phys. C **14**, 325 (1982); A. Barroso et al., Z. Phys. C **28**, 149 (1985).

[17] L. D. Landau, Dokl. Akad. Nauk. S.S.S.R. **60**, 207 (1948);
C.N.Yang Phys. Rev. **77**, 242 (1950).

[18] A. I. Akhiezer and V. B. Berestetskii, *Quantum Electrodynamics* (Interscience Publishers, New York, 1965).

[19] C. Itzykson and J.B. Zuber, *Quantum Field Theory* (McGraw-Hill, 1980).

[20] L. D Landau and E. M. Lifschitz, *Quantum Mechanics Non-Relativistic Theory* (Oxford, Pergamon Press, 1977).

[21] M. H. Mittleman, *Introduction to the Theory of Laser-Atom Interactions* (New York, Plenum Press, 1993); C. J. Joachain, *Laser Interaction with Atoms, Solids and Plasmas* (New York, Plenum Press, 1994).

[22] G. Gabrielse *et al*, ATRAP collaboration, Phys. Rev. Lett, **89**, 213401 (2002);
M. Amoretti *et al*, ATHENA Collaboration, Nature, **419**, 456 (2002).

[23] G. Gabrielse *et al.*, http//cdsweb.cern.ch/record/1234581/files/
CERN-SPSC-2010-006.

[24] M. Amoretti *et al.*, ATHENA Collaboration, Phys. Rev. Lett. **97** 213401;
G. Gabrielse *et al.*, ATRAP collaboration, Phys. Rev. Lett. **100**, 113001 (2008).

[25] T. Pohl, D. Vrinceanu, and H. R. Sadeghpour, Phys. Rev. Lett. **100**, 223201 (2008).

[26] F. Robicheaux, Phys. Rev. A **70**, 022510 (2004); S. Roy, S. Ghosh, and C. Sinha Phys. Rev. A **78**, 022706 (2008).

[27] G. Gabrielse, *Adv. At., Mol., Opt. Phys.* **50**, 155 (2005).

[28] H. R. Reiss, Phys. Rev. A **22**, 1786 (1980); F. W. Byron, P. Francken, and C. J. Joachain, *J. Phys.* B **20**, 5487 (1987); P. Franken, C. J. Joachain, Phys. Rev. A **35**, 1590 (1987); P. Franken, C. J. Joachain, J. Opt. Soc. Am. B **7**, 554 (1990).

[29] L. Shu-Min, C. Ji , Z. Jian-Ge, and Y. Hong-Jun, Phys. Rev. A **47** 1197 (1993); L. Shu-Min, M. Yan-Gang, Z. Zi-Fang, C. Ji,and L. Yao-Yang,Phys. Rev. A **58** 2615 (1998).

[30] M. Stobbe, *Ann. Phys.* **7**, 661 (1930).

[31] M. Jain and N. Tzoar, Phys. Rev. A **18**, 538 (1978).

[32] A. I. Akhiezer and N. P. Merenkov, *J. Phys.* B **29**, 2135 (1996).

[33] W. Rudin, *Principles of Mathematical Analysis* (New York McGraw-Hill, 1976).

[34] G. Bateman and A. Erdelyi, *Higher Transcendental Functions* (New York McGraw-Hill, 1953); I. S. Gradshteyn and I. M. Ryzhik, *Table of Integrals, Series and Products* (New York Academic Press, 1965).

[35] L. V. Keldysh, *Sov. Phys. JETP* **20**, 1307 (1965).

[36] K. C. Kulander, *Phys. Rev.* A **35**, 445 (1987);
J. L. Krause, K. J. Schafer, and K. C. Kulander, Phys. Rev. A **45**, 4998 (1992).

[37] M.L. Mehta, *Random Matrices*, 3rd ed., (Elsevier, Amsterdam, 2004).

[38] A. Bohr and B.R. Mottelson, *Nuclear Structure* (World Scientific, Singapore, 1998).

[39] V. Zelevinsky, B.A. Brown, N. Frazier, and M. Horoi, Phys. Rep. **276**, 85 (1996).

[40] H.-J. Stöckmann, *Quantum chaos an introduction* (Cambridge University Press, 2000).

[41] H.A. Weidenmüller and G.E. Mitchell, Rev. Mod. Phys. **81**, 539 (2009).

[42] T.A. Brody, J. Flores, J.B. French, P.A. Mello, A. Pandey, and S.S.M. Wong, Rev. Mod. Phys. **53**, 385 (1981).

[43] C.E. Porter and R.G. Thomas, Phys. Rev. **104**, 483 (1956).

[44] P. E. Koehler, F. Becvar, M. Krticka, J. A. Harvey, and K. H. Guber, Phys. Rev. Lett. **105**, 072502 (2010).

[45] P.E. Koehler, Phys. Rev. C **84**, 034312 (2011).

[46] H.-J. Sommers, Y.V. Fyodorov and M. Titov, J. Phys. A **32**, L77 (1999).

[47] U. Kuhl, R. Höhmann, J. Main, and H.-J. Stöckmann, Phys. Rev. Lett. **100**, 254101 (2008).

[48] Y. Fyodorov and H.-J. Sommers, J. Math. Phys. **38**, 1918 (1997).

[49] D.V. Savin and V.V. Sokolov, Phys. Rev. E **56**, R4911 (1997).

[50] H.A. Weidenmüller, Phys. Rev. Lett. **105**, 232501 (2010).

[51] G.L. Celardo, N. Auerbach, F.M. Izrailev and V.G. Zelevinsky, Phys. Rev. Lett. **106**, 042501 (2011).

[52] A. Volya, Phys. Rev. C **83**, 044312 (2011).

[53] G.E. Mitchell, J.D. Bowman, S.I. Penttil, and E.I. Sharapov, Phys. Rep. **354**, 157 (2001).

[54] V.V. Flambaum and V.G. Zelevinsky, Phys. Lett. B **350**, 8 (1995).

[55] V.V. Sokolov and V.G. Zelevinsky, Nucl. Phys. **A504**, 562 (1989).

[56] C. Mahaux and H.A. Weidenmüller, *Shell Model Approach to Nuclear Reactions* (North Holland, Amsterdam, 1969).

[57] N. Auerbach and V. Zelevinsky, Rep. Prog. Phys. **74**, 106301 (2011).

[58] S. Mizutori and V. Zelevinsky, Z. Phys. **A346**, 1 (1993).

[59] A. M. Lane and R. G. Thomas, Rev. Mod. Phys. **30**, 257 (1958).

[60] N. M. Larson, Oak Ridge National Laboratory Technical Report No. ORNL/TM-9179/R8, (2008).

[61] V.V. Sokolov and V.G. Zelevinsky, Ann. Phys. **216**, 323 (1992).

[62] N. Auerbach and V. Zelevinsky, Nucl. Phys. **A781**, 67 (2007).

[63] P. von Brentano, Phys. Rep. **264**, 57 (1996).

[64] H. Komano, M. Igashira, M. Shimizu, and H. Kitazawa, Phys. Rev. C **29**, 345 (1984).

[65] G.L. Celardo, A.M. Smith, S. Sorathia, V.G. Zelevinsky, R.A. Sen'kov, and L. Kaplan, Phys. Rev. B **82**, 165437 (2010).

[66] J. Flores *et al.*, AIP Conf. Proc. **1323**, 62 (2010).

[67] A. A. Starobinsky, JETP Lett. **30**, 682 (1979); Phys. Lett. **B91**, 99 (1980).

[68] D. Kazanas, Astrophys. J. **241**, L59 (1980).

[69] K. Sato, Mon. Not. Roy. Astron. Soc. **195**, 467 (1981).

[70] A. Guth, Phys. Rev. D **23**, 347 (1981).

[71] A. D. Linde, Phys. Lett. **B108**, 389 (1982); **114**, 431 (1982); Phys. Rev. Lett. **48**, 335 (1982).

[72] A. Albrecht and P. Steinhardt, Phys. Rev. Lett. **48**, 1220 (1982).

[73] S. V. Mukhanov and G. V. Chibisov, Sov. Phys. JETP Lett. **33**, 532 (1981).

[74] S. Hawking, Phys. Lett. **115B**, 295 (1982).

[75] A. A. Starobinsky, Phys. Lett. **117B**, 175 (1982).

[76] A. Guth and S.-Y. Pi, Phys. Rev. Lett. **49**, 1110 (1982); Phys. Rev. D **32**, 1899 (1985)

[77] J. M. Bardeen, P. J. Steinhardt, and M. S. Turner, Phys. Rev. D **28**, 679 (1983).

[78] W. Fischler, B. Ratra, and L. Susskind, Nucl. Phys. **B 259**, 730 (1985).

[79] N. Seto, S. Kawamura, and T. Nakamura, Phys. Rev. Lett. **87**, 221103 (2001).

[80] T. L. Smith, M. Kamionkowski, and A. Cooray, Phys. Rev. D **73**, 023504 (2006).

[81] G. Efstathiou and S. Chongchitnan, Prog. Theor. Phys. Suppl. **163**, 204 (2006).

[82] B. Friedman, A. Cooray, and A. Melchiorri, Phys. Rev. D **74**, 123509 (2006).

[83] http//www.map.gsfc.nasa.gov

[84] E. Komatsu *et al.*, Astrophys. J. Suppl. **180**, 330 (2009); **192**, 18 (2011).

[85] D. N. Spergel *et al.*, Astrophys. J. Suppl. **148**, 175 (2003); **170**, 377 (2007).

[86] C. L. Bennett *et al.*, Astrophys. J. Suppl. **148**, 1 (2003).

[87] http//www.ligo.caltech.edu

[88] J. Abadie *et al.*, Phys. Rev. Lett. **107**, 271102 (2011);
Nature Physics **7**, 962 (2011); Phys. Rev. D **85**, 022001 (2012).

[89] S. Weinberg, *Cosmology*, (Oxford University Press, 2008).

[90] S. Weinberg, Phys. Rev. D **69**, 023503 (2004).

[91] S. Weinberg, Phys. Rev. D **74**, 063517 (2006).

[92] D. A. Dicus and W. W. Repko, Phys. Rev. D **72**, 088302 (2005).

[93] J. M. Stewart, Astrophys. J. **176**, 323 (1972).

[94] E. T. Vishniac, Astrophys. J. **257**, 456 (1982).

[95] J. R. Bond and A. S. Szalay, Astrophys. J. **274**, 443 (1983).

[96] M. Kasai and K. Tomita, Phys. Rev. D **33**, 1576 (1986).

[97] A. K. Rebhan and D. J. Schwarz, Phys. Rev. D **50**, 2541 (1994).

[98] J. R. Pritchard and M. Kamionkowski, Ann. Phys. (N.Y.) **318**, 2 (2005).

[99] Y. Watanabe and E. Komatsu, Phys. Rev. D **73**, 123515 (2006).